

**Application of a developed tool to visualize newly
synthesized AMPA receptor components *in situ***

Dissertation
zur Erlangung des Doktorgrades
der Naturwissenschaften

vorgelegt beim Fachbereich 15
der Johann Wolfgang Goethe - Universität
in Frankfurt am Main

von

Diplom Biologin Lisa Kochen
aus Frankfurt am Main

Frankfurt 2018
(D 30)

vom Fachbereich Biowissenschaften
der Johann Wolfgang Goethe - Universität als Dissertation angenommen.

Dekan:

Gutachter:

Datum der Disputation:

TABLE OF CONTENTS

1. ACKNOWLEDGMENTS	7
2. ZUSAMMENFASSUNG	8
3. ABSTRACT	13
4. INTRODUCTION	14
4.1 Molecular basis of learning and memory	15
4.1.1 Synapses: transmission of information between neurons	16
4.1.2 Change in synaptic strength allows memory formation	17
4.1.3 Long term potentiation (LTP)	17
4.1.4 NMDA receptors act as co-event detectors	20
4.1.5 Local protein synthesis is an underlying mechanism for learning and memory	20
4.2 Protein synthesis	22
4.2.1 The process of protein synthesis and its machinery	22
4.2.2 Protein synthesis inhibitors	23
4.2.3 Tools to investigate protein synthesis in neurons	23
4.3 AMPA receptor macromolecular complexes	26
4.3.1 AMPA receptors	26
AMPA receptor composition influences signaling properties and trafficking	27
Dynamic regulation of synaptic AMPA receptors	28
4.3.2 Auxiliary proteins	28
Transmembrane AMPA receptor regulatory proteins (TARPs)	29
Impact of TARPs on channel properties	29
TARPs have an impact on receptor trafficking and synaptic localization	30
TARP Gamma 8	31
CNIH2/3	31
4.4 Secretory pathway of membrane proteins	32
4.5 Aims of this study	33
5. MATERIAL AND METHODS	34
5.1 Material	34
5.1.1 Antibody list	34
5.1.2 Reagents and cells	34
5.2 Methods	35
5.2.1 Hippocampal neurons	35
5.2.2 Metabolic labeling with AHA and biotin-alkyne click (FUNCAT)	35
5.2.3 Surface labeling of GluA1 and GluA2	36
5.2.4 Surface labeling of TARP Gamma 8	36
5.2.5 Puromycylation	37
5.2.6 Proximity ligation assay (PLA)	37
5.2.7 Immunocytochemistry	37
5.2.8 Confocal imaging	38
5.2.9 Image representation in figures	38
5.2.10 Data analysis	38
5.2.11 Data representation and statistics	38

5.2.12 Puncta analysis ImageJ and Neurobits	39
5.2.13 GluA1 FUNCAT-PLA puncta intensity measurements (Fig 27)	39
5.2.15 Cumulative distribution of newly synthesized GluA1 and GluA2	39
6. RESULTS	40
6.1 Labeling translation using AHA and puromycin	40
6.1.1 Labeling translation using AHA	40
6.1.2 Labeling translation using puromycin	41
6.2 Proximity ligation assay (PLA)	44
6.3 Development of puncta analysis tools	49
6.3.1 ImageJ macro for puncta detection	49
6.3.2 Neurobits - a MATLAB script for puncta detection	50
6.3.3 Discussion and Outlook for Neurobits and ImageJ scripts	54
6.4 Pore-forming AMPA receptor subunits	55
6.4.1 GluA1 and GluA2	55
Different distributions for newly synthesized GluA1 and GluA2	55
Surface labeling of new GluA1 and new GluA2	58
Site of synthesis of GluA1 and GluA2	62
Pulse-chase experiments of GluA1 and GluA2	64
Inset: Higher FUNCAT-PLA signal in chase time points	65
6.5 Auxiliary proteins	68
6.5.1 TARP Gamma 8	68
Test of custom-produced anti-Gamma 8 antibody	68
Gamma 8 FUNCAT-PLA reveals mainly somatic synthesis	71
Pulse-chase experiments for newly synthesized Gamma 8	72
6.5.2 FUNCAT-PLA reveals high dendritic levels of newly synthesized CNIH2	74
7. DISCUSSION	76
7.1 Method development of FUNCAT-PLA and Puro-PLA	76
7.1.1 Further developments of the PLA technique	78
7.1.2 Future directions of FUNCAT- or Puro-PLA experiments	79
7.2 AMPA receptor complex composition and redistribution kinetics	80
7.2.1 GluA1 and GluA2 surface expression	83
7.2.2 Redistribution kinetics of new GluA1 and new GluA2	85
7.3 Auxiliary proteins TARP Gamma 8 and CNIH2	86
8. REFERENCES	89
9. APPENDIX	95
9.1 List of Abbreviations	96
9.2 List of Figures	97
9.3 List of Info-Boxes	97
9.4 List of Tables	97
9.5 Curriculum vitae	97

1. Acknowledgments

First and foremost, I would like to thank my boss Prof. Dr. Erin Schuman who gave me a warm welcome in the lab when I first started in 2010 and has been supporting and encouraging ever since. I feel very fortunate having had the chance to work on multiple exciting projects under her supervision. My personal development would not have been possible without her.

Next I would like to thank the members of my thesis committee; Prof. Dr. Erin Schuman, Prof. Dr. Amparo Acker-Palmer, Prof. Dr. Manfred Kössl and Prof. Dr. Virginie Lecaudey.

I am grateful to Arjan Vink for his work at the IMPRS graduate school and at the Teaching Lab.

Anne-Sophie has been an awesome coworker, labmate and friend. Her delicious crepes and cannelés bordelais helped through many failed experiments.

I am deeply grateful to Susu who got me first started in the lab and supported me ever since. She does tremendous work backstage to keep the lab running, she organized pilates classes at the Institute and took over babysitting duties so that I could attend pilates classes.

I highly value the administrative work of Nicole Thomsen and Sara Gil-Mast.

First labmate, now husband and father of our son Samuel. Thanks a lot Cyril for introducing me to fascinating live cell imaging, you taught me a lot, and for (mostly) managing to keep home and work life separate.

Ina my favorite technician and good friend, who introduced me to immunostainings and performed countless experiments with me. She always had the "we can do it" attitude and was always helpful.

Excellent support came from the prep team: Ina Bartnik, Nicole Fürst, Christina Thum and Dirk Vogel provided all these beautiful hippocampal neurons (rough estimate of 60 mio cells on 2000 dishes in 8 years) for my experiments. I also acknowledge the rat pups which were sacrificed for my experiments.

Many of these neurons needed to be manually traced after imaging. I am grateful for tracing support from Helene, Laura, Nikhil, Anja, Lea and Anne-Sophie.

Thanks goes also to Dr. Georgi Tushev and Maximilian Heumüller for fruitful script developments for image analysis.

Since most of my experiments include work at various laser scanning microscopes, I am truly grateful to Dr. Stephan Junek, head of the imaging facility, and his team who provided valuable support.

Last but not least, I would like to say a "big thank you" to my family and friends who supported me during my time as a PhD student: my parents Eva and Marcus, my brothers Manuel and Felix, Lisa, Andreas, Lisa, Sebastian, Kleopatra, Katharine, my Scimentogirls and my choir members. These musical intermezzos each Wednesday were one of my weekly highlights.

For critical reading and editing of my dissertation I am grateful to Erin, Susu and Anne-Sophie.

2. Zusammenfassung

Informationsweitergabe zwischen Nervenzellen geschieht an Synapsen, den Kontaktstellen zwischen Nervenzellen. Ein bekannter Mechanismus, der Lernen und Gedächtnis ermöglicht, ist das Verändern der Stärke der Informationsweitergabe in einzelnen Synapsen. Um die gigantische Nachfrage an Membran- und Proteinmaterial in Zellen zu stillen, nutzen Neuronen eine zusätzliche dezentralisierte Proteinproduktionsquelle in Dendriten. Uns ist bereits bekannt, dass diese lokale Proteinsynthese eine wichtige Rolle bei der synaptischen Potenzierung spielt; ein molekularer Mechanismus, der Lernen und Gedächtnisbildung ermöglicht.

Alle Komponenten der Proteinproduktionsmaschinerie sind in Dendriten vorhanden: Polyribosomen für die Translation von mRNAs, Mitochondrien für den energiekonsumierenden Syntheseprozess und Transkripte für Kandidaten vieler verschiedener Proteinfamilien. Viele Proteine, die lokal in Dendriten hergestellt werden, sind bereits bekannt. Es ist jedoch unklar, ob all diese Transkripte auch tatsächlich zur lokalen Synthese benutzt werden. Man kennt zwar die Notwendigkeit von *de novo* Synthese, um Gedächtnisinhalte zu bilden. Die zugrundeliegenden Mechanismen, wie somatische und dendritische Proteinsynthese reguliert werden, müssen jedoch erst noch verstanden werden.

Welche Proteine sind es, die neu hergestellt werden müssen, um Lernen zu ermöglichen?

Werden alle der potentiell möglichen Kandidaten auch tatsächlich lokal hergestellt?

Was ist das lokale Translatom?

Wie verändert sich dies nach einem Stimulus?

Entwicklung einer Methode zum Anfärben spezifischer neu hergestellter Proteine

Bisherige Methoden zur Untersuchung von Proteinsynthese ermöglichen es, entweder Synthesort oder Proteinidentität festzustellen - nicht jedoch beide Informationen innerhalb eines Experiments. Eine Methode, die beides gleichzeitig ermöglicht, ist jedoch von großer Wichtigkeit. Im ersten Teil dieser Arbeit wird die Entwicklung einer ebensolchen Methode beschrieben.

Entwicklung einer "proximity ligation assay" (PLA) basierten Methode: FUNCAT-PLA und Puro-PLA

Eine auf Antikörpern basierende Methode detektiert die Zusammenkunft zweier Events: die Präsenz eines neu hergestellten Proteins und gleichzeitig die Präsenz des zu untersuchenden Proteins. Wenn diese beiden Events in räumlicher Nähe zueinander sind, kann ein DNA-basiertes Amplifikationsprodukt hergestellt werden, welches farblich markiert und unter dem Mikroskop sichtbar gemacht werden kann. Die Präsenz des zu untersuchenden Proteins wird mittels spezifischer Antikörper

detektiert. Das Markieren neu hergestellter Proteine auf der anderen Seite erfolgt auf zwei unterschiedliche Arten, deren spezifische Einsatzgebiete im Einzelnen in dieser Dissertation herausgearbeitet werden.

Proteine werden hier entweder mit dem Aminosäureanalogon Azidohomoalanin (AHA) markiert, das anstelle von Methionin in translatierende Proteine eingebaut wird. In nachgeschalteten Schritten kann AHA mittels "Clickreaktion" chemisch markiert und mittels spezifischem Antikörper in Zellen sichtbar gemacht werden.

Die andere Möglichkeit neu hergestellte Proteine anzufärben, ist die Verwendung von Puromycin, ein Molekül welches mit gerade hergestellten Proteinen interagiert. Beim Einbau von Puromycin kommt es jedoch zum Translationsabbruch und puromycylierte Proteine üben nicht - wie beim AHA-Einbau - ihre eigentliche Funktion aus, sondern werden nach einiger Zeit wieder abgebaut. Nach kurzer Puromycin-Inkubationszeit können neu hergestellte Proteine jedoch mittels Antikörper in nachgeschalteten Schritten sichtbar gemacht werden. Je nach dem, welches Molekül zur Markierung von neuen Proteinen verwendet wird, nennen wir die Methode FUNCAT-PLA (AHA) oder Puro-PLA (Puromycin). Die Entwicklung und durchgeführte Kontrollen dieser neuen Methode werden in dieser Arbeit beschrieben und im zweiten Teil auf eine biologische Fragestellung angewendet.

Hierzu verwenden wir Puro-PLA, um mit kurzen Markierungszeiten den genauen Syntheseort einzelner Proteine nachweisen zu können. FUNCAT-PLA-Experimente hingegen haben den Vorteil, dass sich AHA-markierte Proteine nach ihrer Synthese normal in der Zelle verteilen. Wir verwenden diese Experimente deshalb beispielsweise, um die Umverteilung neu produzierter Proteine zu verfolgen. Hierzu markieren wir einen Pool an neu hergestellten Proteinen mit einer AHA-Inkubationszeit (pulse). Danach werden die lebenden Zellen unterschiedlich lange in Medium ohne AHA überführt (chase). Weiteres Markieren von Proteinen ist hier nicht mehr möglich, die bereits markierten Proteine jedoch wandern zu ihrem Bestimmungsort; wechseln ihre subzelluläre Lokalisation.

FUNCAT-PLA kann nun zudem auch dazu genutzt werden, Proteinhalbwertszeiten zu bestimmen. In den eben erwähnten "Pulse-chase-Experimenten" kann die Menge an PLA-Signal in gesamten Zellen bestimmt werden und der Zerfall der Signalmenge lässt Rückschlüsse darüber zu, wie schnell ein bestimmtes Protein nach seiner Herstellung wieder abgebaut wird.

Mit einem speziellen Trick können selektiv die neu hergestellten Proteine markiert werden, die bis zu einem gewissen Zeitpunkt an die Zellmembran gelangten. Hierzu werden lebende Zellen am Ende der AHA-Inkubation mit einem Antikörper behandelt, der gegen ein extrazelluläres Epitop des zu untersuchenden Rezeptors gerichtet ist. Nach dem Fixieren der Zelle wird reguläres FUNCAT-PLA durchgeführt, wobei dadurch nur die neu hergestellten Proteine angefärbt sind, die sich zum Zeitpunkt der Antikörperinkubation bereits an der Zelloberfläche befanden.

Entwicklung von Bildanalyse-Tools zur Auswertung von FUNCAT- und Puro-PLA Experimenten

FUNCAT- und Puro-PLA führt zu Punktesignal in Zellen (siehe Abbildung am Ende der Zusammenfassung). **Wie viele Punkte befinden sich in welchen Zellkompartimenten? Wie ist die relative Punktedichte in Dendriten und Somata? Wie verändert sich die Punktedichte zwischen verschiedenen experimentellen Konditionen?**

Um die Datenauswertung unserer Experimente qualitativ hochwertig, reproduzierbar und so zeitsparend wie möglich zu gestalten, entwickelten wir zusammen mit Bioinformatikern zwei Skripte. Diese funktionieren semiautomatisch; die Zelldetektion erfolgt manuell, die Punktedetektion jedoch automatisch. Die Funktionsweise und Anwendungsgebiete dieser zwei Skripte wird in dieser Arbeit beschrieben.

Anwendung der Methode zur Untersuchung des Synthesorts und der Umverteilungsdynamik von AMPA-Rezeptoruntereinheiten

Im zweiten Teil wird lokale Proteinbiosynthese in hippokampalen Nervenzellen mit Hilfe dieser neu entwickelten Methode untersucht. Wir konzentrieren uns hierbei auf AMPA-Rezeptoruntereinheiten, da sie bei der schnellen exzitatorischen Erregung eine unentbehrliche Rolle spielen. AMPA-Rezeptoren bilden eine Pore in der Zellmembran, die den Einstrom von Ionen ermöglicht. Bei der Aktivierung einer Nervenzelle werden Botenstoffe ausgeschüttet, die an diese AMPA-Rezeptoren binden und zu deren Öffnung führen. Einströmende Ionen bewirken die Depolarisierung und Aktivierung der nachgeschalteten Zelle und aktivieren zudem Signalkaskaden, die unter anderem zu Transkription von Genen führen kann. Je mehr Rezeptoren sich in der synaptischen Membran befinden, desto stärker wird die Zelle aktiviert. Die aktivitätsabhängige Regulierung der synaptischen AMPA Rezeptoren ist einer der molekularen Mechanismen, die Lernen und Gedächtnisbildung zugrunde liegen. Es ist allerdings noch unklar, wie im Einzelnen die synaptische Menge an AMPA Rezeptoren reguliert wird und in wieweit die aktivitätsabhängige Neusynthese von AMPA Rezeptoren bei der Potenzierung von Synapsen eine Rolle spielt.

AMPA Rezeptoren werden aus unterschiedlichen Untereinheiten gebildet, deren Zusammensetzung jedoch variieren kann. Die Wahl der einzelnen Untereinheiten hat großen Einfluss auf dessen Eigenschaften; von Transportgeschwindigkeit bis hin zu Bindeaffinitäten von Botenstoffen. Es ist jedoch noch ungeklärt, wann und wo sich diese Untereinheiten zu einem Komplex zusammenfügen und wie die Auswahl der Zusammensetzung in Neuronen reguliert wird.

Der sekretorische Weg von Membranproteinen

AMPA Rezeptoren als Mitglieder der Membranproteinfamilie werden von Ribosomen in das Lumen des endoplasmatischen Retikulums (ER) translatiert. Von hier gelangen sie über mehrere Stationen des sekretorischen Wegs an die Zellmembran und ihre eigentliche Wirkstätte: die Synapsen. Über Vesikel geht es vom ER über das ER to Golgi Intermediate Compartment (ERGIC) zum Golgi Apparat. In all diesen Stationen finden posttranslationale Modifikationen wie z. B. Glykosylierung statt. Die Mehrzahl extrazellulärer und Membranproteine ist glykosyliert. Der Glykosylierungszustand eines Proteins hat seinerseits Einfluss auf dessen Stabilität und Leitungseigenschaften von Rezeptoren. Glykosylierung stellt deshalb einen wichtigen zusätzlichen Regulationsmechanismus von synaptischer Stärke dar.

AMPA Rezeptoruntereinheiten des Hippokampus

Im Detail untersuchten wir die vier häufigsten AMPA-Rezeptor-Untereinheiten des Hippokampus, eine Gehirnstruktur, die für ihre Rolle bei der Gedächtnisbildung und Gedächtnisspeicherung bekannt ist. Es handelt es sich bei den Untereinheiten um die porebildenden Untereinheiten GluA1 und GluA2 und die nicht porebildende Untereinheiten (auxiliary subunits = Hilfsuntereinheiten) CNH2 und Gamma 8.

Hilfsuntereinheiten sind nicht Teil der porebildenden Region der AMPA Rezeptoren, sie sind für die korrekte Funktionsweise von AMPA-Rezeptoren jedoch unabdingbar. Das Wirkungsspektrum der Hilfsuntereinheiten reicht hier von korrekter Rezeptorpositionierung in Synapsen bis hin zu Kanaleigenschaftsveränderungen wie Leitfähigkeit.

Die Untersuchung der Herstellung und Umverteilung in der Zelle dieser verschiedenen Untereinheiten hilft uns besser zu verstehen, wie Nervenzellen die Erregungsstärke einzelner Synapsen input-spezifisch verändern können und so final Lernen und Gedächtnisbildung ermöglichen.

Mit FUNCAT-PLA und Puro-PLA Experimenten fanden wir heraus, dass Gamma 8 und GluA1 unter basalen Aktivitätsbedingungen hauptsächlich im Soma hergestellt und im somatischen Golgi Apparat prozessiert werden. Die Umverteilung der beiden Untereinheiten in die Dendriten erfolgt langsam im Verlaufe eines Tages. Unterwegs werden sie evt bereits an die Zelloberfläche gebracht, da neu hergestellte GluA1-Untereinheiten bereits früh einen hohen Anteil an der Plasmamembran zeigen. Aus der Ähnlichkeit der Umverteilungsgeschwindigkeit zwischen GluA1 und Gamma 8 schließen wir außerdem, dass diese beiden Untereinheiten zusammen im sekretorischen Weg an die Zellmembran transportiert werden könnten.

Im Laufe dieser Arbeit stellte sich ausserdem heraus, dass es starke Unterschiede in der Umverteilungsgeschwindigkeit von GluA1 und GluA2 gibt. Im Gegensatz zur langsamen Umverteilung von GluA1 beobachteten wir GluA2-Umverteilung bereits innerhalb einer Stunde.

Auch beschreiben wir im Zuge dieser Arbeit eine potentielle bisher nicht beschriebene Möglichkeit der Regulation von synaptischer Stärke durch die

nichtporebildende Untereinheit CNIH2. Wir fanden heraus, dass CNIH2 lokal in Dendriten hergestellt werden kann und damit evt die synaptische Expression von AMPA-Rezeptoren regulieren kann. CNIH2 wäre somit ein möglicher Kandidat, der auf einen Stimulus hin hergestellt wird und lokal für die synaptische Lokalisation eines AMPA-Rezeptors sorgen könnte. Die lokale Synthese von CNIH2 könnte somit eine spannende Verbindung zwischen neuronaler Aktivität und Änderung der synaptischen Stärke darstellen.

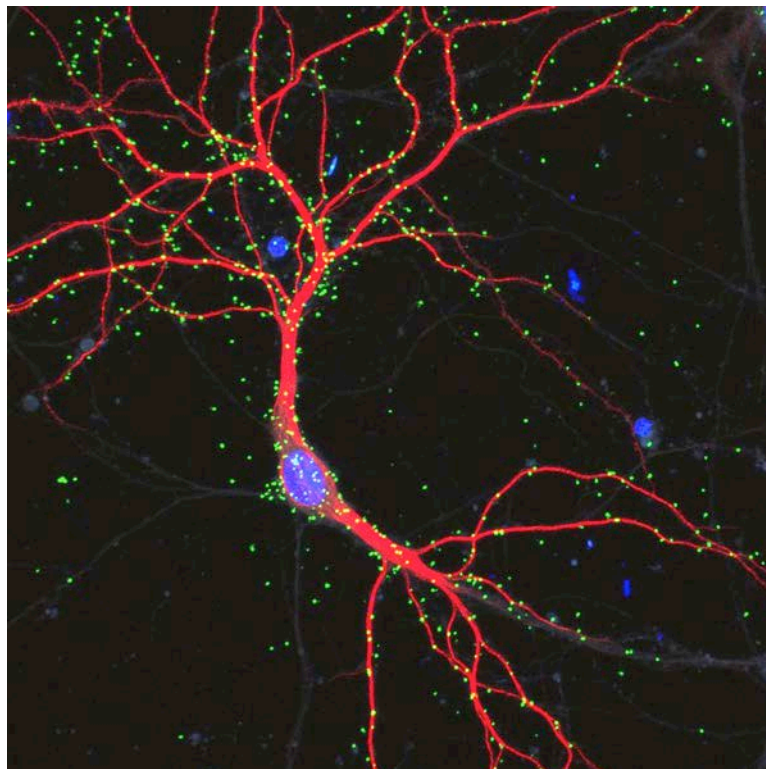
Die neu entwickelte Methode ermöglicht uns, Proteinsynthese spezifischer Proteine in einzelnen Zellen zu untersuchen. Wir verwendeten sie bereits, um ein paar spannende Fragestellung der synaptischen Plastizität zu beantworten. Die Methode wird sicherlich in Zukunft für die wissenschaftliche Community über die Neurobiologie hinaus nützlich sein.

Zentrale Fragen dieser Dissertation:

Wie kann man spezifische endogene neu synthetisierte Proteine in Zellen sichtbar machen?

Welche AMPA-Rezeptor-Untereinheiten können in Dendriten lokal hergestellt und prozessiert werden?

Wie schnell verteilen sich die verschiedenen AMPA-Rezeptor-Untereinheiten nach ihrer Herstellung in der Zelle?



Beispiel eines FUNCAT-PLA Experiments für neu hergestellte GluA2-Untereinheiten (grün) an der Zelloberfläche eines hippocampalen Neurons (rot), Zellkern in blau.

3. Abstract

The information flow between neurons happens at contact points, the synapses. One underlying mechanism of learning and memory is the change in the strength of information flow in selected synapses. In order to match the huge demand in membranes and proteins to build and maintain the neurites' complex architecture, neurons use decentralized protein synthesis. Many candidate proteins for local synthesis are known, and the need of *de novo* synthesis for memory formation is well established. The underlying mechanisms of how somatic versus dendritic synthesis is regulated are yet to be elucidated. Which proteins are newly synthesized in order to allow learning?

In this thesis protein synthesis is studied in hippocampal neurons. The fractional distribution of somatic and dendritic synthesis for candidate proteins and their subsequent transport to their destination are investigated using a newly developed technique. In the first part of this study we describe the development of this technique and use it in the second part to answer biological questions.

We focus here on AMPA receptor subunits, the key players in fast excitatory transmission. AMPA receptors contain multiple subunits with diverse functions. It remains to be understood, when and where in a neuron these subunits come together to form a protein complex and how the choice of subunits is regulated.

The investigation of the subunits' site of synthesis and redistribution kinetics in this study will help us to understand how neurons are able to change their synaptic strength in an input specific manner which eventually allows learning and memory.

Key questions which are addressed in this study:

How can specific newly synthesized endogenous proteins be visualized *in situ*?

What are the neuron's abilities to locally synthesize and fully assemble AMPA receptor complexes?

How fast do different AMPA receptor subunits redistribute within neurons after synthesis?

4. Introduction

4.1 Molecular basis of learning and memory

Synapses connect neurons in the brain. During learning and memory these synapses are altered. *De novo* protein synthesis plays an important role in this alteration.

The brain is a fascinating organ that allows individuals to adapt to their environment and improve their survival through learning and memory. The brain needs to have accurate and constant control over body functions but at the same time needs to be plastic in order to adapt to changes in the environment - the individuals need to learn and memorize new things. In 1950 Katz and Halstead proposed the necessity of new protein synthesis to build memories (Katz and Halstead, 1950). However, it took over a decade for this theory to be tested in experiments with rodents, unable to form new memories when translational inhibitors were injected into their brains, more precisely in a region known as the hippocampus (Agranoff & Klinger 1964; Brink et al. 1966; Flexner & Flexner 1969).

The hippocampus is one of the most studied regions of the brain for its role in memory formation, retrieval and learning (Scoville & Milner 1957; Neves et al. 2008; Remondes & M. Schuman 2004; Squire et al. 1992). This region can be subdivided into three main areas: the dentate gyrus (DG), the *Cornu ammonis* (CA1, 2 and 3) and the entorhinal cortex (EC) (Amaral & Witter 1989; Andersen, P., Morris, R., Amaral, D., Bliss, T., and O'Keefe 2007). Its structure is highly conserved from rodents to primates and humans (Fig 1).

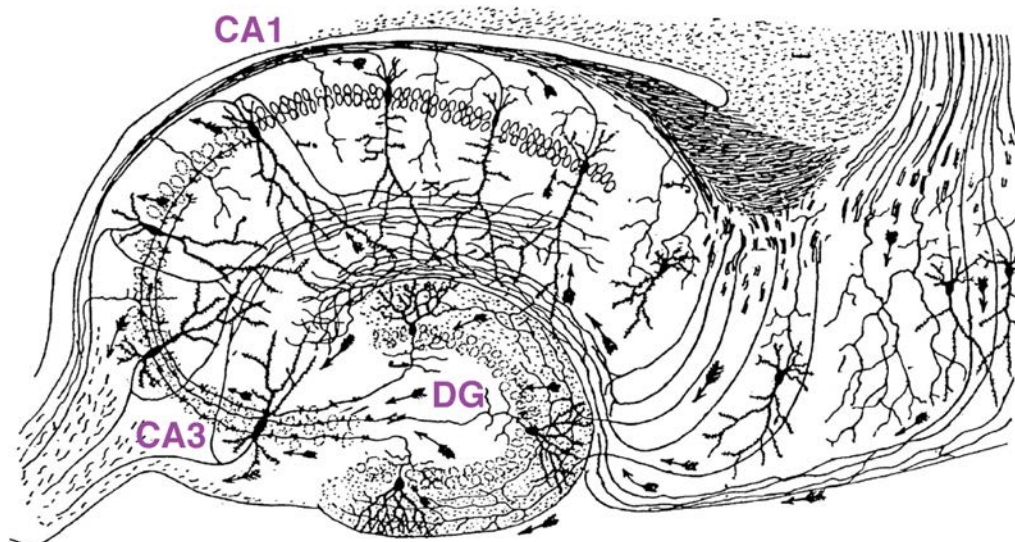


Figure 1: The hippocampal formation

Drawing by S. F. Ramon y Cajal of the hippocampal formation. Pyramidal neurons in the CA1 region, CA2, CA3, dentate gyrus (DG) (Ramón y Cajal 1909).

4.1.1 Synapses: transmission of information between neurons

Synapses, the contact regions between neurons, are the gates of information flow. They play a central role in processing and storing information. A single neuron can have up to ten thousand synapses. At chemical synapses, the topic of this thesis, electrical activity is converted into chemical release of molecules, which again triggers the electrical excitation of the information receiving neuron. Synapses consist of a pre- and a postsynaptic site which are both densely packed with various classes of proteins (Fig 2). Pre- and postsynapses are held together by several classes of adhesion molecules such as cadherins, integrins and neuexins. These adhesion molecules are involved in synapse formation and stabilization but are also dynamically regulated during activity (Bruns & Jahn 1995; Scheiffele 2003; Sheng & Hoogenraad 2007). Adaptor proteins like Homer, Shanks and PSD-95 connect these transmembrane adhesion molecules to the actin-based cytoskeleton. The region in the postsynapse is so densely packed with proteins that it appears as an electron dense part of the synapse in EM images - this is where it got its name from: post synaptic density, PSD. The cytoskeleton in synapses is interconnected with the cytoskeleton of axons and dendrites and therefore allows the dynamic exchange of proteins between neurites and synapses. Various membrane proteins are embedded in pre- and postsynaptic membranes, which allow ion influx or activation of intracellular cascades upon transmitter binding. All these components are dynamically regulated and allow for rapid remodeling of synapses, which as a result alters synaptic function.

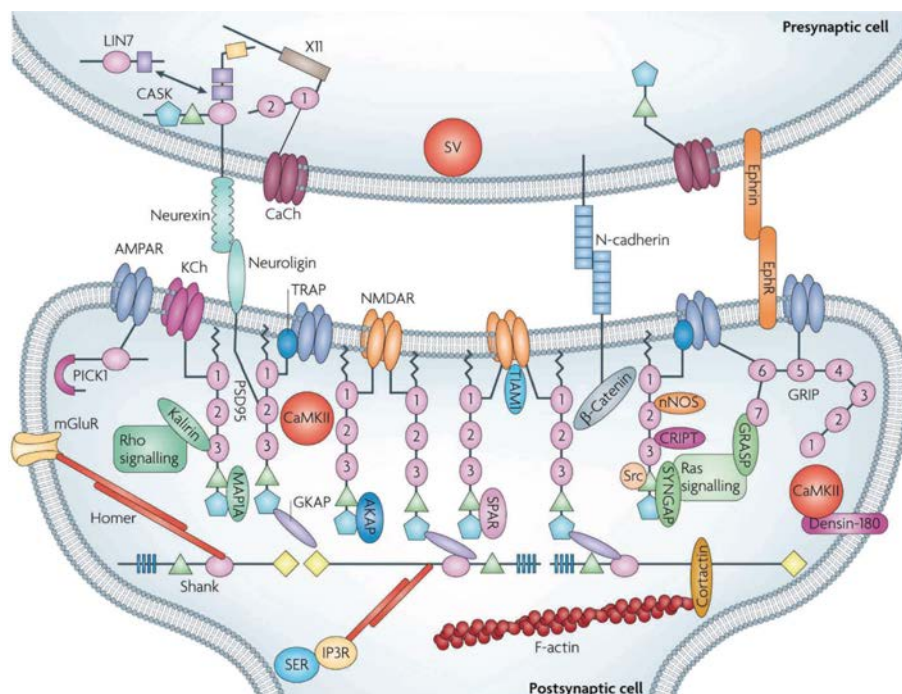


Figure 2: Model of a glutamatergic synapse

The postsynaptic density (PSD) contains scaffolding proteins (e.g. PSD95), membrane receptors (e.g. AMPAR), ion channels (e.g. KCh), cell adhesion (e.g. N-Cadherin) and signaling molecules, and components of the cytoskeleton (e.g. F-actin) (Neff et al. 2009).

Synapses are the point of information transfer between neurons. Information flow happens in the form of electrical currents. In their resting state neurons have a negative membrane potential. Upon activation, this potential gets depolarized and currents (action potentials, APs) flow in axons. At synapses these electrical currents are transformed into chemical transmitter release which then again lead to current flow in the receiving neuron.

The released neurotransmitters define a neuron as either inhibitory (e.g. GABA-releasing) or excitatory (e.g. glutamate-releasing) and connected postsynapses with the appropriate receptors get hyperpolarized or depolarized, respectively. Incoming inhibitory and excitatory inputs (EPSCs and IPSCs) from all synapses of one cell are summed up. When the integrated signal reaches a certain threshold, an action potential (AP) is generated and propagates along the axon to reach presynaptic terminals and induce neurotransmitter release (Clark et al. 2009; Colbert & Johnston 1996; Stuart et al. 1997).

At an excitatory synapse - the topic of this thesis - upon action potential arrival at the presynaptic bouton, glutamate-containing vesicles - the main excitatory neurotransmitter in the CNS - fuse with the presynaptic membrane and release the transmitter into the synaptic cleft. At the postsynapse glutamate binds to and activates ionotropic and metabotropic glutamate receptors. Ionotropic receptor activation leads to ion influx into the postsynapse. These receptors are classically divided into the subtypes AMPA, NMDA and Kainate receptors. Metabotropic glutamate receptor (mGluRs) activation triggers an intracellular signaling cascade by phosphorylation of target proteins and their resulting activation or inhibition. Due to the analog nature of the signal transmission, synaptic strength can be altered by tuning all of the above mentioned components of a synapse. This alteration is one of the known molecular substrates for learning and memory.

4.1.2 Change in synaptic strength allows memory formation

Experience-dependent long-term synaptic plasticity is a major cellular substrate for learning, memory and behavioral adaptation (Bliss & Collingridge 1993; Bi & Poo 2001; Sjöström et al. 2008; Collingridge et al. 2010; Cooper & Bear 2012; Hughes 1958). As early as the 1940s Donald Hebb postulated that "what fires together wires together" meaning that two neurons which are active at the same time strengthen their synaptic connection. Experimental proof of this postulated Hebbian synaptic plasticity came from Bliss and Lømo where they repeatedly stimulated the perforant path in the hippocampus of anesthetized rabbits and observed a lasting increase in postsynaptic responses in neurons from the dentate gyrus (Bliss & Lømo 1973).

4.1.3 Long term potentiation (LTP)

The potentiation of a synapse is achieved by a stronger activation of the postsynapse. This increase in current flow can be achieved by multiple means on both the pre and the postsynaptic site (Fig 3). At presynapses, more vesicles can be released upon stimulation leading to a stronger activation of postsynaptic membrane proteins. More ion influx on the postsynaptic site is achieved by having

more ion channels in the postsynaptic membrane or the pre-existing channels staying open for longer.

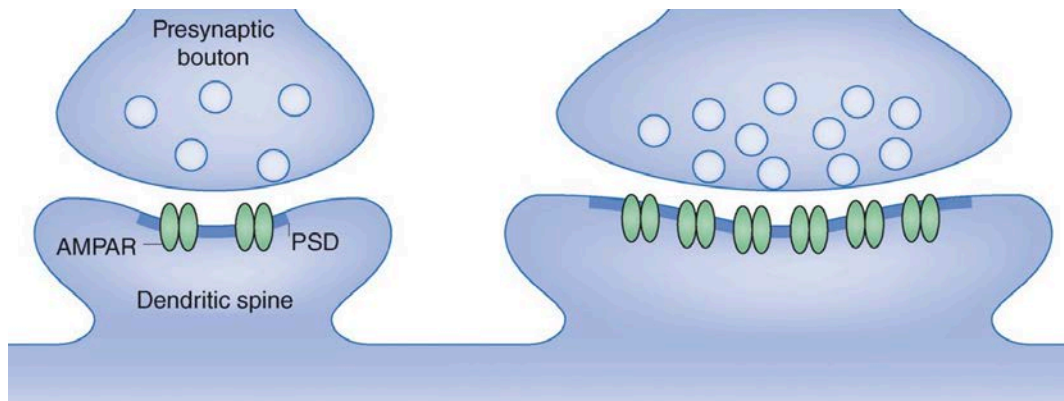


Figure 3: Pre and postsynaptic changes during synaptic potentiation

Potentiated synapse (right) contains bigger PSD (blue line), more synaptic AMPA receptors (green) or releases more neurotransmitter vesicles presynaptically (adjusted from Vitureira & Goda, 2013).

Even though the presynaptic locus for long-term synaptic plasticity is known for almost 30 years (Zalutsky & Nicoll 1992; Salin et al. 1996), the postsynaptic mechanisms underlying synaptic potentiation and depression are more widely described and are focused on in this study. The postsynaptic mechanisms of synaptic potentiation can be broadly divided into two categories: a protein synthesis independent and a protein synthesis dependent part.

The potentiation can be either transient and does not require *de novo* synthesis: early LTP (E-LTP) lasts typically less than three hours where pre-existing AMPA receptors are stabilized at synapses in a protein kinase-dependent way (Andersen, P., Morris, R., Amaral, D., Bliss, T., and O'Keefe 2007). However forms of plasticity with fast protein synthesis dependent changes of synaptic strengths are known as e.g. immediate early gene expression is necessary for learning and required for long-term potentiation (Kang & Schuman 1996; Huber et al. 2000).

Long lasting potentiation is achieved by *de novo* synthesis: late LTP (L-LTP) lasts more than three hours and requires new transcription (Nguyen et al. 1994) as well as it depends on the synthesis of new proteins (Bliss & Collingridge 1993; Sutton & Schuman 2006). Whereas the targets of E-LTP are quite well known and understood, the full newly synthesized proteome for L-LTP remains to be elucidated. Even though the synthesis dependent insertion of AMPA receptors at synapses upon triggering has been shown (Sutton et al. 2006), it however lacks direct proof that it is indeed the AMPA receptor itself which is synthesized. Work from our lab recently showed that for one specific plasticity paradigm it is indeed AMPA receptors which are newly synthesized, using the in this study newly developed technique (tom Dieck et al. 2015). Another hypothesis posits that the synthesis of mediator proteins which facilitate or trigger the synaptic targeting and exocytosis of pre-existing intracellular AMPA receptor pools is important. One piece of the puzzle of synaptic plasticity is hence to understand the dynamics of AMPA receptors. The synthesis and redistribution of various subunits of AMPA receptor complexes will be focused on in this study.

How does the synapse sense that it needs to be potentiated? Which molecular mechanism allows the detection of the before mentioned Hebbian plasticity? This mechanism of co-event detection is well understood and involves NMDA receptors.

4.1.4 NMDA receptors act as co-event detectors

The signaling cascade to achieve AMPA receptor insertion to allow synaptic plasticity is mediated by NMDA receptors (Granger et al. 2013). At resting potential NMDA receptors are blocked by magnesium. This blockage is voltage dependent and after activation of synaptic AMPA receptors and resulting membrane depolarization the removal of magnesium is triggered. The activation of NMDA receptors leads to calcium influx into the postsynapse (Nowak et al. 1984). Intracellular calcium acts as a second messenger for kinases (e.g. PKA, PKC, CamK2 α) leading to changes in AMPA receptor phosphorylation levels and their signaling properties. It also triggers diverse signaling cascades mediating transcription (e.g. PKC mediated gene expression) and protein synthesis that eventually leads to more AMPA receptors at the synapse (Tao et al. 1998; Bliss & Collingridge 1993; Tsien et al. 1996). NMDA receptors hence play a crucial role in regulating the composition and trafficking of AMPA receptors (Granger et al. 2013). Ultimately the AMPA receptor abundance at synapses is altered to either potentiate or downscale synapses. *The dynamic regulation of AMPA receptors at the postsynaptic membrane is thus important to understand the underlying mechanisms of learning and memory.*

4.1.5 Local protein synthesis is an underlying mechanism for learning and memory

Given their gigantic and complex architecture neurons have a high demand in protein production to meet the high need. Neurons make use of an additional supply of proteins to assure maintenance of the big dendritic arbor: local protein synthesis. This local source of protein production is especially important in the alteration of synaptic strength to allow learning and memory.

LTP and LTD are alterations in synaptic strength that are known to be important to form new memory traces. As described earlier some forms of these alterations in synaptic connectivity are protein synthesis dependent as synthesis inhibitors prevent memory formation. A specific form of protein synthesis - the local protein production in dendrites is crucial to allow neurons to rapidly change synaptic strength upon stimulation. Evidence for that finding was coming from increased numbers of polyribosomes in spines along with synaptic potentiation in the hippocampus (Ostroff et al. 2002; Bourne et al. 2006). This data suggests active translation near spines that undergo synaptic plasticity. In addition to ribosomes virtually all other components of the protein synthesis machinery can also be found in dendrites (Fig 4). We can detect mRNA transcripts (Cajigas et al. 2012) using high resolution FISH and sequencing of the hippocampal neuropil layer. These localized transcripts may serve as local templates for protein production. Mitochondria (Popov et al. 2005) reach distal tips of axons and dendrites shown in EM, immunolabeling and live cell imaging of fluorescently tagged mitochondria. They provide ATP for the energy demanding process of protein synthesis.

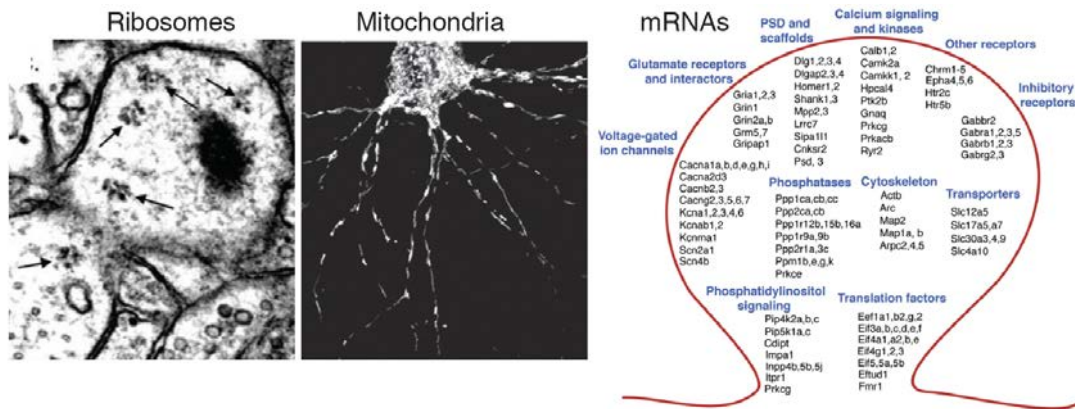


Figure 4: All components of the translational machinery are present in dendrites
 Polyribosomes, mitochondria for energy supply and mRNAs for many different proteins are present in neuronal dendrites (Bourne et al. 2006; Li et al. 2004; Cajigas et al. 2012).

More evidence that local protein production is crucial and sufficient to allow synaptic potentiation is provided by Kang and Schuman. In these classic experiments dendrites of rat hippocampal slices were mechanically isolated from their cell bodies and a neurotrophin (BDNF) was applied. This stimulation led to synaptic potentiation in these dendrites even though they did not have access to the somatic source of protein production machinery (Kang & Schuman 1996). Local dendritic application of protein synthesis inhibitors showed the necessity of local protein synthesis for synaptic potentiation (Bradshaw et al. 2003; Vickers & Wyllie 2007). Locally induced homeostatic plasticity was also found to be protein synthesis dependent (Sutton et al. 2004; Sutton & Schuman 2006; Sutton et al. 2007).

One can speculate that local production combined with local insertion of newly synthesized proteins would be beneficial for the cell in multiple ways. Energy could be saved by locally translating multiple protein copies from one localized mRNA compared to somatic synthesis and active, energy consuming transport of each protein copy individually. Local production and local insertion would enable the neuron to react quickly to external stimuli. Given the complex morphology of neurons with dendritic arbors comprising ca 50.000 μm and 5.500 μm^3 of length and volume, it is hard to imagine how the concentration of a specific protein can be locally changed at synapses with only somatic production.

Different proteins have different half lives depending on their synthesis and degradation rate. They can range from hours (e.g. TrkB isoform 1) to weeks (e.g. Agrin; Cohen et al. 2013). A very short lived protein with exclusively somatic synthesis would be degraded by the time it could reach distal synapses. On the other hand, a very stable protein could remain at a synapse for a very long time, constantly exerting its function. The regulatability of proteins must be assured especially in compartments with small volumes like synapses. Local translation must be tightly regulated in time and space in order to assure right amounts of protein copies per synapse.

The local transcriptome includes mRNAs for many different classes of synaptic proteins (Cajigas et al. 2012). Whether all of them are indeed used for local production is less clear, the local translome is currently unknown. The before mentioned studies show the direct link between neuron's capacity for synaptic

plasticity and local protein synthesis. They however do not shed light onto which newly synthesized proteins exactly are responsible for these changes in activity - **which proteins are newly synthesized in an input specific manner?** What is the activity dependent translome?

During synaptic plasticity synaptic strength can be theoretically altered on different levels. AMPA and NMDA receptors could be synthesized and inserted locally. Alternatively more pre-existing receptors could be stabilized at synaptic sites by the local production of tethering molecules. This would require a ready-to-use pool of receptors in the synaptic vicinity. Locally produced cytosolic proteins must be efficiently tethered since they would otherwise diffuse away rapidly. The diffusion would prevent the local usage of these proteins produced on demand to alter one specific synapse or a stretch of dendrite.

As mentioned above, all of these protein classes could be potentially synthesized in the vicinity of synapses. And yet very little is known about the actual local translome of dendrites and single synapses. In this study we focus on the question whether or not AMPA receptors are synthesized locally and how they redistribute after synthesis. Before describing AMPA receptor components in greater detail I will elaborate on the general protein synthesis machinery and which experimental tools are already available to study protein synthesis.

4.2 Protein synthesis

4.2.1 The process of protein synthesis and its machinery

Ribosomes are protein producing machines. During translation their two main subunits link amino acids together to form proteins. Protein synthesis can be studied with the help of a vast set of translation inhibitors specific to different steps of translation.

Protein translation is executed by ribosomes. In cells, ribosomes either exist as freely diffusible in the cytoplasm or attached to the endoplasmic reticulum. In eukaryotes ribosomes are built out of a small (40 S) and a large subunit (60 S). These two subunits are multiprotein complexes also containing ribosomal RNAs (rRNAs). The process of translation can be divided into three steps: initiation where the two subunits come together with an mRNA, elongation where the amino acids are linked together and termination where the fully translated protein is released and the two ribosomal subunits detach. In particular initiation and elongation are targets of regulation (Graber et al. 2013; Sonenberg & Hinnebusch 2009; Sutton & Schuman 2005). During elongation the small ribosomal subunit enables the binding and decodes the mRNA by facilitating accurate base pairing between triplet mRNA codon and the complementary anticodon of a tRNA linked to their respective amino acid (aminoacyl-tRNA). The mRNA codon sequence dictates the amino acid sequence of the synthesized protein. The new amino acid is added to the pre-existing stretch of newly synthesized protein by the peptidyl transferase in the active center of the large subunit. The catalytic activity is performed by an rRNA. The

newly formed peptide bond between two amino acids is very stable. Once the peptide bond is formed a new aminoacyl-tRNA enters the ribosome and an amino acid then again is added and elongates the pre-existing peptide. Elongation speeds of three to ten amino acids per second have been measured (Iwasaki & Ingolia 2016; Ingolia et al. 2011). The translation of an AMPA receptor protein with 1000 amino acids would hence take a couple of minutes. This however does not include additional necessary post translational modifications such as glycosylation.

4.2.2 Protein synthesis inhibitors

Ribosomes of the three domains bacteria, archea and eukaryotes resemble each other to a remarkable degree, even though their protein composition and protein to rRNA ratio vary. Antibiotics make use of the structural differences between the domains. It gives humans the opportunity to take an antibiotic which inhibits bacterial protein production to eventually kill bacteria without affecting their own human ribosomes and metabolism. In research, these substances are used as translation blockers to study protein synthesis. A broad variety of translation blockers are known. They target different steps of the translation process. Initiation inhibitors such as pactamycin or pateamine A prevent formation of the two ribosomal subunit complex. Elongation inhibitors such as anisomycin, puromycin or emetine inhibit either the peptidyl transferase, the translocation step or lead to truncation of the protein. Apart from translation inhibitors other tools are available to study protein translation.

4.2.3 Tools to investigate protein synthesis in neurons

In order to distinguish pre-existing and newly synthesized proteins in cells, various techniques use incorporation of labeled amino acids or the separation of translating ribosomes from inactive ribosomes. In this study, we make use of bio- orthogonal amino acids carrying a small functional group which can be visualized or purified after incorporation.

A vast set of tools have been developed in the past to study protein synthesis in cells. Various inhibitors of translation can be used to study the impact of protein production on the biological process e.g. synaptic plasticity. Their selectivity for different translation phases can dissect out the dynamics, the interaction partners and regulation of protein production in different organisms. Instead of blocking protein synthesis and observing which other processes in cells are impaired, a broad cast of tools is available to label newly synthesized proteins using the cells' own translational machinery. With these tools in hand, we can study the temporal and spatial dynamics of protein production in cells.

The use of radiolabeled amino acids to tag newly synthesized proteins has been used for several decades. Artificially synthesized amino acids carrying radiolabeled atoms can be visualized once incorporated into proteins using radiography. Pre-

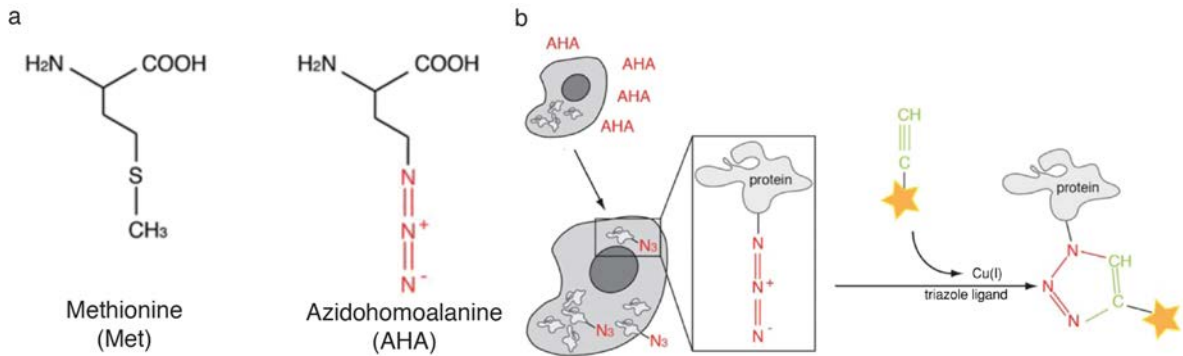
existing proteins only carry normal amino acids and are hence not detected on the autoradiograph. Using this technique, local protein synthesis was visualized for the first time using synaptosomes (a biochemical preparation of synaptic spines and presynaptic terminals which still contain intact membranes and are able to respond to electrical stimulation, (Blaustein & Goldring 1975; de Belleruche & Bradford 1972). Synaptosomes were able to incorporate radiolabeled amino acids into new proteins indicating the fully functional translational machinery present in neurites. The use of radiolabeled amino acids requires however long labeling times of hours (Rao & Steward 1991; Edward 1967; Torre & Steward 1992; Weiler & Greenough 1991). Nevertheless those methods can be used to detect and visualize newly synthesized proteins *in situ* or to purify them via biochemical approaches.

In the above mentioned experiments, only the pool of newly synthesized proteins can be measured. More recent approaches include the usage of stable isotope carrying amino acids. By combining this heavy amino acid labeling with mass spectrometry (MassSpec), one is able to resolve protein identities. Quantitative proteomics additionally gives information about how much of each protein is present in a sample. In a special form of MassSpec experiments, the impact of a stimulus can be investigated in a less biased way where control and stimulus group are analyzed together in one MassSpec experiment. In these so-called SILAC experiments (Stable Isotope Labeling using Amino acids in Cell culture) stably heavy isotope labeled amino acids and normal amino acids are combined. One dish is incubated with normal amino acids and the other one with stably heavy amino acids. Cell lysates of these two dishes can be mixed and analyzed using MassSpec. The slightly heavier nature of the heavy amino acid labeled proteins gives an indication of the dish it was coming from.

To go one step further, the impact of neuronal activity or certain stimuli on protein half lives and turnover rates can be tested performing pulse-chase SILAC experiments. In these experiments a pulse incubation time with labeling medium is followed by periods of label-free medium of various lengths. Labeled proteins are degraded in these chase times and decay curves can be generated. For additional information of translation rates, parallel mRNA isolation and sequencing can be performed.

Instead of labeling translated proteins, the transcriptome of a cell can also be identified by sequencing actively translated mRNA transcripts. Polyribosomes are purified from cell lysates and UV-crosslinked with their bound transcripts. Digestion of unbound mRNA fragments and bound ribosomes leaves mRNA fragments which are "footprints" of currently translated sequences at the time of lysate harvesting (Ingolia et al. 2009; Ingolia et al. 2011). Use of transgenic cell lines and animals, where ribosomes of a specific celltype or brain region are tagged, enables us to selectively purify tagged ribosomes and cell type specific transcriptomes can be generated (Doyle et al. 2008; Heiman et al. 2008). Techniques identifying translated transcripts however lack the information of how many protein copies were generated of a given mRNA species.

For labeling of endogenous proteins more recent approaches use non-canonical amino acids which are incorporated into nascent proteins under very controlled conditions. These amino acid homologues can be subsequently tagged either for visualization *in situ* (FUNCAT, fluorescent non-canonical amino acid tagging) or purification followed by mass spectrometric analysis (BONCAT, bio-orthogonal non-canonical amino acid tagging, see infobox 1).



Infobox 1: FUNCAT and BONCAT - chemistry and principle

a) The chemical structure of the non-canonical amino acid AHA (azide-bearing) is similar to methionine (Met). b) FUNCAT procedure steps during metabolic labeling and click reaction. AHA uptake by amino acid transporter, charging of AHA onto Met-tRNA by MetRS, ribosomes accept AHA-charged Met-tRNAs and incorporate AHA into nascent proteins. A variety of azide- or alkyne-functionalized fluorophores are available to covalently ligate a fluorophore to AHA by Cu(I)-catalyzed azide + alkyne[3+2]-cycloaddition. The Cu(I) catalyst is produced in the reaction mixture from Cu(II) and TCEP and is stabilized by the triazole ligand (TBTA) = "Click-reaction". BONCAT procedure includes cell lysate and purification of clicked newly synthesized proteins over columns and subsequent MassSpec identification. AHA labeling can be performed on cell culture, brain slices, organs and even entire organisms (e.g. zebrafish larvae, mice, adjusted from tom Dieck et al. 2012).

As for heavy isotope labeling, pulse-chase experiments for protein turnover estimations are possible because full length and functional proteins are obtained after labeling. Labeling durations on the order of hours are needed for non-canonical amino acid tagging.

In a parallel approach, puromycin, a translational inhibitor can also be used as a translational marker. Its similarity to tRNAs allows its incorporation into nascent proteins leading to protein truncation. Labeling times of minutes are sufficient to obtain significant signal. Puromycylated proteins can be fluorescently labeled or purified using an antibody directed against puromycin.

In all these approaches either the identity of the newly synthesized proteins remain unknown (e.g. FUNCAT) or the information about the subcellular location is lost (e.g. BONCAT). In candidate-based approaches the overexpression of fusion proteins that carry e.g. photoconvertible fluorescent tags makes it possible to have a timepoint zero of synthesis. In parallel photobleaching experiments one can estimate how fast a pool of a certain protein can be replenished. Overexpression experiments however always come with their own caveats and direct conclusion about endogenous proteins cannot be drawn. In conclusion, techniques developed

thus far to study protein synthesis either lack protein identity or cellular location or they use exogenous proteins.

There is hence a need for a new technique that enables us to visualize the location of specific endogenous newly synthesized proteins. Such a technique will be described in this thesis.

With such a tool at hand we could start answering questions like the following:

Which proteins are synthesized locally in dendrites?

How is their local synthesis regulated by neuronal activity?

What are the redistribution dynamics of newly synthesized proteins after synthesis?

Which cellular volume is investigated by a given newly synthesized protein?

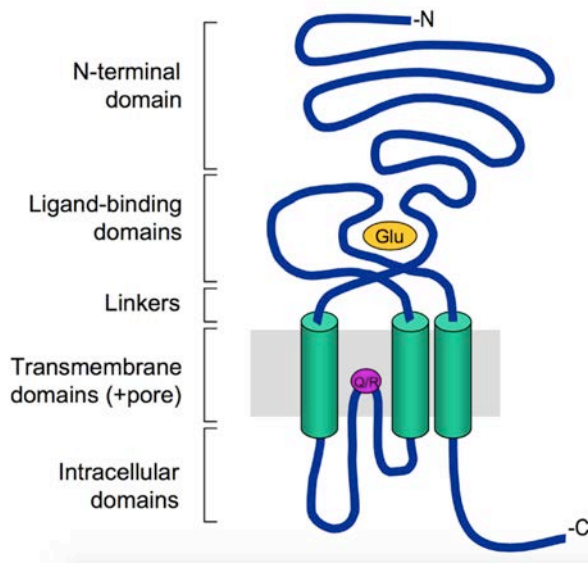
Given the very direct impact on changes in synaptic plasticity, AMPA receptor subunits are a good and obvious candidate for local translation. We now take a closer look at AMPA receptor complexes, a keyplayer of fast excitatory transmission at synapses.

4.3 AMPA receptor macromolecular complexes

AMPA receptors are the main mediators of fast excitatory transmission in the CNS. Their signaling properties and trafficking dynamics depend on the composition of their tetrameric pore-forming and non-pore-forming subunits and their posttranslational modifications like phosphorylation.

4.3.1 AMPA receptors

Fast excitatory neurotransmission in the CNS is primarily mediated by AMPA receptors. Their pore-forming structure allows ion influx into the neuron upon activation. One AMPA receptor is a multiprotein complex in which the pore is built by a tetramer of the GluA subunits. This tetrameric structure exists as homo- or heteromer comprising the combinatorial assembly of the four different subunits GluA1, GluA2, GluA3 and GluA4. Their topology in a membrane is depicted in infobox 2 (Bennett & Dingledine 1995; Nakagawa et al. 2005; Hollmann & Heinemann 1994).



Infobox 2: Topology of AMPA GluA subunits

ca 1000 amino acids and 100 kDa. Its relatively large (ca 500 amino acids) extracellular N-terminus is followed by one transmembrane domain, one C-loop that only crosses the inner lipid layer and forms the ion permeable pore, another two transmembrane domains and ends with an intracellular C-terminus. This C-terminal domain (CTD) is a target for regulation via phosphorylation. The glutamate binding site is built between the extracellular N-terminus and the second extracellular loop. The channel opens when at least two binding sites of the AMPA receptor tetramer are occupied. AMPA receptors are highly conserved during evolution and there is 70 % sequence overlap between GluA1-4. The general topology is shared between NMDA and kainate receptors (Jackson & Nicoll 2011b).

After their synthesis in the ER, GluA dimers are first formed, dimerize then again to form tetramers (Tichelaar et al. 2004). AMPA receptor composition varies between brain regions, cell types and synapses. *In vivo* not all possible combinations are present since only GluA1 homomers, GluA1/2, GluA2/3, GluA2/4 and GluA4 homomers have been detected (Greger & Esteban 2007). In the hippocampus, the brain region of this study due to its central role in memory formation, the dominant subunits are GluA1 and GluA2 (Schwenk et al. 2012; Schwenk et al. 2014) and less abundant also is GluA3 (Lu et al. 2009). In the following paragraph we describe how AMPA receptor subunit composition influences biophysical channel properties and pharmacology.

AMPA receptor composition influences signaling properties and trafficking

The signaling properties of AMPA receptors vary greatly with their subunits tetrameric composition. Calcium ions for example are only capable of passing through GluA2-lacking tetramers. This is due to RNA editing exclusively for GluA2. A positive charge in the pore-forming region (purple circle in infobox 2) is created by the transformation of a glutamine to an arginine (Q/R editing) making it energetically unfavorable for calcium ions to enter the pore. Since nearly all GluA2 subunits in adult neurons are edited (Sommer et al. 1991) they are all calcium impermeable. The editing of GluA2 has also an impact on subunit trafficking since edited GluA2 contains an ER retention signal which is absent in the other subunits. Hence, GluA2 homomers do not leave the ER and GluA2 rather serves as an intracellular pool

where GluA1/2 heteromers can be formed that are rapidly exported from the ER (Sommer et al. 1991; Henley & Wilkinson 2016; Greger et al. 2003).

Dynamic regulation of synaptic AMPA receptors

AMPA receptors are highly mobile proteins that undergo constitutive and activity-dependent translocation (Borgdorff & Choquet 2002; Ehlers et al. 2007; Heine et al. 2008; Tardin et al. 2003) to, recycling at, and removal from, synapses. Their synaptic delivery and internalization is mediated via phosphorylation. Each of the four different subunits can be phosphorylated at various sites on their intracellular C-terminal domain (CTD). This leads to changes in conductivity and is a signal for synaptic surface targeting, synaptic retention or internalization depending on the subunit and phosphorylation site. Activity-dependent phosphorylation of GluA1 delivers AMPARs to synapses, dephosphorylation is a signal for their internalization and LTD. Phosphorylation of GluA2 on the other hand is required for AMPA receptor internalization (PKC-dependent) and its dephosphorylation is important in synaptic retention. GluA1-containing AMPARs are delivered to synapses in an activity-dependent manner and are then replaced by GluA2/3 which do not require activity for insertion.

C-terminal modifications are not the only aspect that influences synaptic targeting. A group of stably interacting proteins exists that have a high impact on AMPA receptor trafficking and signaling properties. They are called auxiliary proteins.

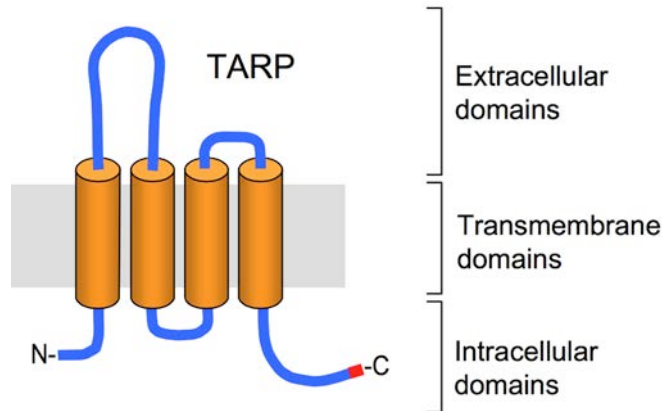
4.3.2 Auxiliary proteins

Auxiliary proteins interact stably with AMPA receptors. They influence various properties of AMPA receptors ranging from trafficking to pore opening probabilities. TARP Gamma 8 and CNIH2 are two representative auxiliary proteins this study focuses on due to their high abundance in the hippocampus.

AMPA receptors are not the naked tetramers they were thought to be for a long time. They are rather part of a multiprotein complex where different proteins interact stably without taking part in the pore-forming region. These auxiliary proteins are critical regulators of AMPA receptor trafficking, pharmacology and channel kinetics. They may play a role in the etiology of disorders as diverse as epilepsy, bipolar disorder, schizophrenia, neuropathic pain and depression since these patients reveal aberrant expression of auxiliary proteins (Beneyto & Meador-Woodruff 2006; Silberberg et al. 2008). A well characterized group of auxiliary proteins are the transmembrane AMPA receptor regulatory proteins (TARPs).

Transmembrane AMPA receptor regulatory proteins (TARPs)

TARPs are found in both neurons and glia cells and display complex, cell-type-specific expression patterns that vary over the course of development (Tomita et al. 2003; Yamasaki et al. 2016; Lein et al. 2006). CA1 pyramidal neurons are known to



express multiple TARP family members, including stargazin (Gamma 2), Gamma 3 and Gamma 8. However, a striking and unique feature of the hippocampus is the selective enrichment of Gamma 8 (Tomita et al. 2003; Fukaya et al. 2005; Lein et al. 2006; Cembrowski et al. 2016).

Infobox 3: TARPs

Their common topology is four transmembrane domains, their termini lay both cytosolically. C-termini can be phosphorylated, synaptic targeting is achieved via a PDZ binding motif in the last four residues (red). They possess a relatively small size of ca 38 kDa (330 amino acids). They can be subdivided into two main classes called type I TARPs (stargazin, g-3, g-4, and g-8) and type II TARPs (g-5 and g-7).

Impact of TARPs on channel properties

Interaction of auxiliary proteins with AMPA receptors have a huge influence on their signaling properties (Fig

5). Bound auxiliary proteins slow down deactivation and desensitization kinetics (Tomita et al. 2003; Rouach et al. 2005; Kott et al. 2007; Milstein et al. 2007; Cho et al. 2007; Menuz et al. 2007; Suzuki et al. 2008; Soto et al. 2009; Kott et al. 2009; Shi et al. 2009; Shi et al. 2010; Kato et al. 2010; Jackson & Nicoll 2011a; Jackson & Nicoll 2011b). As a result, more sodium is allowed to flow into the synapse upon activation leading to a stronger postsynaptic response.

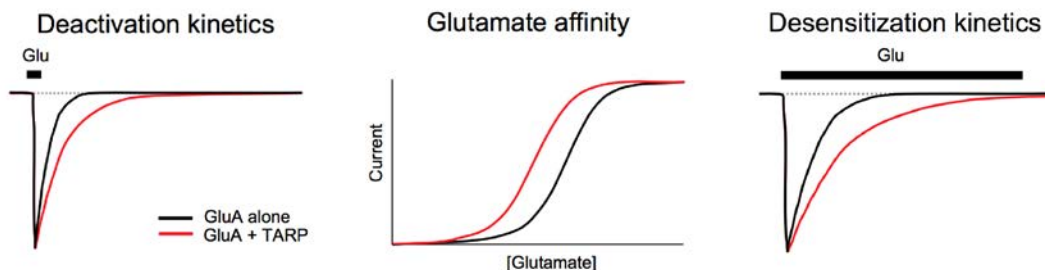


Figure 5: Impact of TARPs on channel properties

AMPA receptor complexes containing TARPs (red) have slower deactivation kinetics, higher glutamate affinity and desensitize slower after glutamate activation compared to AMPA receptor complexes alone (black) (Jackson & Nicoll 2011b).

AMPA receptors interacting with their auxiliary protein have also a higher glutamate affinity compared to the AMPA receptor alone (Bedoukian et al. 2008). They are hence capable of opening in response to a lower glutamate concentration than a naked AMPA receptor tetramer. The same AMPA receptor behaves very differently to a given stimulus depending on its interaction with different auxiliary proteins. Auxiliary proteins represent hence another level of regulation of synaptic strength.

TARPs have an impact on receptor trafficking and synaptic localization

TARPs facilitate AMPA receptor complex forward trafficking by different means. TARPs are known to facilitate ER export by blocking ER-retention sites on AMPA receptor subunits (Bedoukian et al. 2006); they also localize receptors to specific membrane compartments. This was shown by adding the CTD of an auxiliary protein (stargazin) to an unrelated receptor that mediated its ER export and localization to the Golgi (Bedoukian et al. 2008). In the absence of stargazin, no functional AMPA receptor reaches synapses in granule cells (Chen et al. 1999; Hashimoto et al. 1999) indicating its crucial role in synaptic AMPA targeting. Furthermore stargazin is thought to stabilize AMPA receptors at synapses via its CTD-PSD95 interaction (Tomita et al. 2005; Tsui & Malenka 2006; Chen et al. 2000). The dendritically localized kinase CamK2 α , well known for its role in synaptic plasticity, is able to phosphorylate pore-forming and non-pore-forming subunits and with that change their properties and synaptic dwell time. CamK2 α plays hence a crucial role in the regulation of synaptic AMPA receptor complexes in the context of synaptic plasticity (Opazo et al. 2010; Opazo & Choquet 2011; Sumioka et al. 2011; Hafner et al. 2015). In Gamma 8 knock out mice CA1 pyramidal neurons display a modest reduction in synaptic AMPARs but a severe loss of extrasynaptic AMPARs (Rouach et al. 2005). These results indicate the strong involvement of Gamma 8 in AMPA receptor surface targeting.

Stargazin has a lower affinity for desensitized AMPA receptors that still bind glutamate. Since stargazin stabilizes AMPA receptors in the PSD, unbound desensitized AMPA receptors diffuse away more easily. This leads to a fast exchange in the order of milliseconds of desensitized receptors in the PSD. The cell is hence able to respond reliably to high frequency stimulation by exchanging desensitized receptors by inactive ones (Constals et al. 2015; Turetsky et al. 2005). There is still a debate about the subunit stoichiometry of AMPA receptor to auxiliary protein and where their interacting regions are. AMPARs are estimated to associate with either two or four TARPs, suggesting a degree of cooperativity in TARP binding (Milstein et al. 2007). Additionally TARP stoichiometry differs among hippocampal cell types, suggesting that gating effects could be modulated by differential TARP expression (Shi et al. 2009). Expression of CNIH2 in cells expressing a GluA1 construct which is covalently linked to four Gamma 8 molecules does cause further slowing of deactivation, strongly suggesting the presence of two non overlapping binding sites for these two proteins (Herring et al. 2013). Two auxiliary proteins are of special interest in this study given their high and selective abundance in the hippocampus: Gamma 8 and CNIH2. Their main properties are summarized here after.

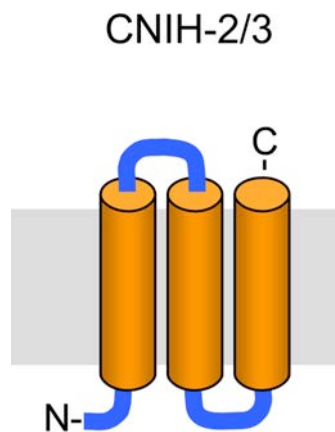
TARP Gamma 8

This auxiliary protein is selectively enriched in the hippocampus. It is involved in AMPA receptor surface targeting as CA1 pyramidal neurons of Gamma 8 knock-out mice exhibit an almost complete loss of extrasynaptic AMPA receptor currents. Synaptic AMPA receptor levels are only slightly affected (35 %) indicating a stronger role in surface targeting rather than synaptic retention of Gamma 8 (Rouach et al. 2005). The enrichment of Gamma 8 in synaptic fractions also points towards its synaptic function. Its implication in synaptic plasticity is shown by an impaired LTP in knock out mice; LTD however is not significantly affected (Rouach et al. 2005).

CNIH2/3

Aside from the structurally similar TARPs, other candidate auxiliary proteins have been identified in coprecipitation mass spectrometry experiments. One example found in the hippocampus are the two transmembrane proteins cornichon homolog 2 and 3 (CNIH2, CNIH3, see infobox), both stably binding AMPA receptors (Schwenk et al. 2009). Despite their very different amino acid sequence and topology compared to TARPs they exert surprisingly similar effects on AMPA receptor trafficking and channel properties.

CNIHs cycle between ER and Golgi apparatus to promote AMPA receptor export



Infobox 4: CNIH2 and 3

Cornichon homologs 2 and 3 span three transmembrane domains, with an intracellular N-terminus and a very short extracellular C-terminus. The entire protein is just 160 amino acids long (18 kDa). CNIH2 is the most abundant auxiliary protein in the brain and hippocampus (modified from (Jackson & Nicoll 2011b)).

from the ER (Schwenk et al. 2014; Harmel et al. 2012). They thereby promote forward trafficking to the plasma membrane and enhance AMPA receptor surface expression (Boudkkazi et al. 2014). CNIHs slow down the deactivation and desensitization kinetics of agonist-evoked currents to an even greater extent than stargazin (Schwenk et al. 2009; Tigaret & Choquet 2009; Jackson & Nicoll 2009; Brockie & V Maricq 2010). There is disagreement about the subcellular localization of CNIH. Shi et al reports no detectable surface CNIH in hippocampal neurons (Shi et al. 2010) whereas the impact of CNIH on AMPA receptor currents indicates the opposite.

Taken together, auxiliary proteins have a high impact on AMPA receptor forward trafficking and channel properties. They hence represent another layer of regulation of synaptic strength. How AMPA receptor complex composition is regulated and how the choice of various auxiliary proteins is made is not well understood.

In order to understand how AMPA receptor complexes can be recruited, stabilized and removed from synapses in an input-specific manner it is hence imperative to understand how their composition of GluA and auxiliary subunits is regulated. As part of the membrane protein family, AMPA receptors are synthesized and distributed via the secretory pathway.

4.4 Secretory pathway of membrane proteins

Membrane proteins, as opposed to cytosolic proteins, traffic through the secretory pathway. Membrane containing vesicles are actively transported along the cytoskeleton as they progress through the different secretory compartments. One posttranslational modification of membrane proteins is glycosylation.

The site of synthesis and site of action differs for most proteins. Proper protein distribution after synthesis is key to proper cell function. Membrane and secreted proteins, as opposed to soluble proteins, are not synthesized in the cytosol but in compartments of the secretory pathway (Fig 6).

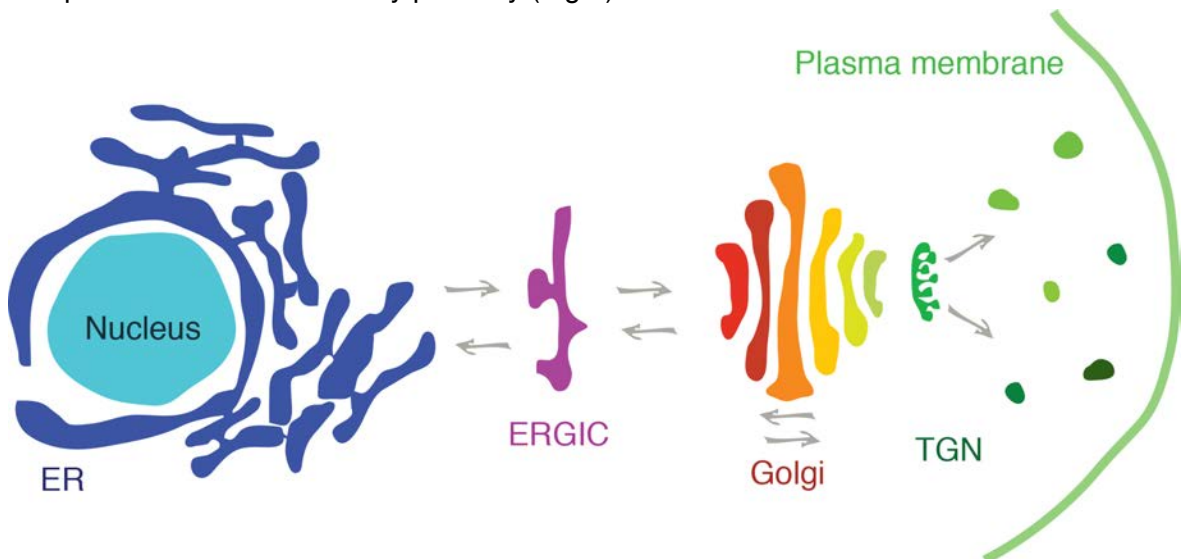


Figure 6: Secretory pathway

Membrane proteins are synthesized in the endoplasmic reticulum (ER), get transported and translationally modified in the ER to Golgi compartment (ERGIC) and the Golgi apparatus and finally sorted and targeted to the plasma membrane via the trans-golgi-network (TGN).

Nascent peptides are translated into the endoplasmic reticulum (ER) lumen by ribosomes located on the rough ER. From here they progress sequentially through the secretory pathway of post ER stations. They leave the ER from ER-exit sites (Cui-Wang et al. 2012), progress through the ER to Golgi intermediate compartment (ERGIC), reach the Golgi as they are sequentially post translationally modified and sorted in the trans-golgi-network (TGN) to reach their final destination e.g. the plasma membrane. Here vesicles fuse mediated by fusion and fission proteins and incorporate their cargo into the membrane.

In order to reach the membrane, proteins must have a proper posttranslational modification status. One very common posttranslational modification is glycosylation, most membrane and extracellular proteins are glycosylated

(Moremen et al. 2012). Defects in the glycosylation machinery lead to severe diseases (Cylwik et al. 2013) and aberrant glycosylation profiles are used as cancer markers. Glycosylation of proteins is achieved sequentially through the secretory pathway starting in the ER and finalized in the Golgi apparatus. The glycosylation status of a protein highly influences its properties like conductivity and stability (Moremen et al. 2012; Scott & Panin 2014; Hanus et al. 2016) and is hence an important additional regulator of synaptic strength.

The progression of membrane protein containing vesicles through the secretory pathway is achieved via active transport using motor proteins. This transport along with components of the cytoskeleton (actin filaments, microtubuli) is accomplished by binding directly or via adaptors to motorproteins (myosins, kinesins and dyneins respectively (Hirokawa et al. 2010; Govindarajan et al. 2011). The regulation of binding and unbinding from these linker proteins is mediated by phosphorylation (Kennedy & Ehlers 2011; Südhof & Rothman 2009). The tunable interactions between these various components are specific and allow tailor made cytoskeletal transport of proteins. Receptor-containing vesicles associate with and dissociate from cytoskeletal proteins depending on their phosphorylation status in a calcium-dependent manner (Wang & Ehlers 2008; Setou et al. 2000; Guillaud et al. 2008). The above mentioned kinase CamK2 α serves as one of the links between receptor trafficking and activity as it is able to phosphorylate the adaptor complex in an input specific manner. It is additionally found to influence post-ER vesicle trafficking as long range traveling vesicles are immobilized and exocytosed under regimes of high neuronal activity and highly mobile with reduced activity respectively in a CamK2 α dependent manner (Hanus et al. 2014).

In summary, regulated active transport of vesicles has a huge impact on protein concentration throughout the cell. The secretory pathway plays hence an important role in AMPA receptor complex composition and distribution.

4.5 Aims of this study

Key players of synaptic function which are known to change rapidly during synaptic plasticity are favorable candidates for local protein synthesis. Local protein synthesis in dendrites is one underlying molecular mechanism for memory and learning. The identity of which proteins are required to be locally produced however remains to be defined. We need a molecular tool to look at specific endogenous newly synthesized proteins *in situ*. The development of this tool will be described in the first part of this study.

AMPA receptor subunits are the key players of fast synaptic transmission and their surface and synaptic abundance is highly regulated during synaptic plasticity. How are synthesis, assembly and secretory processing orchestrated? Using the newly developed technique we aim to investigate the site of synthesis and redistribution dynamics of pore-forming and non-pore-forming AMPA receptor subunits.

5. Material and methods

5.1 Material

5.1.1 Antibody list

Antibodies were used in the following dilutions: ms-anti-biotin (Sigma, B7653, 1:1000), rb-anti-biotin monoclonal (Cell Signaling, 5597, 1:5,000), rb-Bassoon-N-term (sap7f, 1:2000 for Puro-PLA), rb-Bassoon-C-term (Synaptic Systems, 141002, 1:2500 for Puro-PLA), ms-anti-Bassoon mab7f (Enzo, VAM-PS003, 1:1000 for FUNCAT-PLA), rb-anti- CamK2 α (Millipore, 04-1079, 1:1000), ms-anti- CamK2 α (Thermo Scientific, MA1-048, 1:2000), rb-anti-CNIH2 (C-term, Synaptic System), rb-anti-TARP Gamma 8 (custom made from Agrobio under supervision of Anne-Sophie Hafner, anti-1st extracellular loop + intracellular C-terminal domain) dilutions indicated in figure legends, rb-anti-GluA1 (Abcam, ab31232, 1:500-1:1000), rb-anti-GluA1 (custom Agrobio under the supervision of Dr. Anne-Sophie Hafner, N-terminal, 1:200 pulse-chase), ms-anti-GluA2 (gift from Vollum Institute, Gouaux lab, 1:1000), rb-anti-GluA2 (monoclonal Abcam 133477, aa 150-250), ms-anti-Puromycin (Kerafast, EQ0001, 1:2500–1:3500), rb-anti-TGN38 (Sigma, 1:1000), gp-anti-MAP2 (Synaptic Systems, 188004, 1:2000). Secondary antibodies used as PLA probes were developed in donkey and coupled to Duolink PLA^{plus} and PLA^{minus} oligos (Sigma; 1:10), fluorescent secondary antibodies all from Life Technologies and used 1:1000: anti-rabbit-488, anti-rabbit-594, anti-mouse-405 dylight, anti-mouse-488, anti-mouse-594, anti-guinea pig-405 dylight, anti-guinea pig-488, anti-guinea pig-594.

5.1.2 Reagents and cells

AHA	Inhouse production by Erwin Noll and Dr. Susanne tom Dieck, 4 mM in methionine free Neurobasal-A + GlutaMax + B27
Anisomycin	Tocris, stock 100 mM in DMSO, 40 μ M final
Aqua Polymount	Polysciences
B27 50 x	Gibco
Biotin-alkyne	Jena Bioscience, stock 50 mM in DMSO, 25 μ M final, acetylene-PEG4-Biotin
Blocking buffer	4 % goat serum (Sigma-Aldrich) in PBS pH 7.4
CaCl ₂	Roth
COS cells	Thermo scientific
CuSO ₄	Sigma, 200 mM in water, 200 μ M final
DAPI	Roth, stock 1 mg/ml in water, 1 μ g/ml final in PBS
DMSO	Sigma-Aldrich
FUNCAT-fix	4 % PFA in PBS-Sucrose
GlutaMax 100 x	Gibco
HEK cells	Thermo scientific
Immersion oil 40x	Zeiss 518 F
Methionine	Sigma

Magnesium chloride	Roth
Magnesium sulfate	Sigma Aldrich
MatTek dishes	VWR
Neurobasal-A	Gibco
Neurobasal-A wo Met	Gibco
Neurons, hippocampal	Inhouse preparation, see methods
Pipettes	Gilson and Eppendorf
PLA reaction mixes	Sigma Aldrich
PFA 16%	Alfa Aesar
Poly-D-Lysine	BD Biosciences
Puromycin dihydrochloride	Sigma, stock 90 mM in water
Sucrose	Sigma-Aldrich
Table centrifuge	Eppendorf
TBTA	Sigma, stock 200 mM in DMSO, 200 μ M final
TCEP	Thermo scientific, 500 μ M final
Triton	Sigma Aldrich
Vortexer	VWR
X-treme Gene Transfection	Sigma Aldrich

5.2 Methods

5.2.1 Hippocampal neurons

Dissociated rat hippocampal neuron cultures were prepared and maintained essentially as described previously (Aakalu et al. 2001; Banker & Goslin 1991). Briefly, we dissected hippocampi from postnatal day 0-1 rat pups of either sex (Sprague-Dawley strain; Charles River Laboratories), dissociated them with papain (Sigma) and plated them at a density of $30 - 40 \times 10^3$ cells/cm² onto poly-d-lysine-coated glass-bottom Petri dishes (MatTek). Hippocampal neurons were maintained, fed weekly with neuronal growth medium and allowed to mature in a humidified atmosphere at 37 °C and 5% CO₂ in growth medium (Neurobasal-A supplemented with B27 and GlutaMax) for >18 days *in vitro* to ensure synapse maturation. All experiments complied with national animal care guidelines and the guidelines issued by the Max Planck Society and were approved by local authorities. Neuronal preparation was executed by the lab technicians Ina Bartnik, Nicole Fürst, Anja Staab, Christina Thum and Dirk Vogel on a weekly basis (adapted from tom Dieck et al. 2015).

COS7 cells (Fig 8) and HEK cells (Fig 30) were grown and maintained in DMEM with 5% GlutaMax, 1% Pyruvate and 10% fetal calf serum in a humidified atmosphere at 37 °C and 5% CO₂.

5.2.2 Metabolic labeling with AHA and biotin-alkyne click (FUNCAT)

The FUNCAT part of the assay was performed as described previously (tom Dieck et al. 2012) with the following modification: we used a biotin-alkyne as a tag in the copper-catalyzed [3+2] azide-alkyne cycloaddition (CuAAC) click reaction. Cells on MatTek dishes were incubated in methionine-free Neurobasal-A supplemented with

4 mM AHA (prepared as described in Link et al. 2007) in house by Erwin Noll and Dr. Susanne tom Dieck) for indicated times. In methionine control experiments, AHA was replaced by 4 mM methionine. In protein synthesis inhibitor control experiments, cells were preincubated for 15 - 30 min with 40 μ M anisomycin in their full conditioned medium; the same concentration of anisomycin was present during AHA incubation. For experiments with neurons, the B27 supplement and GlutaMax was present in all incubation media. Different chase periods (AHA free incubations) up to 24 h were used when indicated. Subsequently, cells were washed quickly two times with PBS-MC (1 \times PBS, pH 7.4, 1 mM MgCl₂, 0.1 mM CaCl₂) and fixed for 15 min in PFA-sucrose (4% paraformaldehyde, 4% sucrose in PBS-MC) at room temperature, washed, permeabilized with 0.5% Triton X-100 in 1 \times PBS, pH 7.4, for 10 - 15 min and blocked with blocking buffer (4% goat serum in 1 \times PBS) for 1 h up to 3 h at room temperature. To optimize conditions for the CuAAC click reaction, we equilibrated cells by washes with 1 \times PBS, pH 7.8. For the CuAAC click reaction, to avoid copper bromide derived precipitates, we used the reducing agent Tris(2-carboxyethyl)phosphine (TCEP) in combination with CuSO₄ to generate the Cu(I) catalyst for CuAAC. A click reaction mix composed of 200 μ M triazole ligand TBTA (Tris (1-benzyl-1H-1,2,3-triazol-4-yl)methyl)amine), 25 μ M biotin alkyne tag, 500 μ M TCEP and 200 μ M CuSO₄ was mixed in PBS, pH 7.8, with vigorous vortexing after each addition of a reagent from stock solutions. The click reaction mixture was prepared immediately before application to the cells, and CuAAC was performed light protected overnight at room temperature. After the click reaction, cells were washed intensely with 1 \times PBS, pH 7.4 and 0.5% Triton X-100 in PBS for 15 min and either processed directly for immunocytochemical detection of biotin (equivalent to regular FUNCAT) and cell markers or processed for PLA detection (adapted from tom Dieck et al. 2015).

5.2.3 Surface labeling of GluA1 and GluA2

For live labeling of the surface fractions of GluA1- and GluA2-containing receptors neurons were incubated in their own growth medium with HEPES (10 μ M) and antibodies targeting the N-terminal extracellular domains of the subunits GluA1 or GluA2, at the dilution 1:200 and 1:500 respectively for 8 min at room temperature. Following two brief washes with PBS-MC, cells were fixed, permeabilized and blocked as for regular immunocytochemistry.

5.2.4 Surface labeling of TARP Gamma 8

HEK cells were transfected with a Gamma-8-GFP construct (transfection with XtremeGENE HP DNA Transfection Reagent from Sigma Aldrich according to the manufacture's recommendations). After overnight expression anti-Gamma-8 antibody was applied for 20 min at a 1:500 dilution at 37 °C in a humidified atmosphere on living cells. Two brief washes with PBS were followed and cells subsequently fixed. For total staining cells were first fixed, permeabilized and blocked and the antibody applied for 1.5 hours at the same concentration.

5.2.5 Puromycylation

Neurons were incubated with (or, in “no puro” controls, without) 1-5 μ M puromycin (as indicated) for 2-15 min (as indicated) in full medium at 37 °C in a humidified atmosphere with 5% CO₂. Puromycylation was stopped by two fast washes in PBS-MC at room temperature, and cells were fixed for 15 min in PFA-sucrose. In protein synthesis inhibitor control experiments, cells were pretreated with 40 μ M anisomycin for 15-30 min before addition of puromycin to the medium (adapted from tom Dieck et al. 2015). After fixation, cells were washed, permeabilized and treated as described in the sections “Proximity ligation assay (PLA)” (using puromycin antibody and protein of interest antibody as primary antibody pair for 1.5-2 h) and “Immunocytochemistry.”

5.2.6 Proximity ligation assay (PLA)

"Detection of newly synthesized proteins by proximity ligation was carried out using anti-biotin antibody or anti-puromycin antibody in combination with protein-specific antibodies and detection using Duolink reagents according to the manufacturer's recommendations with slight modifications. We routinely used rabbit (rb) PLA^{plus} and mouse (ms) PLA^{minus} probes as secondary antibodies and the “Duolink Detection reagents Red” for ligation, amplification and label probe binding. Briefly, after metabolic labeling, permeabilization and washing (see sections “Metabolic labeling with AHA and biotin-alkyne click (FUNCAT)” and “Puromycylation”), cells were blocked in blocking buffer (4% goat serum in PBS, 1 h up to overnight) and incubated with primary antibodies including anti-MAP2 (microtubule associated protein-2) guinea pig diluted in blocking buffer (1.5 h at room temperature). After washing with PBS, PLA probes were applied in 1:10 dilution in blocking buffer including anti-guinea pig-488 1:500 for 1 h at 37 °C in a humidified chamber, washed four times with wash buffer A (0.01 M Tris, 0.15 M NaCl, 0.05% Tween 20) and incubated for 30 min with the ligation reaction containing the circularization oligos and T4 ligase prepared according to the manufacturer's recommendations in a prewarmed humidified chamber at 37 °C. Amplification and label probe binding was performed after further washes with wash buffer A with the amplification reaction mixture containing Phi29 polymerase and the fluorophore-labeled detection oligo prepared according to the manufacturer's recommendations in a pre-warmed humidified chamber at 37 °C for 100 min. Amplification was stopped by three washes in wash buffer B (0.2 M Tris, 0.1 M NaCl, pH 7.5). If needed DAPI was applied in PBS 1:1000 for 2 min for nuclear staining and washed with wash buffer B. Cells were imaged immediately in wash buffer B."

5.2.7 Immunocytochemistry

After fixation and permeabilization (only immunocytochemistry) or the click reaction step (FUNCAT), cells were blocked in blocking buffer for 1 h, which was followed by incubation with the respective antibodies for 1.5 h, washes in PBS and incubation with fluorophore-coupled secondary antibodies for 45 min. Cells were washed, counterstained with DAPI in PBS for 2 min if required and mounted with AquaPolymount or imaged directly in PBS. Samples were imaged soon after the experiment and stored at 4°C.

5.2.8 Confocal imaging

Images were acquired with an LSM780 or an LSM880 confocal microscope (Zeiss) using a 40x/1.4-NA oil objective (Plan Apochromat 40x/1.4 oil DIC M27) and a pinhole setting of 90 μm . All lasers were used at 2 % power. Images were acquired in 8-bit or 16-bit mode as z stacks with 1024 \times 1024 pixel (or 2048 \times 2048 for better visualization) xy resolution through the entire thickness of the cell, pixel dwell times of 0.39 - 0.79 μs and the detector gain in each channel adjusted to cover the full dynamic range but to avoid saturated pixels. Imaging conditions were held constant within an experiment. Imaged neurons were chosen using the MAP2 channel (e.g. absence of microtubule fragmentation and when applicable homogeneous nuclear DAPI staining). For experiments with dendritic analysis, only cells with clearly distinguishable dendritic trees were imaged. However it was avoided to image completely isolated cells to ensure synaptic contacts to other neurons (adapted from tom Dieck et al. 2015).

5.2.9 Image representation in figures

Contrast and brightness parameters were adjusted for optimal visualization. Images from single experiments and single figures were scaled similarly. For representations with soma and dendrites separately (e.g. Fig 28 and 29), somata were cropped and dendrites digitally straightened using the ImageJ plugin Straighten (-> edit -> selection -> straighten). In Fig 7, 9, 20 to 22, 30 and 31 one color channel was separated and converted to grey scale image. In Fig 31 the Gamma 8 antibody channel was converted into a fire lookup table for better visualization of differences in signal intensity.

5.2.10 Data analysis

Puromycylation in COS7 cells (Fig 8): Analysis of puromycin signal was done manually in ImageJ by defining ROIs surrounding single cells by hand and plotting the average signal intensity. The DAPI signal was used to define cell location. Cell areas were not significantly different between different labeling conditions.

Puromycylation in neurons (Fig 9): Neuronal somata were outlined by hand and the average intensity measured with ImageJ. Neuronal somata sizes did not differ significantly between labeling conditions.

Gamma 8 antibody labeling (Fig 31): Analysis was done in ImageJ by manually defining ROIs. Mean intensities in somata and straightened dendrites were measured and plotted.

5.2.11 Data representation and statistics

Normality of data distribution was tested using D'Agostino & Pearson omnibus test. If the data followed a normal distribution results were plotted as mean \pm SEM and unpaired t-test for two conditions or one-way ANOVA for more than two conditions was used to test for significant differences. Non-normally distributed data were represented as boxplot with median \pm quartiles and minimum maximum values. Mann-Whitney non-parametric test was used for two data groups, Kruskal-Wallis and Dunn's multiple comparison were used for more than two groups to test for significant differences. Data normalization: If not stated otherwise experiments with

multiple biological replicates were normalized to the mean of their control groups and pooled together.

5.2.12 Puncta analysis ImageJ and Neurobits

For half-automated puncta analysis in cells custom built scripts were developed in cooperation with Maximilian Heumüller and Dr. Georgi Tushev (head of the scientific computing facility of MPI-BR). Both are extensively described in the results section (Fig 15-17). In brief, puncta were either detected by a fixed intensity threshold or by local intensity maxima and only puncta overlapping with the cell of interest were measured. Puncta number per cell of interest, integrated puncta intensity or puncta area were normalized to cell area. When plotting percent of puncta in dendrites, cell areas were checked beforehand in order to rule out that observed differences are due to different cell sizes. If data is shown as such, cell areas were not significantly different from one another.

5.2.13 GluA1 FUNCAT-PLA puncta intensity measurements (Fig 27)

Puncta intensities were measured using the Neurobits script. Values of local maxima within puncta were compared among different chase time points.

5.2.14 Data point exclusion

Four values were excluded in Fig 29 (pulse-chase for GluA2) because they deviated more than 2 SDs from the mean (1 data point in dendrite data set, 1 in soma data set).

5.2.15 Cumulative distribution of newly synthesized GluA1 and GluA2

A backwards cumulative distribution was computed for each neuron for the two AMPA receptor subunits with a bin size of 5 μm of dendritic length. All puncta in one cell were set as 100 %. No significant difference in total cell size was observed between GluA1 and GluA2 images. Normalization to neuronal area was hence not required. Cumulative puncta distribution starting from the most distal puncta back to the soma was performed using Prism6 (GraphPad Software Inc.). Somatic puncta were given the distance value zero.

Since the current version of the MATLAB macro Neurobits gives puncta distances from a geometric soma center and not from the soma border (which would be more suited here), soma diameter needed to be subtracted from all distance values for each cell. Since the closest dendritic puncta to the soma did not vary between GluA1 and GluA2, distance values from the closest dendritic puncta were subtracted from all dendritic values on a cell by cell basis. Three independent experiments were processed separately and cumulative probabilities were averaged. Half-lives of a one phase decay was calculated for each cell individually and medians were compared using Mann-Whitney test using Prism6 (Fig 19 e inset).

6. Results

In the following we describe the development of a new technique to visualize specific endogenous newly synthesized proteins of interest. In this study we successfully developed two different methods each of which has its own advantages and disadvantages that will be discussed.

As elaborated in the introduction, investigating protein synthesis in neurons is key to understand the underlying mechanisms of learning and memory. Prior to this work, the available tools could either investigate global protein synthesis without knowledge of protein identity or identify single newly synthesized proteins with no information about their subcellular localization. Knowledge about protein identity and location, however, is crucial to understand how local protein synthesis can shape and influence synaptic plasticity.

6.1 Labeling translation using AHA and puromycin

6.1.1 Labeling translation using AHA

The use of non-canonical amino acid tagging is a well established method for labeling newly synthesized proteins. For example, newly synthesized proteins can be metabolically labeled with the methionine analog azidohomoalanine (AHA). "In FUNCAT (fluorescence non-canonical amino acid tagging), azidohomoalanine (AHA) is taken up by cells and loaded onto methionine tRNAs. During translation, AHA is incorporated into newly synthesized proteins. A biotin-based tag is then added by click chemistry, and the newly synthesized protein is visualized using an anti-biotin antibody." (Quote here and all further quotes from tom Dieck et al., 2015).

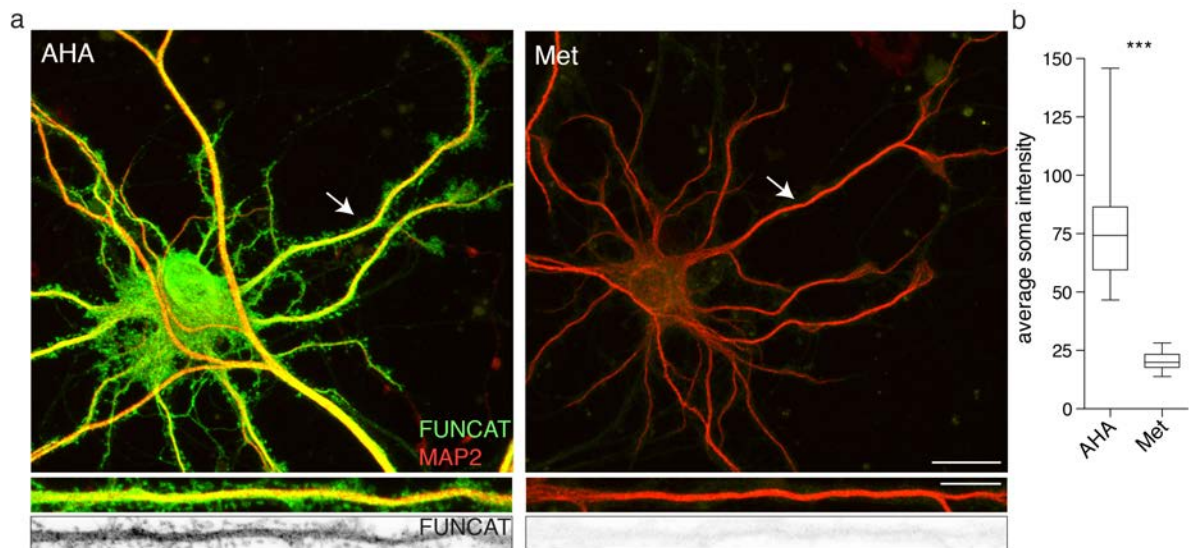


Figure 7: AHA labeling of newly synthesized proteins in cultured hippocampal neurons

a) FUNCAT signal (green) is visible both in soma and dendrites (arrow and bottom panel) of a representative cultured hippocampal neuron (DIV 25) after 1 h of AHA labeling. Note the visible signal even in synapses. MAP2 protein (red) marks the cell outline. Straightened dendrites at the bottom are marked by the arrow. Adding methionine to the labeling medium instead of AHA leads to negligible FUNCAT signal in the entire cell, scale bar = 20 and 10 μm respectively. b) Analysis with median \pm quartiles and min max values of soma intensities in AHA and methionine (Met) treated cells from one representative experiment with $n = 12\text{-}32$ cells, $***p < 0.0001$, Mann-Whitney test.

In Fig 7 a representative FUNCAT experiment is shown in which the pool of newly synthesized proteins of a neuron was labeled and visualized using a 1 h labeling period with AHA in cultured hippocampal neurons (DIV 25) at 37 degrees. AHA was bath applied in a 4 mM concentration in methionine-free culture medium. Notably, we could detect newly synthesized proteins in somata and dendrites as well as in dendritic spines (Fig 7 a). Adding methionine (Met) instead of AHA as a negative control led to negligible FUNCAT signal in both somata and dendrites (Fig 7 b, c, three fold difference).

Given the relatively long 1 h AHA labeling period, the position of the fluorescent signal within the neuron does not allow one to discern the exact site of synthesis, since proteins can exhibit diffusion and transport and hence redistribute within the cell. As a minimum labeling period of several tens of minutes is required using AHA, this method might not be best suited for a real snapshot of site of synthesis. Another labeling approach must be used where very short labeling times are sufficient to obtain significant labeling of newly synthesized proteins.

6.1.2 Labeling translation using puromycin

Puromycin is a translational inhibitor that resembles the 3' end of an aminoacyl-tRNA (Pestka 1971) and is typically used as such. "Puromycin incorporation into the nascent protein terminates translation and releases the truncated protein, which is then recognized by an anti-puromycin antibody". This enables us to detect newly synthesized proteins with puromycylation (Schmidt et al. 2009). First and foremost

we had to determine the concentrations and labeling times that are suitable for such assays in our test system - cultured hippocampal neurons.

Different puromycin concentrations and incubation times were first tested in COS7 cells (Fig 8). Puromycin was added to cell's original medium and cells were incubated at 37 degrees with controlled CO₂ levels (5%) to maximize puromycin incorporation. As negative controls, puromycin was either omitted or added in the presence of anisomycin, another translational inhibitor. Anisomycin at the used concentration stalls the ribosomes completely and interacts at a site competing with puromycin. Background signal detected in the puromycin+anisomycin condition would indicate potential translation-independent labeling. After puromycin incorporation cells were washed briefly to clear free puromycin in cells, fixed and processed for immunostaining against puromycin. DAPI staining was used to label all cell nuclei for knowledge of cell localization. After 5 min of labeling at 1 μ m concentration we could already observe a significant staining (Fig 8 b) compared to the anisomycin pretreatment and the puromycin leave-out control conditions. Increasing labeling times to 15 min at 5 μ m did not further increase puromycin labeling as compared to 5 min but increased background staining. The signal to noise ratio was around 3-fold for 5 and 10 min labeling and decreased to 1.5 fold in the 15 min labeling condition.

A low concentration of 1 μ m was hence sufficient for visualizing newly synthesized proteins in COS7 cells. Are these labeling times and concentrations also sufficient to label protein synthesis in cultured hippocampal neurons?

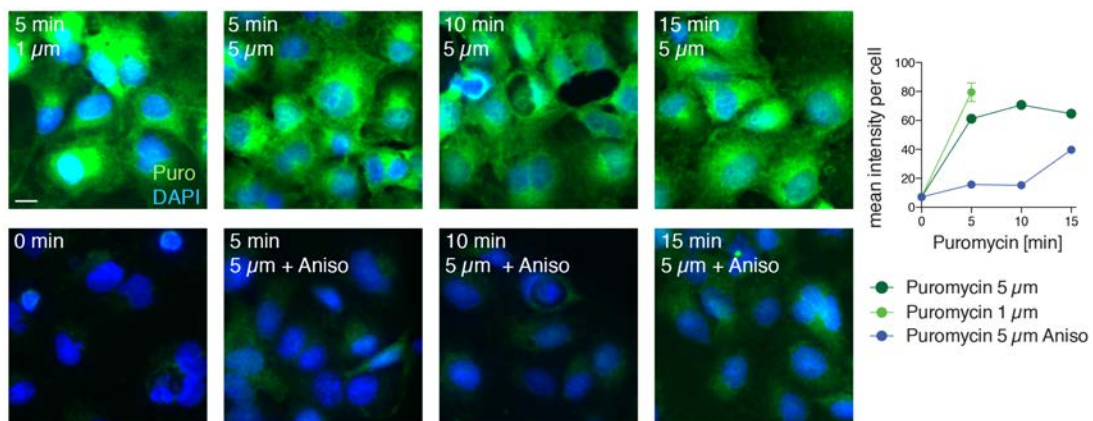


Figure 8: Puromycylation in COS7 cells

Different puromycin concentrations and labeling durations were tested on COS7 cells. Puromycin signal visualized with the anti-puromycin antibody (green), nuclei with DAPI (blue). As a negative control the translation inhibitor anisomycin was present 30 min prior and during puromycin labeling (bottom row). Analysis showing mean \pm SEM of puromycin intensities of n = 32-58 cells from one representative experiment, scale bar = 20 μ m.

We conducted experiments labeling hippocampal neurons with puromycin in their own medium. Testing different puromycin labeling times with 5 μ M puromycin in neuronal somata and dendrites (Fig 9 a) revealed that five minutes was sufficient for significant labeling with a signal to noise ratio of greater than 3. Increasing

puromycin concentrations to 15 μM did not further increase the signal (data not shown), consistent with what was observed previously in COS7 cells (Fig 8).

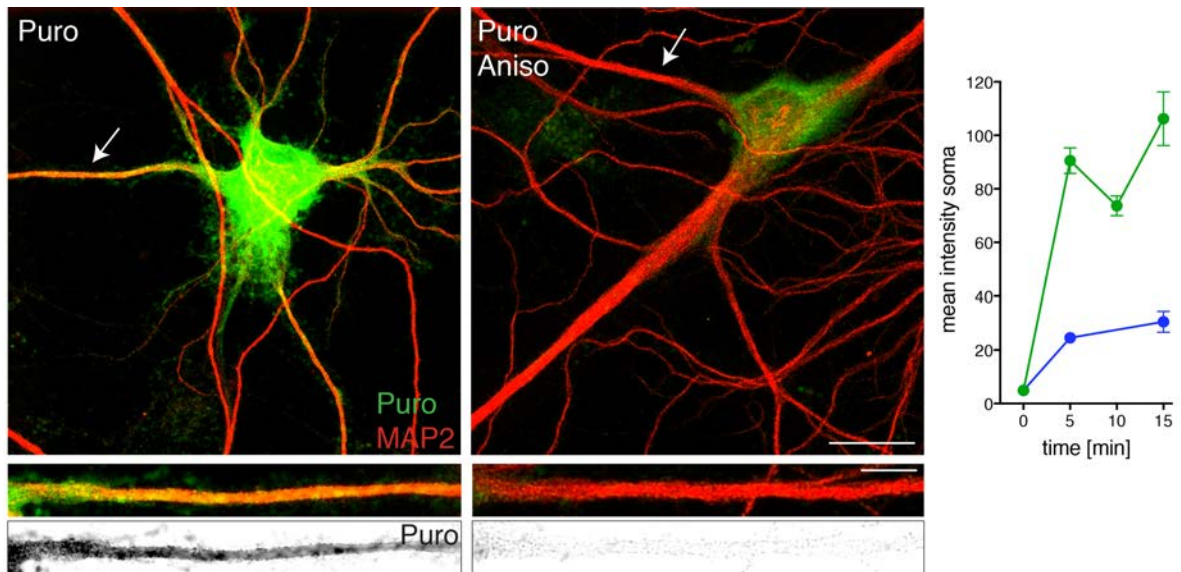


Figure 9: Puromycin labeling in cultured hippocampal neurons

Representative images of hippocampal neurons (DIV 20) labeled with 5 μM puromycin for 5 min. Puromycylated proteins (green) overlap with cell outline (MAP2, red). As a negative control anisomycin was present 30 min prior and during puromycin labeling. Arrows indicate the straightened dendrites in the lower panel (coloured and greyscale image of puromycin signal only). A faint background signal is detected in the soma and negligible staining is observed in dendrites, scale bar = 20 and 10 μm respectively. Analysis of mean puromycin intensity in neuronal somata, mean \pm SEM, n = 10-27 from one experiment.

Puromycin can be successfully used to label protein synthesis in hippocampal neurons. Labeling times on the order of few minutes are sufficient to label newly synthesized proteins indicating promise for obtaining snapshots of protein synthesis. Since the labeling period can be kept very short, proteins do not have much time to redistribute after labeling. With such a tool in hand we can answer questions like the following: how much protein synthesis occurs locally in dendrites compared to neuronal somata? How are the synthesis rates changed with synaptic activity - under paradigms of learning and memory?

Summary of labeling methods

Two different approaches are available in the lab to visualize the pool of newly synthesized proteins in neurons. They allow to investigate the difference in general protein production levels between cells, cell types and neurons in different regimes of activity. The identity of these labeled newly synthesized proteins remains however completely unknown.

Complementary approaches such as mass spectrometry on samples with labeled newly synthesized proteins are not fully satisfactory. Indeed while the identity of newly synthesized proteins can be determined, their subcellular origin are entirely lost. We hence developed a technique to visualize specific newly synthesized proteins of interest in cells to preserve and study their subcellular distribution.

6.2 Proximity ligation assay (PLA)

"Advancements in transcriptomics and proteomics have arguably delivered both what can potentially be translated (the transcriptome) and the tissue-wide population of proteins that are in fact translated in a certain time window (the proteome). What is clearly missing, however, is the subcellular resolution of the site of synthesis and the ensuing spatial redistribution of newly synthesized proteins. To accomplish this, we developed a proximity ligation assay (PLA) - based strategy that detects the spatial coincidence of two antibodies: one that identifies a newly synthesized protein tagged with either FUNCAT or puromylation and another that identifies a specific epitope in a protein of interest (POI) (Fig 10). Next, respective secondary antibodies coupled to different oligonucleotides (PLA^{plus} and PLA^{minus} probes) are introduced; when the two probes are in proximity, linker oligonucleotides and a ligase promote formation of a 'circle' subsequently amplifiable by rolling-circle amplification. Ultimately, the coincidence detection ('new' and 'POI') is visualized *in situ* by fluorescently labeled probes complementary to the amplified sequences, as shown for newly synthesized CamK2 α in neurons (Fig 11). We extensively tested and optimized the dependence of FUNCAT-PLA and puromylation-PLA (Puro-PLA) on the presence of the antibodies, AHA or puromycin, intact protein synthesis (Fig 11 for AHA and Fig 12 for Puro) and of the POI (data not shown, see Supp Fig 3 in tom Dieck et al. 2015).

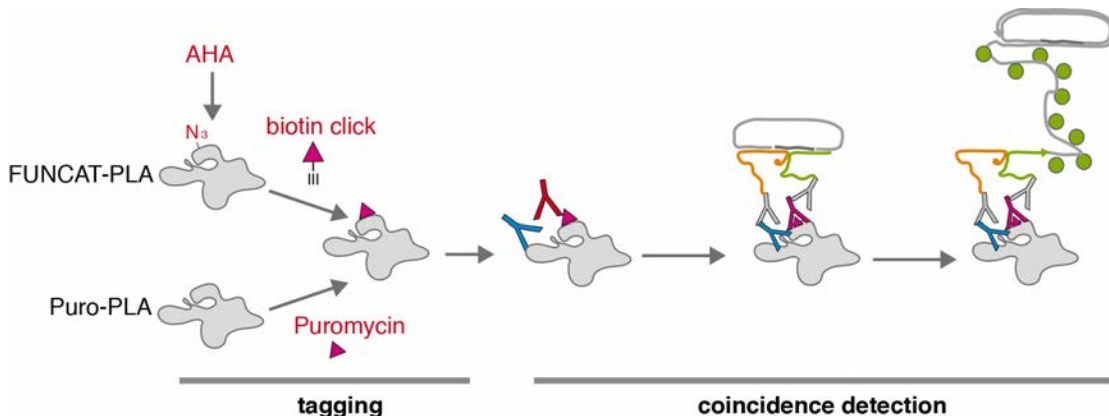


Figure 10: Working principle of FUNCAT- and Puro-PLA

Newly synthesized proteins incorporate either AHA or puromycin. AHA is biotinylated by click chemistry. Antibody (magenta Y) recognition of the 'newly synthesized' tag (biotin or puromycin, magenta triangle) and recognition of a POI by a protein-specific antibody (blue Y) detects close proximity when PLA^{minus} and PLA^{plus} oligonucleotides (yellow and green squiggles) coupled to secondary antibodies (gray Y) are close enough to serve as a template arranging linker oligonucleotides such that subsequent formation of a circular product by a ligase and rolling-circle amplification is possible. Signal is obtained by binding of fluorescently coupled detection probes (green circles, from tom Dieck et al 2015).

Recently, deep sequencing and high-resolution *in situ* hybridization have led to the identification of an unexpectedly high number of mRNA species in mature neuronal processes. We used FUNCAT-PLA to investigate whether the distribution of candidate newly synthesized proteins is consistent with their local synthesis in dendrites or axons. Cultured rat hippocampal neurons were treated with AHA (2 h) to pulse-label a population of newly synthesized proteins and were then processed

as described above (Fig 11). The FUNCAT-PLA signal for the postsynaptic density protein CamK2 α was detected throughout dendrites, a result consistent with the abundance of CamK2 α mRNA in dendrites."

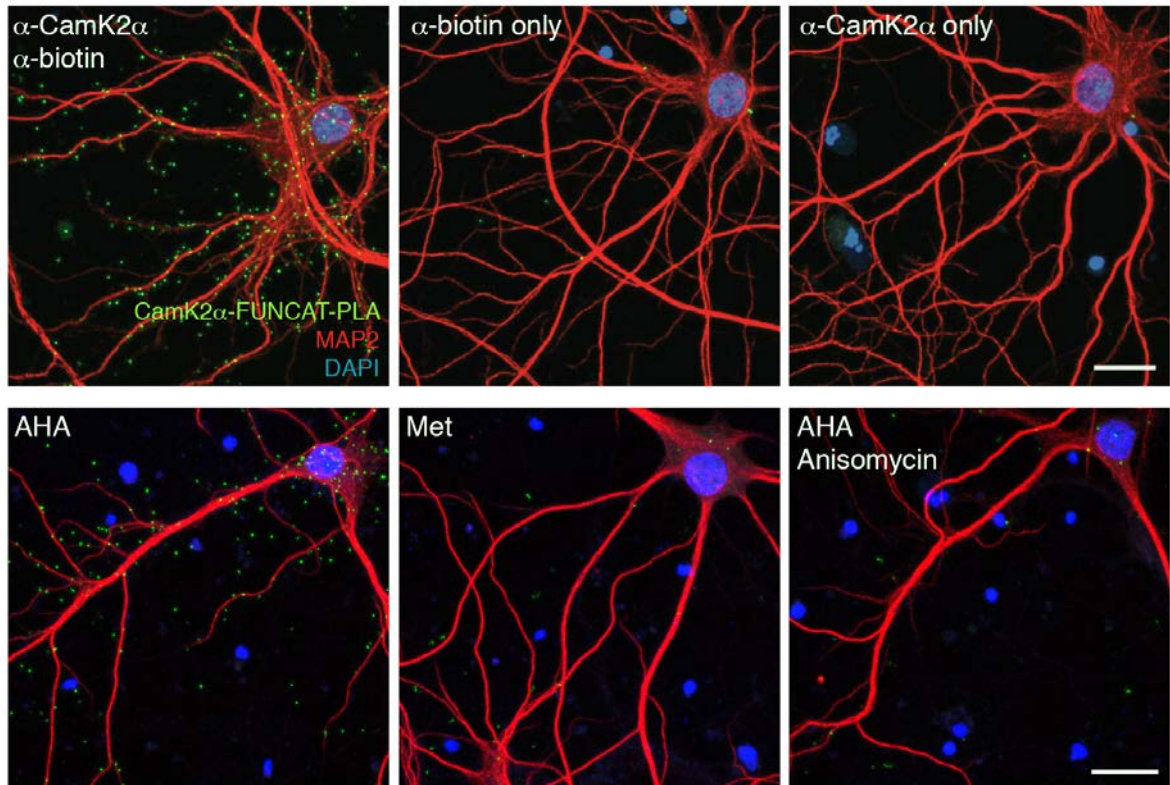


Figure 11: FUNCAT-PLA for newly synthesized CamK2 α and negative controls

"Images of FUNCAT-PLA signal (green) for newly synthesized CamK2 α (2 h AHA) in cultured hippocampal neurons and controls without either anti-CamK2 α antibody or anti-biotin antibody (top panel) or omitting AHA (Met) or with protein synthesis inhibitor anisomycin (bottom panel), scale bar = 10 μ m."

As AHA labeling times must be relatively long, a parallel approach to obtain signal close to the site of synthesis, as described above, is labeling with puromycin. Here we are now able to examine the same POI after a very short labeling pulse. If the protein of interest is synthesized exclusively in neuronal somata and then rapidly redistributed into dendrites we would expect a soma restricted PLA labeling when using short puromycin incubations. If this protein is however locally translated, dendritic signal should occur even after short labeling times. Dendritic Puro-PLA signal would be expected in the following experiment since CamK2 α is one of the most abundant mRNAs in dendrites.

"In puromycylation experiments, we treated rat hippocampal neurons with puromycin (5-15 min) and processed them to detect nascent CamK2 α (Fig 12). We observed that, consistent with the results obtained by FUNCAT-PLA, abundant newly synthesized CamK2 α signal was present in both soma and dendrites.

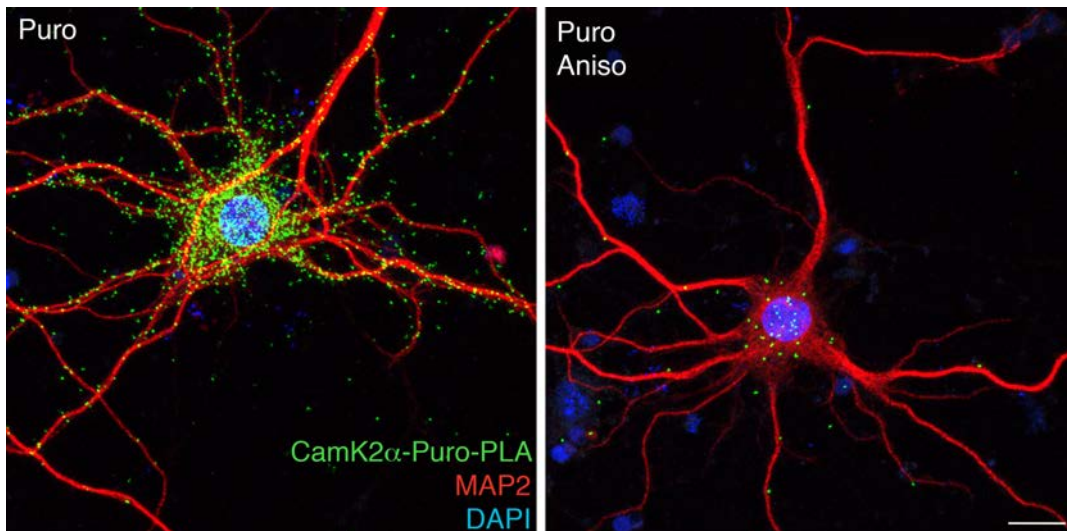


Figure 12: Puro-PLA for newly synthesized CamK2 α and negative control

"Puro-PLA images of newly synthesized CamK2 α (green) after 15 min of puromycin (Puro, 1 μ M) labeling without (left) or with (right) the protein synthesis inhibitor anisomycin (Aniso), scale bar = 10 μ m."

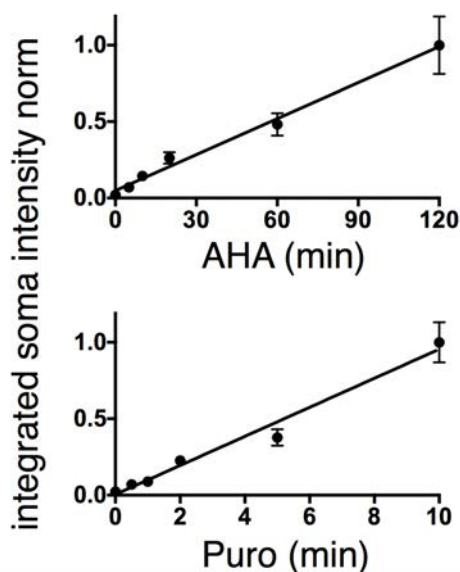


Figure 13: Linear relationship between labeling time and signal density

"Correlation of TGN38 FUNCAT-PLA and Puro-PLA signal (integrated PLA intensity in the soma, normalized) dependence on incubation time with AHA and Puro (1 μ M). $R^2 = 0.99$ and 0.98 from two and three independent experiments, $n = 20$ or 27 cells and $n = 15-20$ cells, AHA and Puro, respectively. Mean \pm SEM and the linear regression are shown."

Here both variants of metabolic labeling, FUNCAT-PLA and Puro-PLA, led to qualitatively similar results, with the major difference being the apparent extent of labeling (for example, number of particles). Whereas incubation times in the range of seconds to minutes were sufficient to obtain a Puro-PLA signal that was linear with time, a detectable FUNCAT-PLA signal required longer metabolic labeling times, but it was also linear over time (Fig 13)."

One big difference between the two labeling techniques is the absence of methionine in AHA labeling medium. Since methionine starvation is known to potentially cause cellular stress (Dikic 2017; Mazor et al. 2018) we assessed whether it has a strong influence on global protein synthesis (Fig 14). We performed a Puro-PLA experiment for TGN38 with and without a 30 min incubation in methionine-free Neurobasal-A medium prior to a 15 min puromycylation. No difference was detected in the Puro-PLA signal suggesting that the influence of methionine starvation is not substantial under these conditions.

Another good stress indicator in neurons is the fragmentation of the Golgi apparatus (Alvarez-Miranda et al. 2015). We assessed Golgi morphology after incubation with methionine free medium for 1 h (data not shown). Cells showed normal stacked Golgi morphology providing another indication of no or low cellular stress in methionine starvation conditions as used for our experiments.

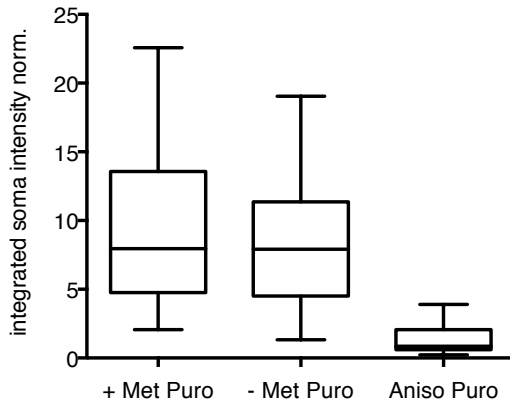


Figure 14: No obvious influence of methionine starvation on global protein synthesis

"Puro-PLA experiment for TGN38 in cultured hippocampal neurons (DIV 20) with (+Met) and without (-Met) incubation in methionine-free Neurobasal-A (30 min) prior to a 15 min puromycylation. Data is displayed as box plot with median \pm quartiles and min max values, $n = 42-43$ cells, two independent experiments."

"The two methods of metabolic labeling - AHA incorporation and puromycylation - have distinct advantages and disadvantages and, as such, provide different insights (Table 1). AHA uptake and activation by the methionyl tRNA synthetase is rate limiting for AHA incorporation and therefore requires relatively long pretreatment times (minutes to hours). In contrast, incorporation of puromycin as a tRNA analog is considerably faster (seconds to minutes). Furthermore AHA replaces only methionine residues, whereas puromycylation can occur at any residue. AHA labeling is more efficient with a prior methionine-starvation step and is ideally implemented in a

methionine-free medium that might be sensed as cellular stress signal (but see also Fig 14). Note, however, that an increase in overall toxicity was not observed in previous experiments. Thus, for experiments in which brief labeling is necessary, puromycylation is preferred. AHA incorporation is the method of choice for pulse-labeling a fraction of proteins to follow their fate over a longer timescale (hours to days) to examine protein distribution changes, turnover or half-life. There is no indication that AHA incorporation changes a protein's spatial fate. In contrast, puromycin incorporation results in premature truncation of polypeptide chains and enhanced degradation of truncated proteins. Thus, FUNCAT-PLA and Puro-PLA each has advantages and drawbacks. Both have the potential to answer a broad spectrum of questions related to protein synthesis rate and site and the spatial fate of endogenous newly synthesized proteins within cells."

Table 1: Properties and range of applications for Puro-PLA and FUNCAT-PLA

	Puro-PLA	FUNCAT-PLA
Incorporation	Fast	Slow
	No activation required	Uptake by amino acid transporter and activation by MetRS needed
	Competition with all activated tRNAs	Competition with methionine, labeling depending on number of methionine positions in protein of interest
	Labeling in full conditioned medium	Labeling in methionine-free medium
	No starvation necessary	Methionine starvation conditions promote labeling (either with pre-starvation or at least during incubation)
	C-terminal incorporation, possible at any site but limited to one puromycin per protein	Only replacement of methionine residues possible, more than one methionine replacement possible per protein
Protein	Full labeling (one puromycin per protein) would lead to protein synthesis block	Full labeling in theory possible
	Truncated, premature termination of labeled protein	Full length protein with small bio-orthogonal groups
	Enhanced degradation/ turnover of truncated proteins expected, non-physiological protein fate	Physiological fate
Method characteristics	Fast, sensitive	Lag phase, especially when used without methionine starvation, less sensitive than Puro-PLA
	Short labeling, unlikely to influence short term physiology	Labeling conditions might impact short term physiology
	Puro antibodies needed, N-terminal POI antibodies are predicted to work better than C-terminal	Biotin antibodies needed, Epitope for antibody against POI can be N- or C-terminal
	Direct detection with anti-puromycin antibody	Additional step required (biotin click)
	Estimating intra- vs intermolecular detection with N-/C-term antibody against POI possible	Modification by direct click of a PLA oligo possible
Recommended method use	Short term measurements Site of synthesis Synthesis rate at a time point	Long term measurements Turnover Half-life Distribution changes Synthesis in time interval

Each technique independently is a useful tool to estimate how the synthesis of a given protein varies between cell types, state of activity or cell compartments. Biological tool development must be accompanied by an appropriate analysis pipeline. We will now describe how we dealt with these new type of images.

All experiments described below deal with puncta distributions in neurons. Analyzing puncta abundance and properties manually is very labor intensive and time consuming and might not include all parameters which could be of interest. It was thus important to have an analysis pipeline to study many parameters in a reasonable timeframe with high accuracy and reproducibility. We will now describe two different analysis tools we developed to perform in depth analysis of puncta density, distribution and redistribution in neurons.

6.3 Development of puncta analysis tools

In many neuronal cell biology labs, images of various punctate signals in neurons need to be analyzed: e.g. mRNA, miRNA, Puro- and FUNCAT-PLA. A puncta analysis tool box is hence useful. In collaboration with Maximilian Heumüller (Schuman lab) and Dr. Georgi Tushev (head of scientific computing facility at the MPI-BR) we developed two different scripts for puncta analysis in neurons. Both scripts use MAP2 staining (or any other cell fill or cell marker) to obtain an outline of a neuron which is semiautomatically detected in single cells. The program then recognizes puncta automatically and exports the information in excel files for further analysis.

6.3.1 ImageJ macro for puncta detection

An ImageJ based macro was developed by Maximilian Heumüller to measure overall labeling in neurons with the distinction between somata and dendrites. For the above described experiments, this distinction is necessary to estimate the fraction of local synthesis in dendrites or somata for a given protein.

The general workflow is depicted in Fig 15. The MAP2 outline (1.) of neuron's dendrites and soma is transformed into a thresholded image by manually setting a threshold value on a cell-to-cell basis (2.). MAP2 signal from other cells or cell debris is manually cut out by the experimenter (3. and 4.). Since MAP2 labeling can be weak in neuronal somata compared to dendrites, we inserted an optional step of filling the soma manually (5.). Puncta detection is done based on a fixed intensity threshold which is initially defined by the experimenter by thoroughly testing multiple values on multiple images. That threshold value is kept constant throughout the entire experiment. MAP2 staining labels dendrites but not synapses. In order to analyze synaptically localized puncta in the vicinity of MAP2, the outline can be optionally dilated. Puncta that occur within the mask are analyzed (6.). The number of detected puncta, the sum of the PLA signal area or the integrated intensity of the PLA signal overlapping with the cell mask is divided by the non-dilated cell area and data is exported as a text file for further processing in Excel (8.). After the analysis is completed for one cell, the macro automatically opens the next image in the directory folder to decrease the analysis time per data set.

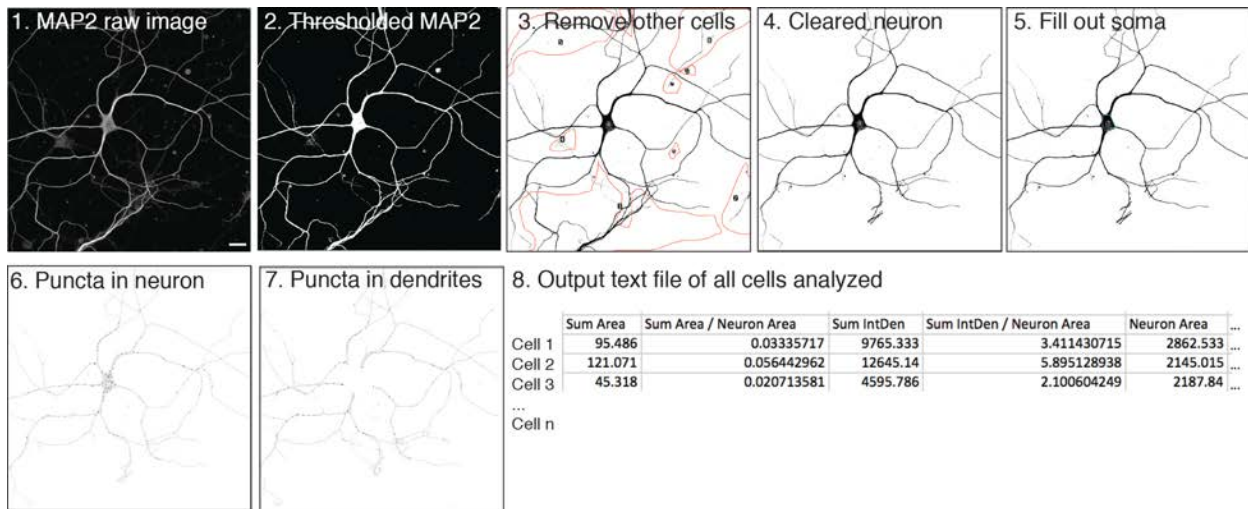


Figure 15: Workflow of puncta analysis with the custom written ImageJ script

1. Raw greyscale image of an example neuron stained with MAP2. 2. Thresholded signal for digitalized cell outline. 3. Manual removal (red outlines) of other cells and dendrites not belonging to the cell of interest. 4. Resulting cleared neuron. 5. Optional manual soma fill. 6. Thresholded puncta (black) which overlap with the cleared neuron (grey). 7. Dendritic puncta where soma was removed. 8. Example output text file, one row per cell. For more details see text.

To investigate puncta density differences between soma and dendrites an additional step can be added in the macro. The neuron's soma is removed manually and only puncta in dendrites are measured (7.). Somata information can be concluded by subtracting dendritic values from total values.

The script has its limitations. Depending on the investigated protein, somatic puncta density can be quite high. Puncta counts may not be accurate in these cells since puncta detection is done on the thresholded PLA image and overlapping puncta are counted as one. Using puncta area as a read out is better suited in these cases. The script is able to detect changes in total amounts of puncta in neurons due to different treatments and conditions as well as in dendrite-to-soma ratios.

Investigating local synthesis and exact puncta distribution in dendrites we needed a more detailed description of dendritic puncta. The analyses below were developed to answer the following questions: How far can puncta be found in dendrites? How does their density depend on somatic distance and numbers of branch points? Are there differences in puncta abundance in between dendrites of one cell?

6.3.2 Neurobits - a MATLAB script for puncta detection

The aim of this part of the project was to develop a MATLAB based script which does not require coding knowledge on the part of the user. At the same time, the script should keep some flexibility in setting parameters to adjust for individual experiments and biological questions. Also, visual inspection should be possible at each step to avoid the "black box" effect where data is fed in and an analysis output file is created without the user comprehending which particular analyses or transformations took place.

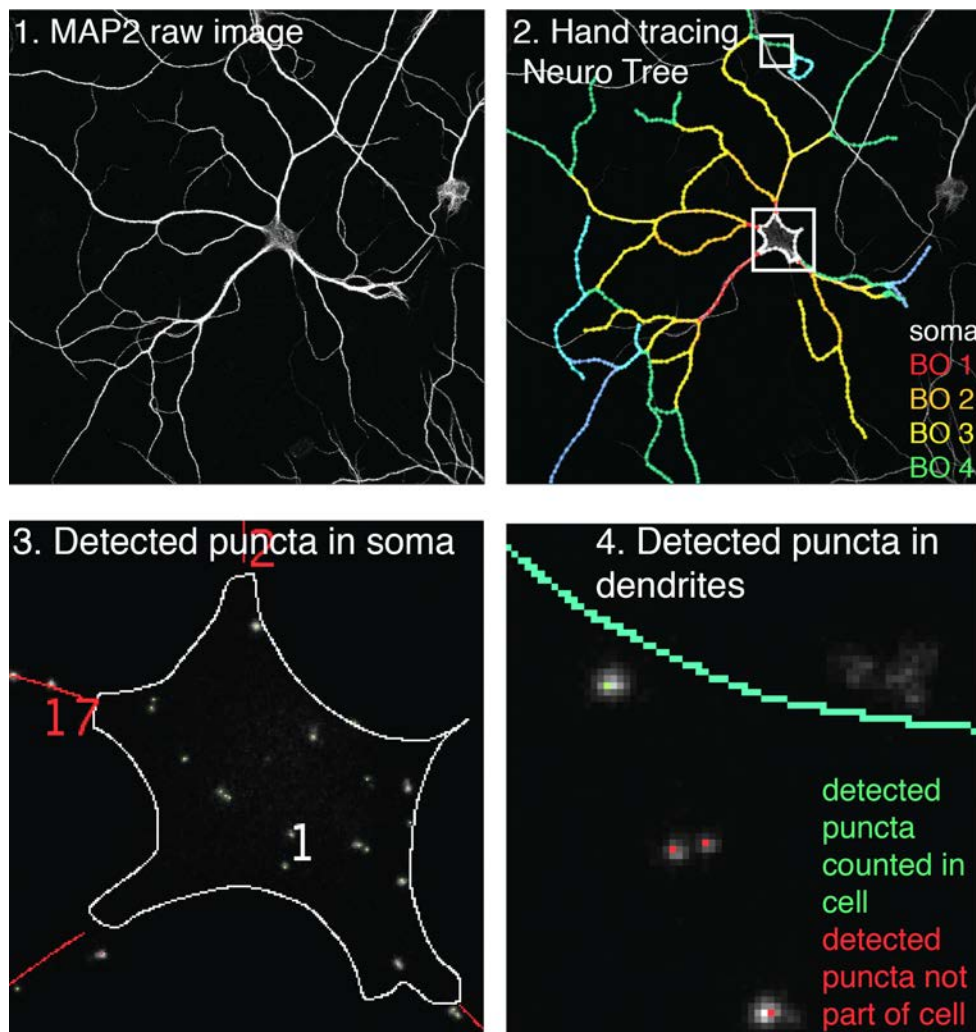


Figure 16: Workflow of puncta analysis in neurons with Neurobits (MATLAB)

1. Example image of a neuron stained with MAP2, 2. MAP2 signal is manually traced. After each branch point a higher branch order (BO) is indicated by the experimenter, 3. puncta detection on the PLA channel in soma (cropped region from 2.) red and white numbers indicate branch IDs for exact identification, 4. puncta detected in a stretch of dendrite (cropped region from 2.). Detected puncta assigned to the neuron (green) and detected puncta not corresponding to neuron (red). For more details see text.

Neurons are manually traced, puncta detection is done automatically and attribution to individual neurons is based on a defined puncta distance to the traced skeleton. The main difference with the ImageJ script described above is the method by which puncta are detected and that neuronal morphology is described in great detail. Using this script, we sought to answer how far in dendrites local synthesis (puncta) can be detected and to which extent branch points influence puncta density. We also sought to plot puncta density as a function of distance from the soma as well as a function of branch order.

The workflow of Neurobits is depicted in Fig 16. During the manual tracing the experimenter surrounds the soma and traces all dendrites of a cell via mouse clicks in the cell outline channel (MAP2 or a comparable cell staining or cell fill, 1.). Input files are stacks (3D) and maximum intensity projections can be generated in the

program directly. It is additionally possible to create sum and average intensity projections if required.

Branch points are indicated by the experimenter by higher branch order (BO) (2.) indicated by pressing numbers on the computer keyboard. Soma is assigned the BO zero, primary dendrites BO one, secondary dendrites BO two, etc. Single stacks of the image can be examined to clarify which of the overlapping dendrites belong to which cell. The X-Y coordinates of each click are saved in a text file and can be reused later if needed. In the current MATLAB version one cell per image is traced. Puncta detection is done by automatically detecting local intensity maxima of the puncta channel (3.). This represents an improvement compared to a fixed threshold in the ImageJ script. With this method even adjacent puncta can be detected as two separate puncta. This method is also less prone to misdetection due to variations in puncta intensities. Whether or not puncta correspond to a neuron or not is defined by a defined perpendicular distance from the traced skeleton. Satisfactory values can be defined by visual inspection of different values on multiple example images. Detected puncta belonging to the cell (3. and 4.) are marked by the script with a green spot, detected puncta outside of the cell are marked with a red spot.

For visual control of the analysis' accuracy, pictures are exported for each cell for the traced skeleton overlapping with the MAP2 signal and the traced skeleton overlapping with the puncta channel; in these images the detected puncta are marked in green and red. Branches are numbered so that each branch in the analysis can be unambiguously traced back to their exact location in the original image and cell (see 3.: soma = 1, dendrite = 17).

Certain analysis parameters can be adjusted to account for varying image parameters in different experiments (channel of puncta signal, image resolution, puncta brightness and abundance, background staining):

- Minimal distance (in pixel) of two adjacent puncta (intensity maxima): useful for high resolution images where single puncta comprise many pixels and puncta with non gaussian intensity distributions.
- Minimal brightness of puncta (maximum value of background). Value needs to be set between 0 and 1. 1 equals the brightest intensity value found in the puncta channel of a given image. Values smaller than 1 represent fractions of this value. The closer the value is to 1 the less puncta that are detected.
- Puncta distance to skeleton (in pixel) to be defined as part of the analyzed cell.

Once the experimenter is satisfied with the puncta detection a command will analyze the entire folder containing all cells from one experiment. Text files are generated for each cell with a list of all detected puncta with the analyzed properties and a png file for visual inspection of the puncta detection quality.

A summary text file of all cells of an experiment with the information of one cell per line is generated for now with Terminal (MacOS) but will be integrated soon into the Neurobits script. In Table 2 all output parameters of Neurobits are listed.

Table 2: Output parameters for Neurobits (MATLAB)

Image name
Number of puncta in soma
Number of puncta in dendrites
Area soma (in pixel, 2D)
Arbor span (in pixel, 1D)
Puncta density per cell (total puncta/cell area)
Density soma
Density dendrite
Ratio density arbor/soma
Number of puncta BO 1 etc
Span BO 1 etc
Density BO 1 etc
Puncta distances (pixel) from soma (geometric center) separated in different BOs
Puncta distances (pixel) to soma (Sholl)
Puncta distances (pixel) to proximal branch point
Puncta distances (pixel) to distal branch point

The outcome of the analysis should not vary greatly with different users. In order to exclude that possibility and to test the reproducibility of the data we let two different high-school students trace the same dataset of cells (14 cells of a FUNCAT-PLA experiment for GluA2 where puncta density is high in soma and dendrites) and compared the outcome. Fig 17 shows that the variability between the two tracers was very low. The branch order of detected puncta within cells showed only a 6 % difference, the puncta distance to soma showed a 2 % difference and total number of puncta per neuron 3 %. The slightly bigger SEM observed in puncta number per neurons is due to the smaller n (14 cells vs over 2000 datapoints from these 14

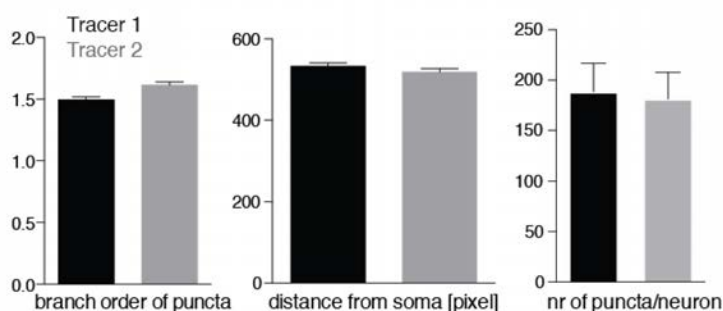


Figure 17: High reproducibility of neuron tracing with different script users

One dataset of FUNCAT-PLA for GluA2 in cells was traced by two different tracers (black and grey). Mean \pm SEM of branch order of puncta, puncta distance from soma (2359 and 2571 datapoints from 14 cells) and total number of puncta per cell (from 14 cells) are plotted. Similarities of mean 94 %, 98 % and 97 % respectively. Note no significant difference detected between the two tracers.

cells for branch order and soma distance). The high reproducibility is a good indication that tracing is very reproducible between different individuals. To be on the safe side, however, we tried to have one full dataset traced by one person.

This script is still under development but with the current version we are already able to make elaborate statements about puncta

distributions in neurons. The script is used for most of the data analysis presented in the biological results section. We will now briefly summarize the two scripts and discuss their future perspectives and improvements.

6.3.3 Discussion and Outlook for Neurobits and ImageJ scripts

Analysis involving manual tracing in neurons is labor intensive. To date no algorithm is as good as the human brain in detecting a neuron's complex architecture with potential overlap from other neurons in our type of images. Additionally, given the relatively small number of cells per condition, analysis must be as accurate as possible to detect eventual small differences between conditions. For the datasets used in this thesis (maximum 10 conditions à ca 15 cells) the tracing can still be done in a reasonable time frame (up to a week). For datasets with more than 200 cells, however, a different approach must be used.

The ImageJ script was a good first step to simplify and reduce the time needed for a crude puncta analysis. It was sufficient to detect changes in total puncta abundance and, to a certain degree, also shifts between soma and dendrites. Subtle changes in puncta distributions between conditions and a more detailed puncta distribution within dendrites, however, is not possible.

This was the rationale to develop Neurobits. We made sure that the data of the traced neuronal skeleton is stored in a way that the information can be accessed easily by an updated script version and other programs.

Future directions will improve the script as follows:

3D analysis: the current analysis is done on 2D images. Since the original files are three dimensional stacks, optimally the information about the third dimension should be analyzed as well. Overlapping puncta in the z-axis could be separated if analyzed in 3D. Given the relative roundness of somata compared to relative flat dendrites, puncta densities in 2D are overestimated in somata. For a direct density comparison between soma and dendrites in addition to the third dimension the actual dendritic width must be detected rather than a fixed dilation of the traced skeleton. The best approach would be an automated MAP2 detection to define dendritic width. Preliminary attempts in this direction with promising first results have been obtained but are not yet implemented in the main Neurobits script.

Cell type classification using mathematical description of neuron's morphology: A big step is the full reconstruction of neuron's morphology. The current script treats branches individually and does not yet reconstruct the entire dendritic tree. A full reconstruction would allow one to track which child branches arise from which parent branch. This information would be useful to compare puncta densities between different dendrites of one cell. In addition, a mathematical description of the full dendritic arbor could potentially be used to identify different cell types. Cluster analysis of parameters like number of primary dendrites, average branch and total dendritic length, angle of branches and soma sizes could identify clusters of cells which share some common features. Hippocampal cell cultures consist of a mix of cell types. If a sufficient number of cells are imaged, cell heterogeneity of puncta abundance could be reduced by only analyzing cells of a

single morphological type. This would enable us to detect subtle changes in puncta distributions which are otherwise masked by variations within one condition.

Interpuncta distances and distances to branch points: Puncta distances in relation to branch points are already generated. Cui-Wang et al. showed local hot spots of ER exit sites at branch points (Cui-Wang et al. 2012). The analysis of branch point proximity could thus answer, for example, whether or not newly synthesized membrane proteins accumulate at branch points and are more likely to be exported there. This interesting hypothesis could be already tested with the existing datasets but was not yet conducted due to time limitations. It would be additionally helpful to know interpuncta distances. How far is the closest puncta from a given puncta? If local synthesis in dendrites occurs at hotspots or if newly synthesized proteins are transported together this would be visible by an interpuncta distance histogram analysis.

With these analysis tools at hand we will now move on to biological questions and experimental data.

6.4 Pore-forming AMPA receptor subunits

AMPA receptors are the key players of fast synaptic transmission in the brain (Schwenk et al. 2012). Their current flux (e.g. opening probability and ion conductivity) depend on their subunit composition. Pore-forming and non-pore-forming subunits build functional receptor complexes. Where are the different subunits synthesized and where in the secretory pathway do they assemble? If the same routes of the secretory pathway are employed for each subunit the distribution for different newly synthesized subunits should be the same. Differences in newly synthesized receptor distribution would suggest different initial routes of processing. With the FUNCAT- and Puro-PLA technique described in this thesis, we will now investigate the site of synthesis and redistribution dynamics of AMPA receptor subunits.

6.4.1 GluA1 and GluA2

Different distributions for newly synthesized GluA1 and GluA2

The pore-forming subunits GluA1 and GluA2 are the most abundant AMPA subunits in the hippocampus (Schwenk et al. 2012). We hence performed FUNCAT-PLA experiments for GluA1 and GluA2 to address whether there are differences in the newly synthesized protein distribution of the subunits.

Cultured hippocampal neurons were incubated with AHA and as a negative control anisomycin was added prior and during AHA labeling. A relatively short AHA labeling time of 50 min was chosen to limit the redistribution after synthesis (Fig 18). Robust signal for both subunits could be seen in AHA-treated cultured hippocampal neurons. In anisomycin control conditions very little signal was present in cells leading to a very good signal to noise ratio of 10- and 7-fold for GluA1 and GluA2, respectively (Fig 18 c).

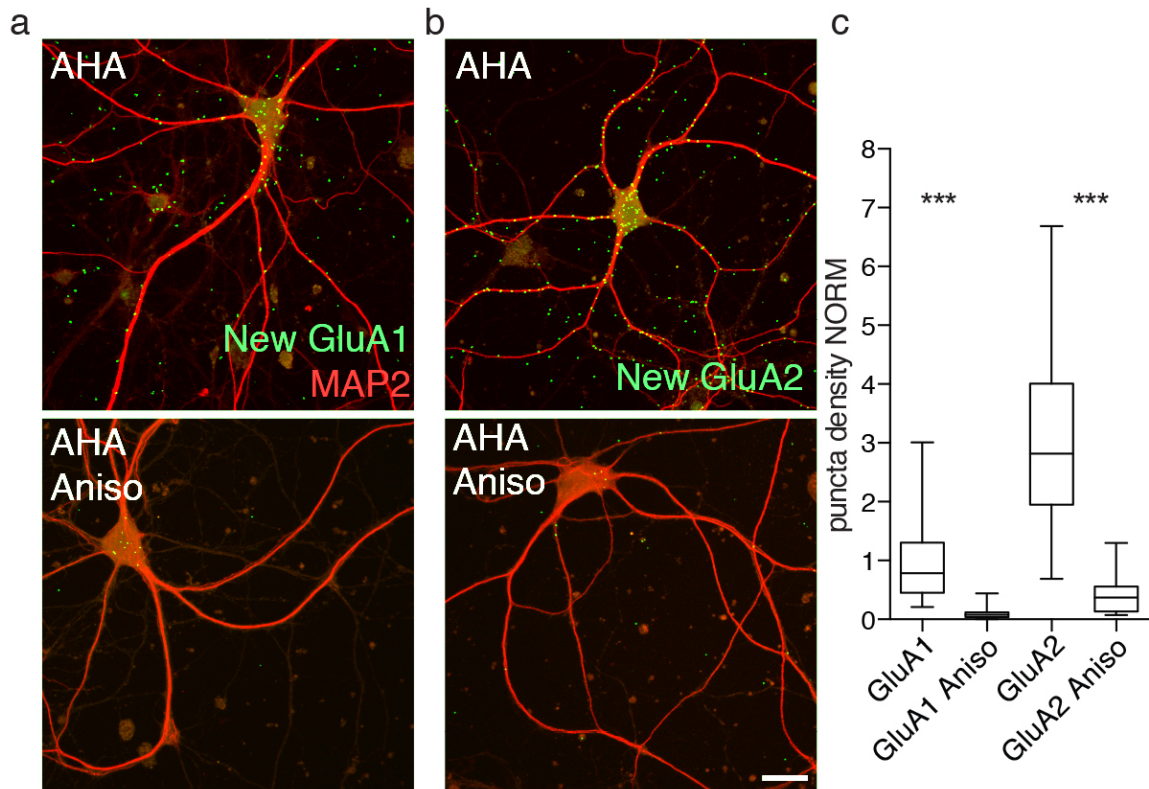


Figure 18: FUNCAT-PLA for AMPA receptor subunits GluA1 and GluA2

a) Newly synthesized AMPA subunit GluA1 (green) and b) GluA2 in cultured hippocampal neurons (50 min AHA, DIV 18-21). Bottom panel: Respective negative controls with the translation inhibitor anisomycin, scale bar = 20 μm . c) Analysis of normalized puncta density (PLA intensity per cell area including cell body and dendrites), box plot with median \pm quartiles and min max values, $n = 31-41$ cells of 3 independent experiments, Mann-Whitney test *** $p < 0.0001$.

GluA2 showed more than threefold higher general labeling compared to GluA1. Both proteins displayed abundant signal in neuronal somata. To our surprise, clear differences were seen in relative dendritic levels of FUNCAT-PLA. GluA2 showed substantial dendritic labeling whereas GluA1 was sparsely present in dendrites. Since GluA2 showed higher labeling in general we needed to verify whether we indeed find relatively more newly synthesized GluA2 in dendrites compared to GluA1. Analyzing dendritic puncta distributions and relative abundances (Fig 19) we could indeed find qualitative and quantitative differences in the puncta distribution of GluA1 and GluA2. There was relatively more signal in dendrites compared to soma with a dendritic fraction of 47 % in GluA1 and 66 % in GluA2 (Fig 19 b). This represented an increase of 40 %. The increase in dendritic signal was also visible when comparing puncta densities of dendrites and somata. The median increased by 50 % (Fig 19 c).

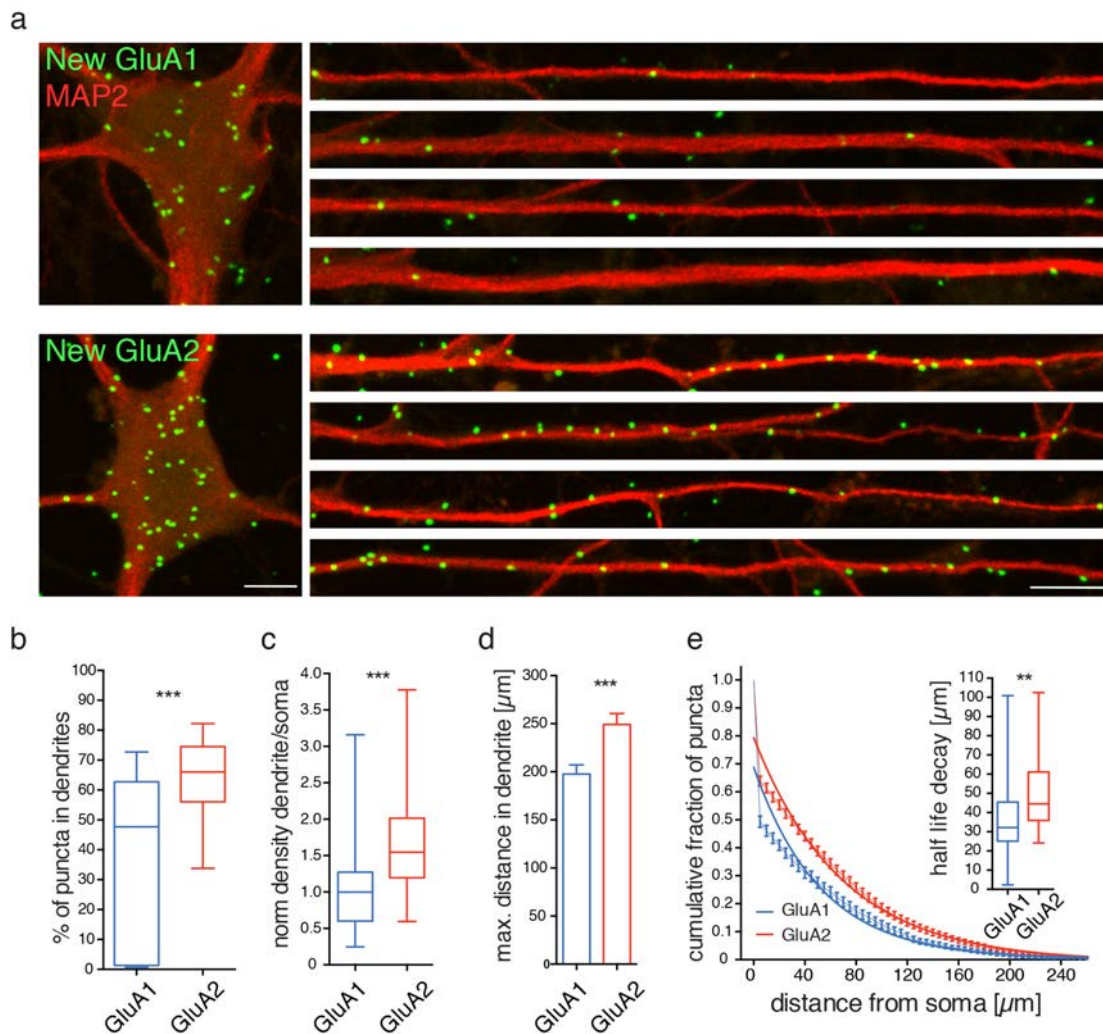


Figure 19: Newly synthesized GluA2 is relatively more abundant in dendrites than GluA1

a) FUNCAT-PLA for GluA1 or GluA2 (green) in neuronal somata (left panel) and dendrites (right panel) of cultured hippocampal neurons (DIV 18-21), scale bar = 10 μm . b) Box plot of dendritic puncta fraction with median \pm quartiles and min max values, Mann-Whitney test, $***p < 0.0001$. c) Box plot of normalized puncta density in dendrites to soma, Mann-Whitney test, $***p < 0.0001$. d) Bar graph of mean \pm SEM of maximal puncta distance from soma, unpaired t-test, $***p = 0.0008$. e) Backwards cumulative distribution of puncta distances to soma, mean \pm SEM and nonlinear fit, inset: box plot with median \pm quartiles and min max values of half-life for non linear curve fit (one phase) for individual cells in e), Mann-Whitney test, $**p = 0.0014$, $n = 40$ cells per subunit from 3 independent experiments. For more details see method section.

GluA2 puncta were detected further from the cell body in distal dendrites since the average maximum puncta distance from the soma was 200 μm in GluA1 and 250 μm in GluA2 samples. This represented 25 % further away from the soma (Fig 19 d). The backwards cumulative distribution of puncta distances to soma illustrated which fraction of puncta in a given cell was further away from the soma at a certain distance (Fig 19 e). The curve for GluA1 decreased more rapidly showing again the lower dendritic puncta fraction. A nonlinear curve fit was applied to each cell individually and half lives of the decay was computed (Fig 19 e inset). For GluA1 50 % of puncta were further than 32 μm away from the soma (see Fig 13 e when

curves drop to 0.5 on y axis). For GluA2 half of the puncta were further away than 45 μm .

After 50 min of AHA labeling newly synthesized GluA2 was detected in more distal aspects of the dendrites compared to GluA1. These two subunits show hence very different distributions shortly after synthesis. To exert their function, AMPA receptor subunits need to be present on the plasma membrane, and more specifically at synapses. In the next experiments, we therefore asked whether the above differences in dendritic signals between GluA1 and GluA2 are also observed when the surface expression of the receptors is examined. Does, for example, the higher dendritic GluA2 level lead to faster access to the surface and synapses?

Surface labeling of new GluA1 and new GluA2

We investigated what fraction of the newly synthesized subunit can be detected on the plasma membrane. FUNCAT-PLA was performed and PLA signal for newly synthesized AMPA receptor subunits present at the surface was detected. This was achieved by “live labeling”. Primary antibody recognizing an extracellular epitope of the subunit was added to neuronal growth medium on living cells, at the end of the AHA labeling period, just before fixation. After fixation, cells were permeabilized and blocked as for regular staining (for more details see methods section).

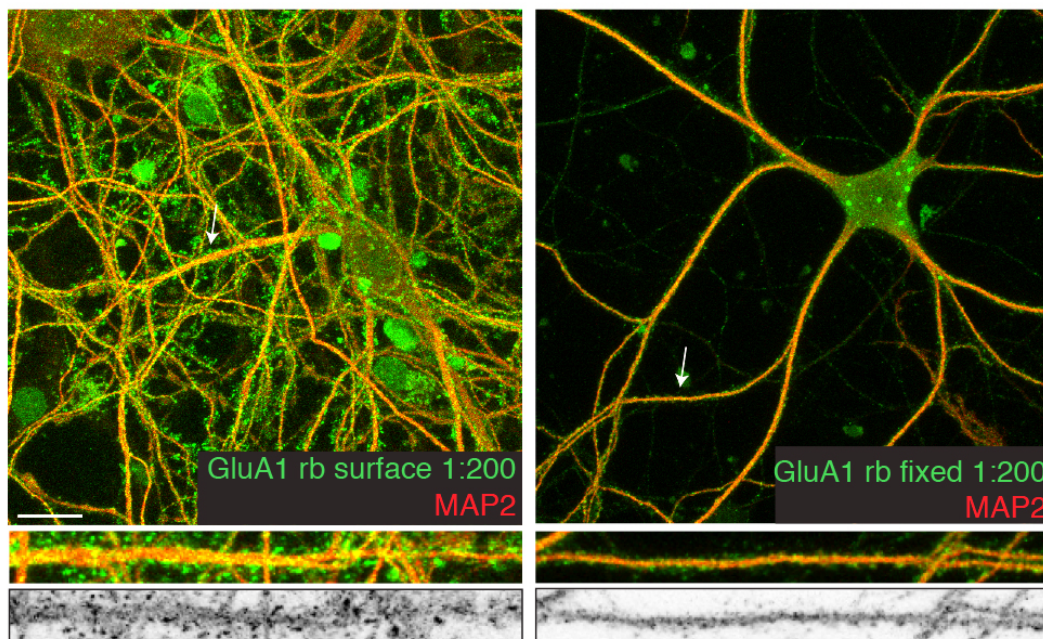


Figure 20: Surface labeling of GluA1 using an N-terminal antibody

Immunocytochemistry for GluA1 (green) on live (left) and fixed (right) cultured hippocampal neurons (DIV 49). Bottom panel: Two color image and GluA1 staining only for straightened dendrites indicated by arrows, scale bar = 20 μm .

First we needed to validate if the used antibodies were suitable for surface labeling. Regular immunohistochemistry was hence performed prior to FUNCAT-PLA experiments. For both subunits (Fig 20 and 21) surface immunolabeling where the antibody was applied to living neurons was compared to total immunolabeling where the antibody was added after fixation, permeabilization and blocking.

GluA1 surface (live) and total (permeabilized) labeling resulted in signal in neuronal somata and dendrites, nicely overlapping with the dendritic marker MAP2 (Fig 20). Some nuclear background staining could be observed in live labeling conditions. This nuclear staining was unexpected given the synaptic function of GluA1. Synaptic like pattern was observed under live labeling conditions and less under fixed conditions. This suggested a synaptic enrichment of the labeling. This antibody showed expected labeling pattern for GluA1 and gave significant labeling when used live. It was therefore used for surface FUNCAT-PLA experiments.

Anti-GluA2 antibody staining also resulted in a signal detectable in both somata and dendrites (Fig 21). Labeling was detected consistently throughout dendrites. Staining overlapped with the dendritic marker MAP2. Synaptic like pattern was observed in both labeling conditions. No somatic background staining was visible. This antibody gave an expected labeling pattern and resulted in significant signal when used under live, non-permeabilizing conditions. It was hence used for surface FUNCAT-PLA experiments.

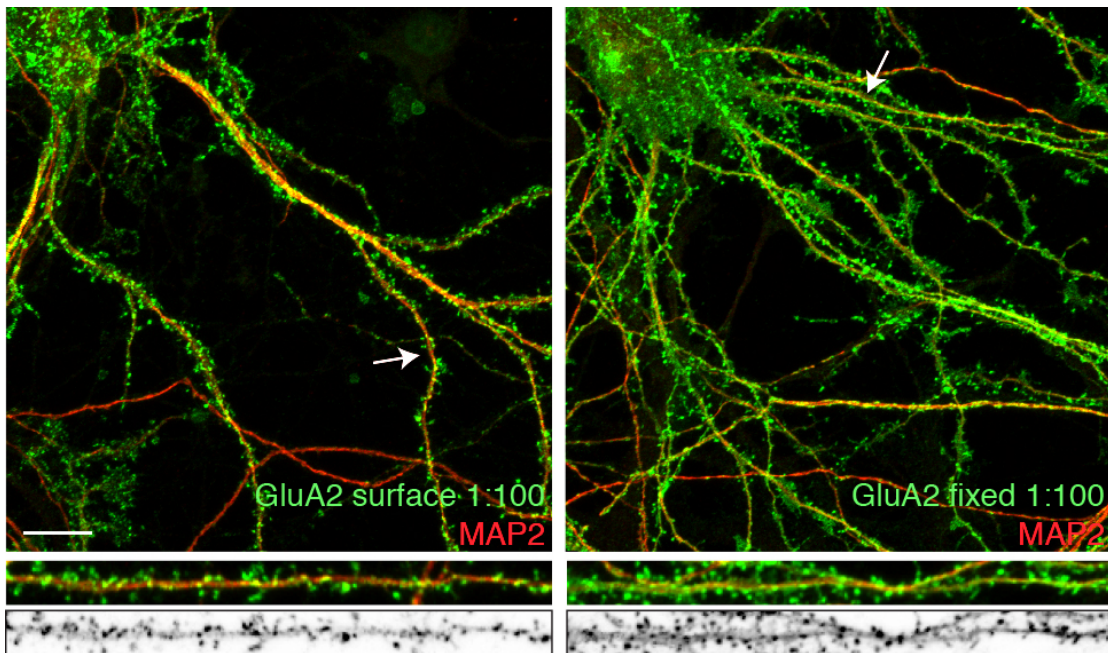


Figure 21: Surface labeling of GluA2 using an N-terminal antibody

Immunocytochemistry on live (left) and fixed (right) cultured hippocampal neurons (DIV 28) using an anti-GluA2 antibody (green). Arrows indicate straightened dendrites at the bottom. An apparently synaptic pattern is visible with both staining methods (green and grey), scale bar = 20 μm . Staining performed by Dr. Anne-Sophie Hafner, antibody kind gift from Gouaux lab, Vollum Institute.

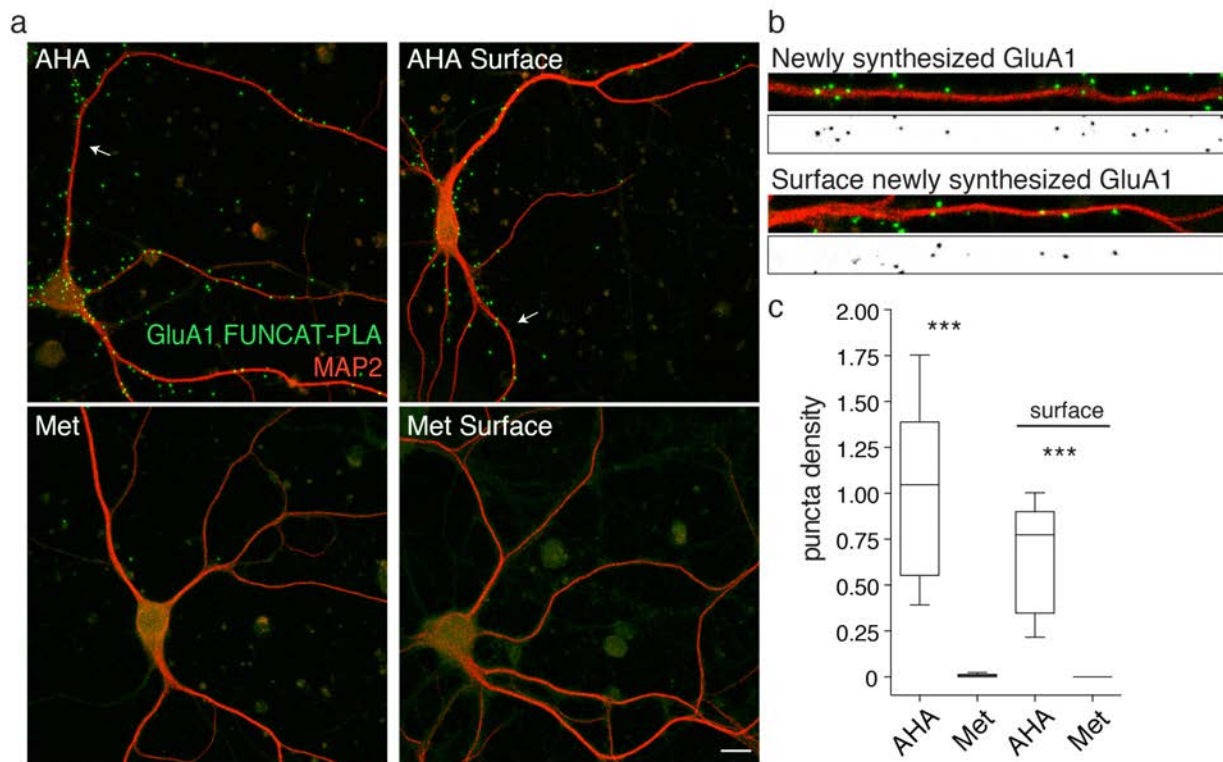


Figure 22: High fraction of newly synthesized GluA1 at the cell surface

a) Newly synthesized GluA1 subunit (green) and MAP2 (red) in cultured hippocampal neurons (DIV 19, 2 h AHA labeling) and respective methionine (Met) negative controls (bottom panel). Total pool of new GluA1 (left) and surface fraction of new GluA1 (right), scale bar = 15 μm . b) Straightened dendrites indicated by arrows in a). c) Analysis of puncta density in entire cells for total new and surface new GluA1, median \pm quartiles and min max values, n = 10-16 cells from one experiment, one-way ANOVA: *** $p < 0.0001$. Note the total absence of puncta in Met Surface condition.

We next investigated how much of the newly synthesized GluA1 or GluA2 subunit made it to the neuron's surface in a given time. AHA labeling durations had to be chosen such that significant puncta labeling was present in surface conditions. For GluA1, two hours of AHA incubation was needed to get sufficient signal for surface labeling (Fig 22). For the total pool of newly synthesized GluA1 robust labeling could be observed in somata as well as in dendrites (note the longer labeling time compared to Fig 18 and 19). When only labeling the surface fraction of newly synthesized GluA1, a reduction of approximately 25 %, relative to the total, was observed in entire cells (Fig 22 c). Dendritic puncta were often localized adjacent to MAP2 staining, at presumed synapses. Methionine-treated cells showed no labeling in total and surface labeling conditions. A robust labeling compared to methionine treated negative control samples was observed for total and surface labeling.

For GluA2 a much stronger labeling in general was observed and a shorter AHA labeling time, of only one hour, was used (Fig 23). Total new GluA2 was present in both somata and dendrites. Labeling was often so strong that single puncta were not distinguishable in some neurons. Signal was drastically reduced in soma and dendrites (by 68 %) when the surface fraction was identified. Many puncta were localized right next to the MAP2 signal indicating their presumed synaptic localization.

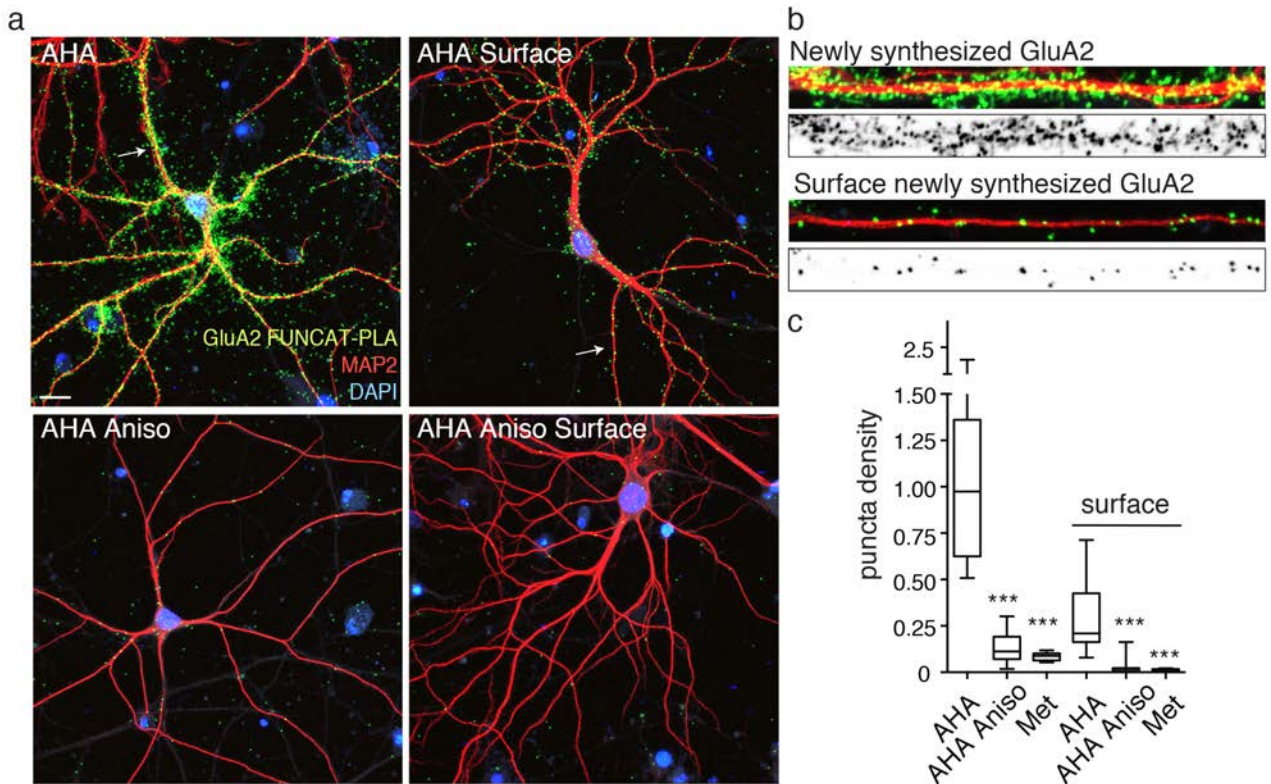


Figure 23: Low fraction of newly synthesized GluA2 at the surface

a) Newly synthesized GluA2 (green) in entire cultured hippocampal neurons (DIV 25, 1 h of AHA, left panel) or at the cell surface (right panel) and their respective negative controls (bottom, anisomycin), scale bar = 15 μm . b) Arrows in a) indicate straightened dendrites. c) Box plot of puncta densities with median \pm quartiles and min max values, $n = 9-20$ cells from 1 to 2 experiments, DIV 21 and 25. Puncta intensity normalized to cell area. Kruskal-Wallis test was performed for total and surface separately, $p^{***} < 0.001$.

The addition of the translation inhibitor anisomycin or substituting AHA with methionine led to a significant signal reduction. Comparing medians of puncta densities from all analyzed cells (Fig 23 c) signal to noise ratio was high (6 and 11 for total and surface respectively for the anisomycin control and 8 and 15 for the methionine control).

Did the surface fraction differ between the dendrites and the somata? For GluA1 a slight trend of higher surface fraction in dendrites, however not significant, was observed (Fig 24).

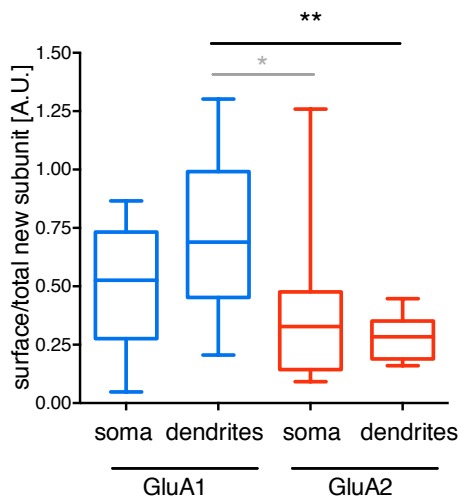


Figure 24 Comparison of surface to total fraction of newly synthesized AMPA receptor subunits

Analysis of experiments shown in Fig 16 and 17. Surface fraction of PLA signal compared to total in soma and dendrites, median \pm quartiles and min max values, n = 16 and 10 cells, Kruskal-Wallis multiple comparison, *p = 0.03 and **p = 0.0018.

For GluA2 very comparable fractions of newly synthesized protein were present at the surface in soma and dendrites. This result indicates that exocytosis did not differ between these two compartments.

Comparing the exocytosis between subunits however, GluA1 exhibited a higher surface fraction of newly synthesized protein (Fig 24 and compare 25 % GluA1 with 68 % GluA2 signal reduction for total cells, Fig 22 and 23), most pronounced in dendrites.

Taken together a big fraction of newly synthesized GluA1 in dendrites is relatively rapidly detectable at the plasma membrane whereas most of newly synthesized GluA2 in dendrites is located intracellularly. As seen in the direct comparison of relative dendritic signal for newly synthesized AMPA receptor subunit there were qualitative distributional differences between the two subunits.

The above observed differences in dendritic signal for newly synthesized subunits could in principle arise from either higher local synthesis of GluA2 or a faster redistribution after somatic synthesis.

Site of synthesis of GluA1 and GluA2

In previous FUNCAT-PLA experiments we observed more newly synthesized GluA2 in dendrites than new GluA1. In order to investigate whether this is due to more local synthesis of GluA2, Puro-PLA experiments were performed for the two subunits. After a short pulse of 5 to 10 min with puromycin newly synthesized GluA1 or GluA2 was labeled using the before described Puro-PLA technique (Fig 25 a - c). Both subunits showed very clean negative controls when puromycin was omitted and displayed high puncta density in somata under puromycin labeling conditions. To our surprise the signal in dendrites was very low (Fig 25 d). Both subunits had only 17 % on average of their total puncta present in dendrites. This is a rather low fraction given the much bigger area of the entire dendritic tree compared to the small soma.

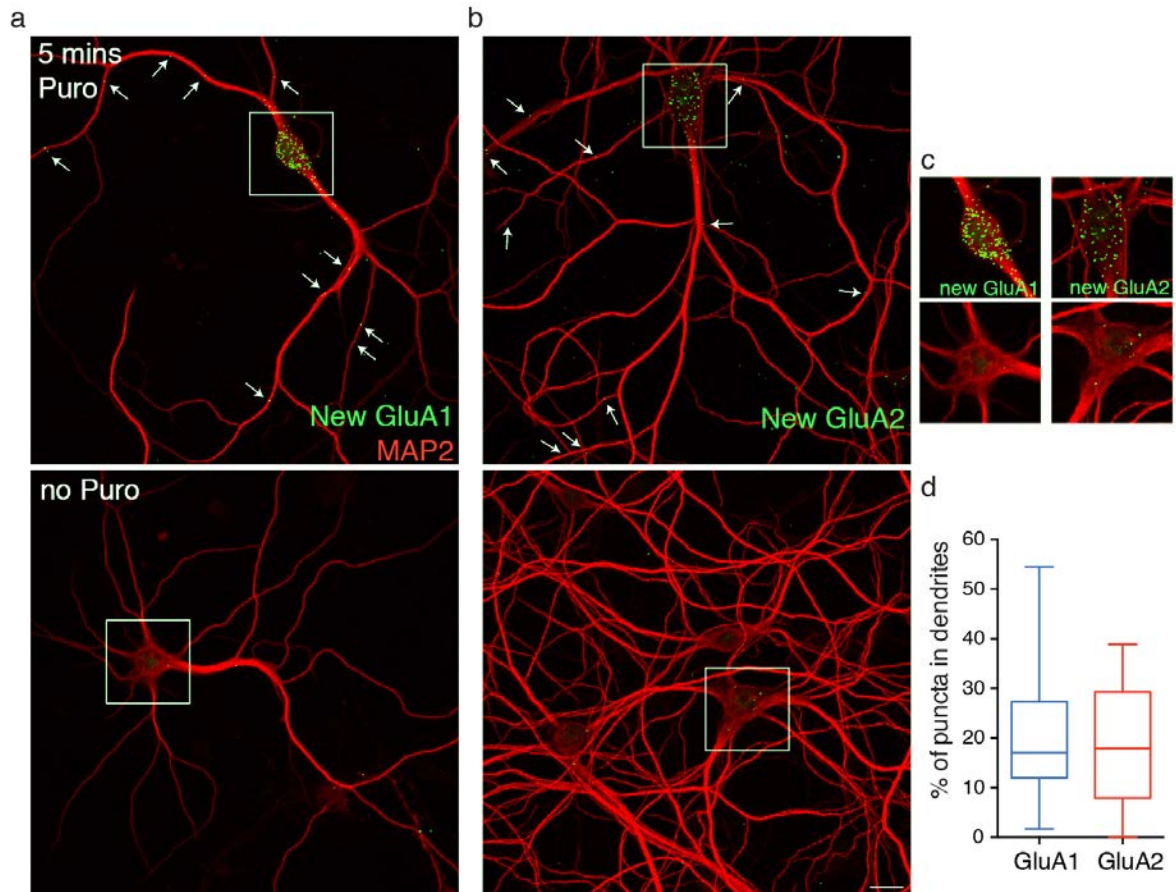


Figure 25: Puro-PLA for GluA1 and GluA2 shows very low dendritic signal

a) Puro-PLA signal (green) for GluA1 and GluA2 b) in cultured hippocampal neurons (DIV 20-34) and their respective negative controls (bottom) where no puromycin was added, scale bar = 20 μm . Arrows highlight dendritic puncta. c) Zoom in on somata in a) and b). d) Boxplot with median \pm quartiles and min max values for fraction of puncta in dendrites for both POIs. Note the low dendritic puncta abundance and no significant difference between the two POIs, Mann-Whitney test, ns = 0.89, median of 17.86 and 17.06 for GluA2 (17 cells from 4 experiments, 1-3 μM , 5-7 min Puro) and GluA1 (26 cells from 3 experiments, 1-2 μM , 5-10 min Puro) respectively.

In summary no differences were seen for site of synthesis of the two AMPA receptor subunits. Given the pronounced difference in dendritic puncta abundance in before mentioned FUNCAT-PLA experiments (Fig 18, 19) we hypothesized that newly synthesized GluA2 would redistribute more quickly into dendrites. We hence conducted pulse-chase FUNCAT-PLA experiments in which redistribution over time could be observed for the two subunits.

Pulse-chase experiments of GluA1 and GluA2

Pulse-chase experiments of GluA1

We performed pulse-chase experiments with AHA to examine the time-course with which new GluA1 and GluA2 subunits redistribute into dendrites after synthesis. After a two hour AHA labeling pulse, cells were fixed at 0, 6, 12 and 24 hours chase (in AHA free medium) and FUNCAT-PLA was performed for GluA1 (Fig 26 a). No protein degradation was evident since total puncta abundance did not decrease over the chase time course (Fig 26 b and c).

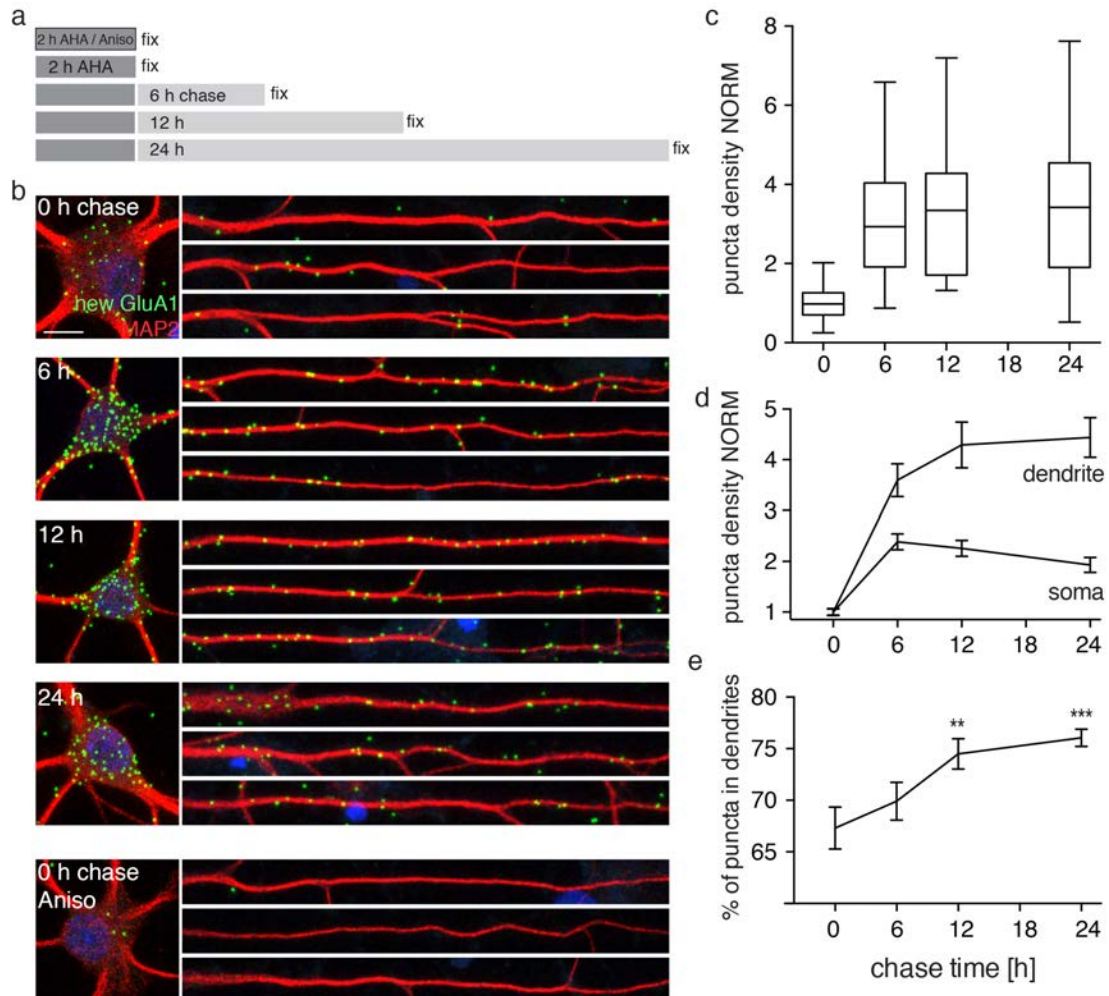


Figure 26: Pulse-chase experiment for GluA1 suggests a slow redistribution into dendrites

a) Incubation scheme for AHA labeling followed by different chase times in label-free medium. b) Representative somata (left panel, DAPI blue) and straightened dendrites (right panel) of cultured hippocampal neurons (DIV 18) with FUNCAT-PLA for GluA1 (green) for all chase timepoints and anisomycin control (bottom), scale bar = 10 μ m. c) Box plot analysis of total puncta density in cells (median \pm quartiles and min max values). d) Puncta density in somata and dendrites (mean \pm SEM). e) Dendritic fraction of puncta (mean \pm SEM), one-way ANOVA, **p = 0.0069, ***p = 0.0002, n = 29-47 cells from 2 experiments.

Inset: Higher FUNCAT-PLA signal in chase time points

To our surprise, we noticed that the total puncta abundance increased in all chase conditions (three-fold increase at timepoint 6, 12 and 24 h compared to time-point zero). The total puncta abundance should stay constant or decrease in chase time points given the absence of AHA. Without AHA present in the medium not more proteins can be labeled and puncta abundance can not increase. This was however

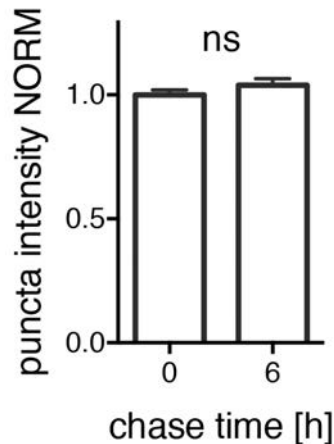


Figure 27: No puncta intensity differences between different chase times for GluA1 FUNCAT-PLA

Analysis of PLA puncta intensities (mean \pm SEM), $n = 31-47$ cells from 2 experiments, unpaired t-test ns $p = 0.24$. Data of each experiment normalized to mean of timepoint zero.

found in two independent experiments. It was hence unlikely to be an experimental error. Such an effect was never observed in similar pulse-chase experiments for other newly synthesized proteins (TrkB, Bassoon, Gamma 8, LaminB1, GluA2 and GM130; Fig 29 and 33 of this study, tom Dieck et al. 2015, Dörrbaum et al. 2018). This fact indicates the specific nature of this unexpected observation for newly synthesized GluA1.

One can only speculate about the biological or experimental reason for this effect. One possible explanation would be the very close proximity of several newly synthesized GluA1 subunits directly after synthesis; these subunits would then get separated over time. This very close proximity could lead to steric hindrance of antibody binding and an underestimation of newly synthesized GluA1 in the no chase condition. Separated subunits in chase conditions could be successfully labeled, leading to higher total puncta abundances.

If several newly synthesized GluA1 subunits in close proximity are still successfully labeled, the resulting puncta would be expected to be brighter compared to the chase time points. We tested this hypothesis and analyzed mean puncta intensities in cells of different chase timepoints. As shown in Fig 27, no significant difference was observed in puncta intensities. The lower puncta abundance in the no chase sample can hence not be explained by concentrated PLA signal in single puncta. The dendrite-to-soma ratio did not differ significantly between the no chase and 6 h chase time point. This result indicated no obvious selective labeling differences in different cellular compartments. We therefore decided to use the generated data in subsequent analyses.

How fast does newly synthesized GluA1 redistribute into dendrites after synthesis? Over the chase time course of 6, 12 and 24 hours a gradual increase in dendritic density and gradual decrease in somatic density was visible (Fig 26 d). As a result the fraction of dendritic puncta increased from 67 to 75 % over the period of 24 h chase (Fig 26 e, compare to 47 % after 50 mins of labeling in Fig 19). Newly synthesized GluA1 hence redistributed slowly into dendrites within a day. For GluA2

we would expect a faster redistribution given the higher dendritic density of newly synthesized GluA2.

Pulse-chase experiments of GluA2

Since significant dendritic GluA2 labeling was already observed after 50 min AHA labeling period (see Fig 19), we first needed to define labeling conditions where dendrites exhibited lower signal but the total labeling was still significantly higher than background. A high level of dendritic labeling at the chase time point zero would make redistribution over time difficult to interpret. 10, 20 and 60 min of AHA labeling times were thus tested and the number of dendritic puncta and signal-to-noise ratio compared to their respective anisomycin controls (Fig 28). Ten minutes of AHA labeling resulted in very weak somatic and no detectable dendritic labeling.

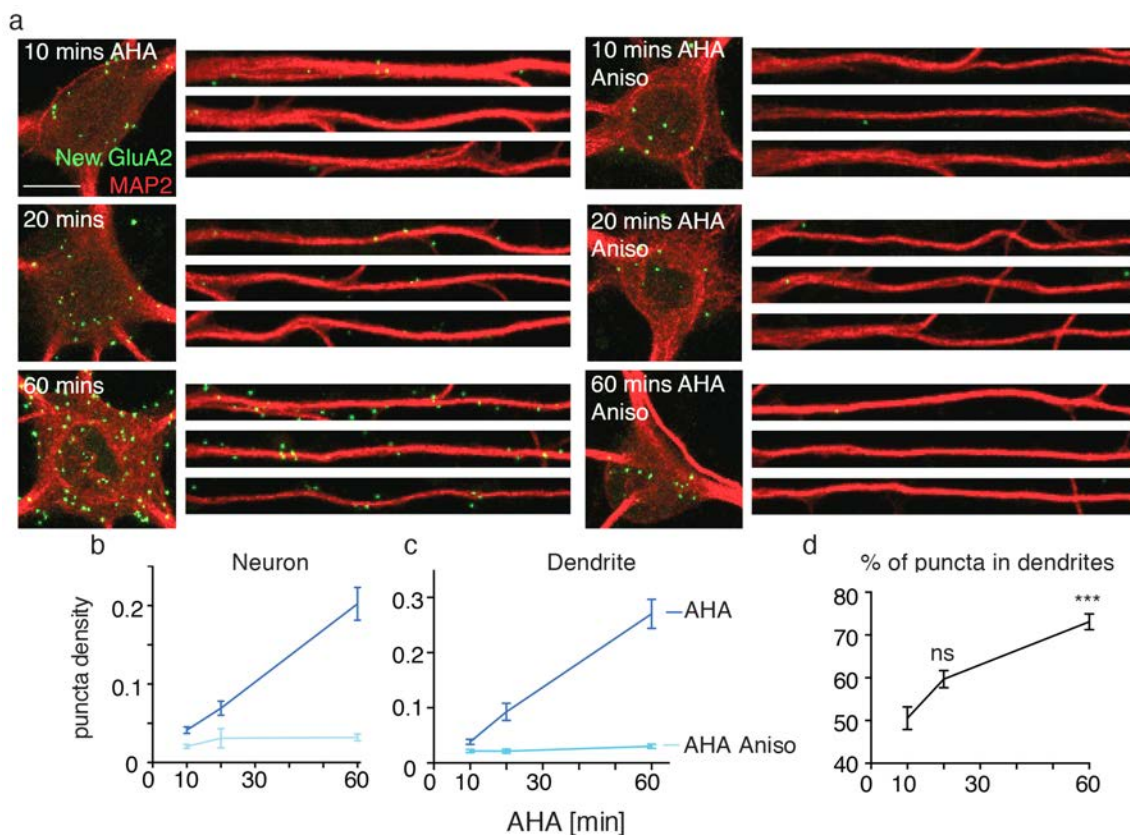


Figure 28: Define AHA labeling conditions for GluA2 pulse-chase experiments

a) Representative images of newly synthesized GluA2 (green) in somata and straightened dendrites of cultured hippocampal neurons (DIV 19) after increasing AHA labeling times (min indicated) and respective anisomycin controls (right panel), scale bar = 10 μ m. b) Analysis of puncta density mean \pm SEM for AHA and AHA + anisomycin in entire cells and c) in dendrites only (7-12 cells from one experiment). d) Dendritic fraction of puncta, n = 19-27 cells from 2 independent experiments, Kruskal-Wallis test compared to 10 mins labeling, ns = 0.069, ***p < 0.0001.

With 20 min of AHA labeling more somatic signal and a few dendritic puncta were observed. Both soma and dendrites showed significantly higher labeling than the anisomycin negative control. After 60 min of AHA labeling, robust signal was detected in soma and dendrites. The dendritic fraction of 73 % in this experiment

after 60 mins labeling corresponded nicely with 66 % of puncta in dendrites after 50 mins of AHA labeling in Fig 19. We decided to perform the subsequent pulse-chase experiments with 20 min AHA labeling since it showed sufficient labeling in somata with relatively low labeling in dendrites. It would thus be possible to follow the potential redistribution of GluA2 into dendrites. Cells were labeled for 20 min with AHA and subjected to chase periods in label-free medium for 0, 20 and 40 min (Fig 29). Relatively short chase times were chosen since 60 mins of AHA labeling resulted already in high dendritic labeling. FUNCAT-PLA for GluA2 was performed as previously described. Total puncta abundance remained constant for the different chase times (Fig 29 c). The signal to noise ratio was 10 fold (data not shown). Without a chase period only a sparse dendritic labeling could be observed (Fig 29 b). After a short 40 min chase time the ratio increased significantly (Fig 29 d and e).

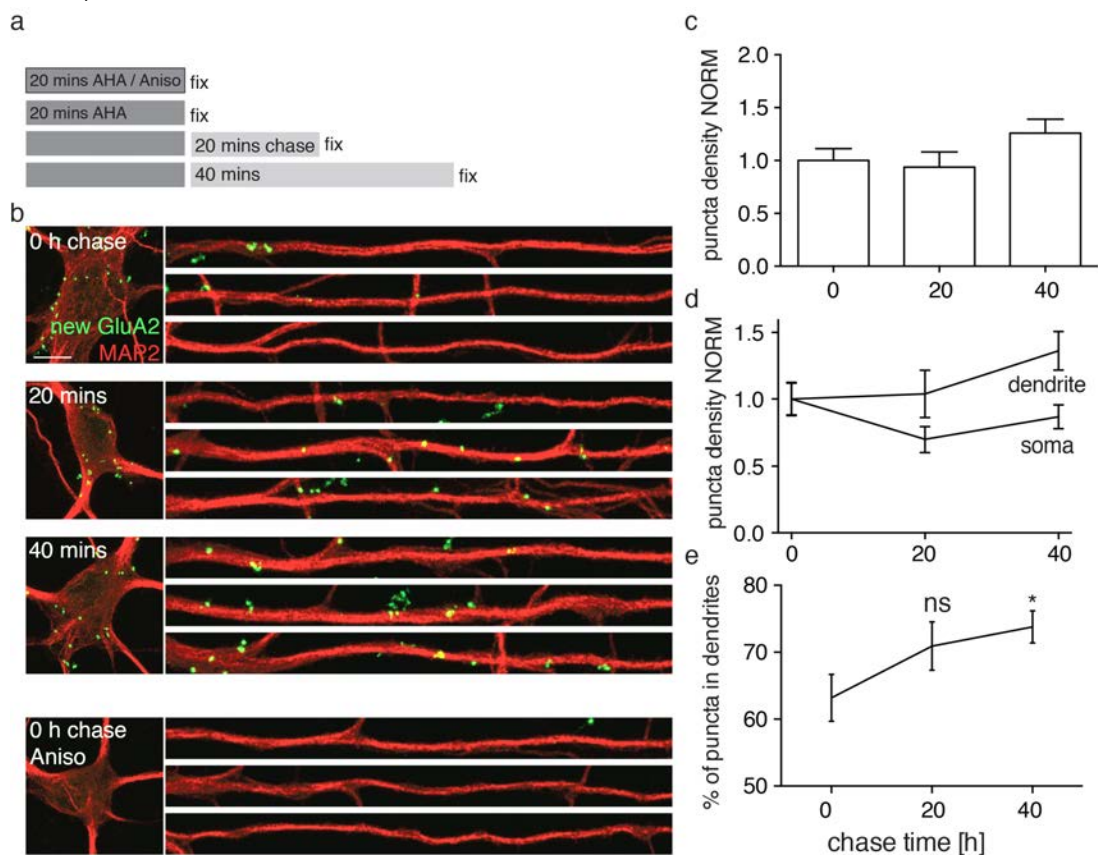


Figure 29: Newly synthesized GluA2 redistributes rapidly into dendrites

a) Incubation scheme of pulse-chase FUNCAT-PLA experiment for GluA2. b) Representative images of newly synthesized GluA2 (green) in somata (left panel) and straightened dendrites (right panel) of cultured hippocampal neurons (DIV 18) after different chase times (min indicated), anisomycin negative control (bottom), scale bar = 10 μ m. c) Analysis of PLA puncta density in entire cells and d) in somata and dendrites separately. e) Analysis of dendritic fraction of puncta, one-way ANOVA, ns = 0.1, *p = 0.0488, n = 12-15 cells from 1 experiment. Mean \pm SEM in c) - e).

Taken together the two AMPA receptor subunits GluA1 and GluA2 were both mainly synthesized in the soma under basal activity conditions and then redistributed into

dendrites. Surprisingly vast differences existed in redistribution kinetics and surface expression. GluA2 redistributed much faster into dendrites after synthesis. The surface labeling experiment however showed that most of the dendritic fraction of new GluA2 was located intracellularly whereas GluA1 was rapidly exported to the surface once present in dendrites.

This data suggests that the two subunits do not take the same route to be delivered to synapses to exert their function.

AMPA receptors are not only composed of pore-forming subunits, but also associate with auxiliary subunits which influence their forward trafficking. We will now investigate the site of synthesis and redistribution kinetics of two candidates of auxiliary proteins, CNIH2 and TARP Gamma 8, because they are the most abundant auxiliary proteins in the hippocampus (Schwenk et al. 2012). This will help us to understand how and when in the secretory pathway the interaction of the different AMPA subunits may occur. How can their delivery to the cell's surface and synapses be regulated?

6.5 Auxiliary proteins

How and when in the secretory pathway are AMPA receptor complexes assembled and how is their membrane incorporation orchestrated? Who are the key players that influence homo- or heterotetramer composition? In which step of the secretory pathway are auxiliary proteins interacting and mediating the export?

6.5.1 TARP Gamma 8

From high resolution *in situ* hybridization data (Dr. Anne-Sophie Hafner and Anne Bührke in the lab, data not shown) we knew that Gamma 8 mRNA was highly restricted to somata of hippocampal neurons. CNIH2 mRNA in stark contrast, could also be found in dendrites. Does translation of these proteins follow their transcript distribution? This hypothesis would open tantalizing opportunities for selective regulation of AMPA receptors in the two different compartments.

Test of custom-produced anti-Gamma 8 antibody

In order to conduct PLA experiments for Gamma 8 and CNIH2, we first needed to identify suitable antibodies. To date, no high quality antibody against Gamma 8 was commercially available. A Gamma 8 antibody was hence custom-produced (Agrobio) targeting an extracellular loop of the protein (under the supervision of Dr. Anne-Sophie Hafner from the lab). Specificity was confirmed in HEK cells naturally lacking Gamma 8 protein (Fig 30). Cells were transfected with a Gamma 8-GFP construct and either surface labeled with the antibody or immunostained after fixation. Antibody specificity was confirmed by labeling restricted to transfected cells.

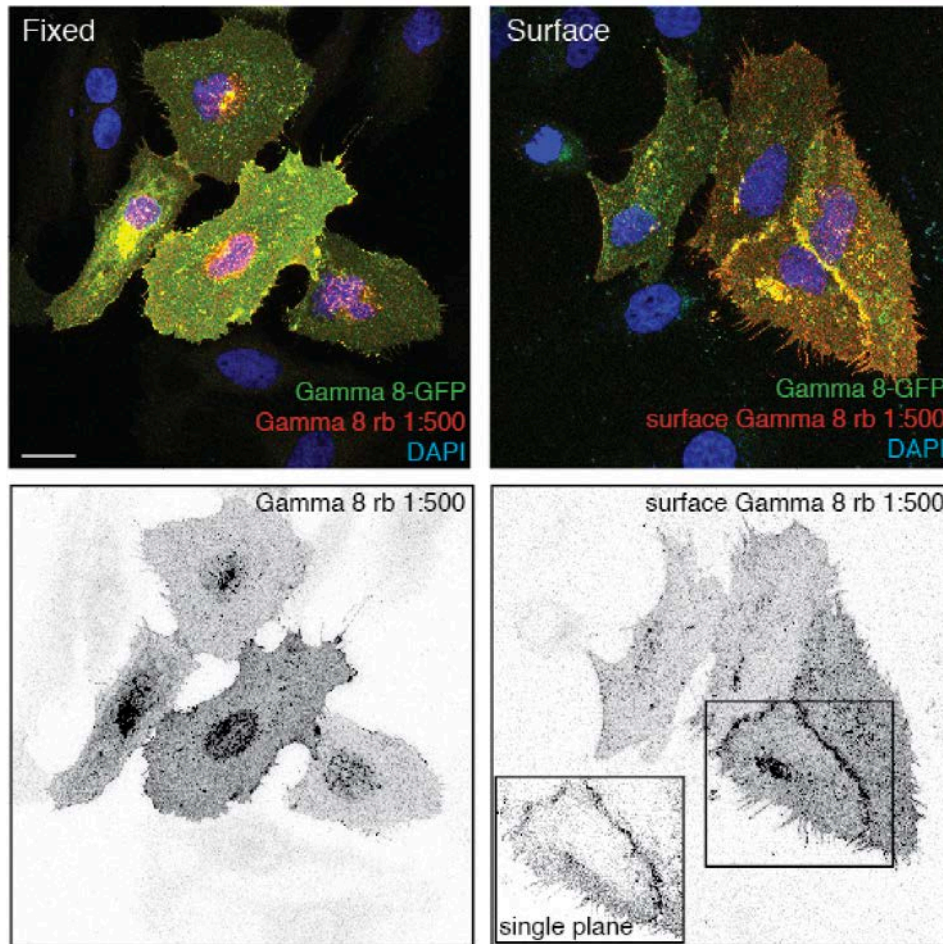


Figure 30: Specific labeling using custom-produced Gamma 8 antibody

Representative images of HEK cells transfected with Gamma 8-GFP (green). Top panel: Gamma 8 immunolabeling (red) for either total pool of Gamma 8 (left) or surface fraction (right). Adjacent nontransfected cells (only DAPI visible) show no staining. Bottom panel: Greyscale image of Gamma 8 immunolabeling. Right: surface labeling in maximum intensity projection and single plane, scale bar = 10 μm .

In surface labeling conditions, typical surface like labeling could be observed in a single plane (Fig 30 inset).

In cultured hippocampal neurons (Fig 31) different levels of Gamma 8 staining could be observed. General labeling was stronger than in the leave-out control experiment where the anti-Gamma 8 primary antibody was omitted (Fig 31 b).

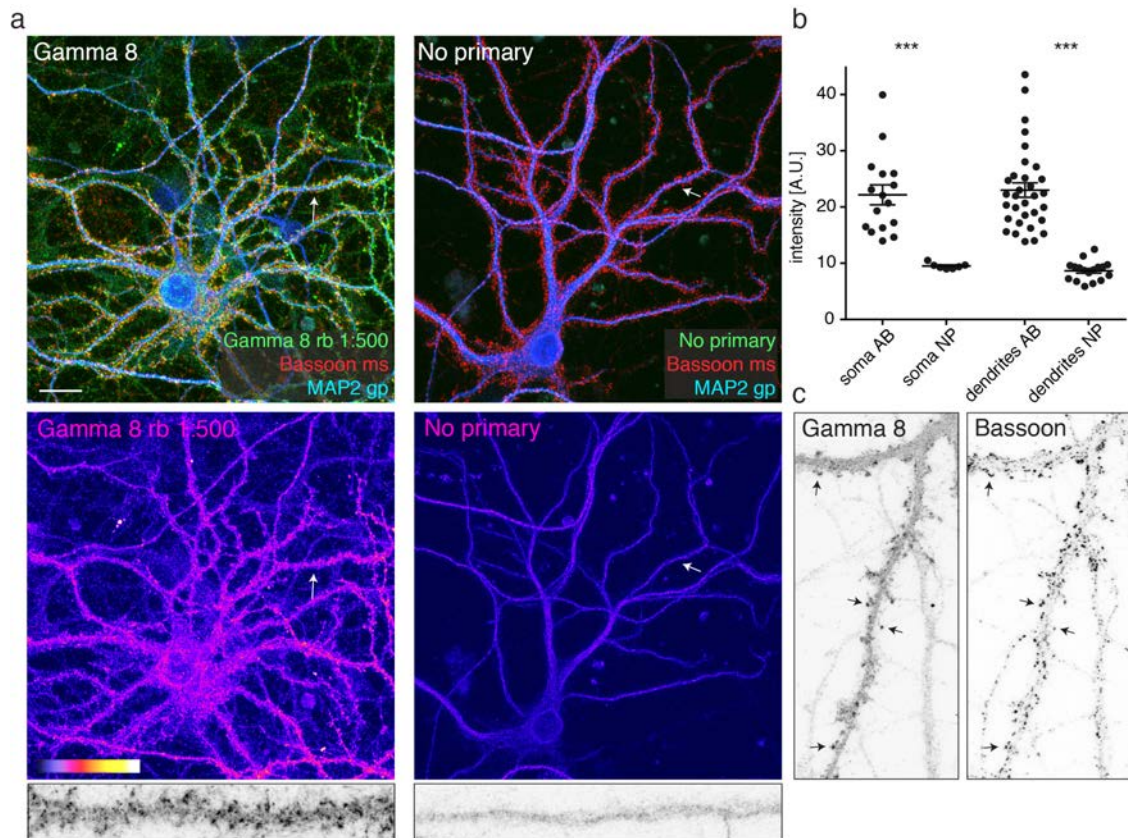


Figure 31: Custom-produced anti-Gamma 8 antibody shows staining enriched at synapses

a) Representative images of Gamma 8 labeling in cultured hippocampal neurons (DIV 26). Gamma 8 protein (green) is present in somata and dendrites (MAP2, blue) and enriched at synapses (Bassoon, red). No primary control (right panel). Bottom panel: fire look up table of Gamma 8 channel. Arrows indicate straightened dendrites shown in greyscale, scale bar = 20 μm . b) Analysis of mean labeling intensities in somata and dendrites in Gamma 8 antibody labeling (AB) and no primary antibody (NP) conditions, unpaired t-test, *** $p < 0.001$. c) Gray scale image of stretch of dendritic arbor. Co-localization of synapses labeled with bassoon and Gamma 8 (arrows).

Anti-Gamma 8 labeling was present in somata and along dendrites without a visible gradient in dendrites. In many cells, synaptic enrichment of Gamma 8 staining was observed. The synaptic nature of this accumulation was confirmed by synaptic co-staining using an anti-bassoon antibody (Fig 31 c). Gamma 8 protein labeling could be observed all along dendrites. Staining in mouse brain slices showed high Gamma 8 expression in the hippocampus with strong labeling in the neuropil layer (Dr. Anne-Sophie Hafner, data not shown). Dendritic mRNA levels for Gamma 8, however, were very low. Is Gamma 8 synthesized mainly in neuronal somata? And if so how fast does it reach dendrites and synapses after synthesis?

Gamma 8 FUNCAT-PLA reveals mainly somatic synthesis

Distribution of newly synthesized Gamma 8 protein was investigated by FUNCAT-PLA experiments after a 2 hour AHA labeling period (Fig 32). A good signal-to-noise ratio compared to the methionine negative control of 14 was achieved (Fig 32 b). Gamma 8 labeling in somata was high; dendritic signal, on the other hand, was rather sparse. Even after a relatively long labeling period of 2 hours many dendrites lacked newly synthesized Gamma 8 protein. This data fits well with the very low dendritic mRNA abundance for Gamma 8.

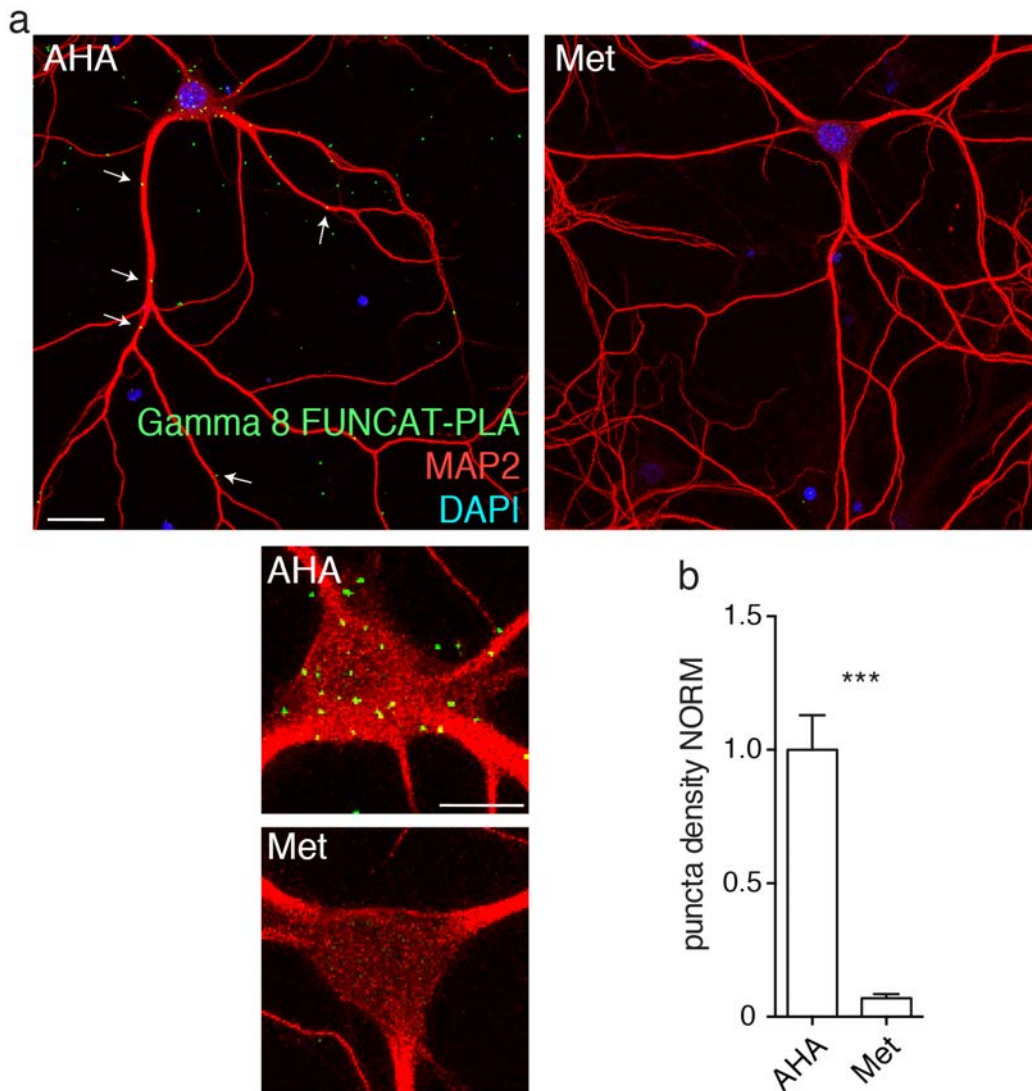


Figure 32: Low Gamma 8 FUNCAT-PLA signal in dendrites

a) Newly synthesized Gamma 8 (green) in cultured hippocampal neurons (DIV 19, 2 h AHA). Negative control methionine (Met). Cropped somatic region enlarged at the bottom, scale bar = 20 μm . b) Analysis of FUNCAT-PLA puncta density for AHA and methionine treated neurons. Means \pm SEM of $n = 13-16$ cells (1 h AHA, DIV 28 and 40) from 2 independent experiments, unpaired t-test *** $p < 0.0001$.

Pulse-chase experiments for newly synthesized Gamma 8

Gamma 8 protein displayed a pronounced dendritic staining. How long does it take for newly synthesized Gamma 8 to redistribute from soma to distal synapses to exert its function? Pulse-chase experiments for newly synthesized Gamma 8 were performed (Fig 33) with a 2 h labeling period and subsequent chase times in unlabeled medium for 0, 6, 12 or 24 h. As a negative control, methionine was added instead of AHA. The signal-to-noise ratio was sufficient (data not shown). No decay was observed in the investigated timeframe of a day (Fig 33 c). A relatively slow redistribution of puncta into dendrites over the time course of 24 h was observed (Fig 33 b, d, e).

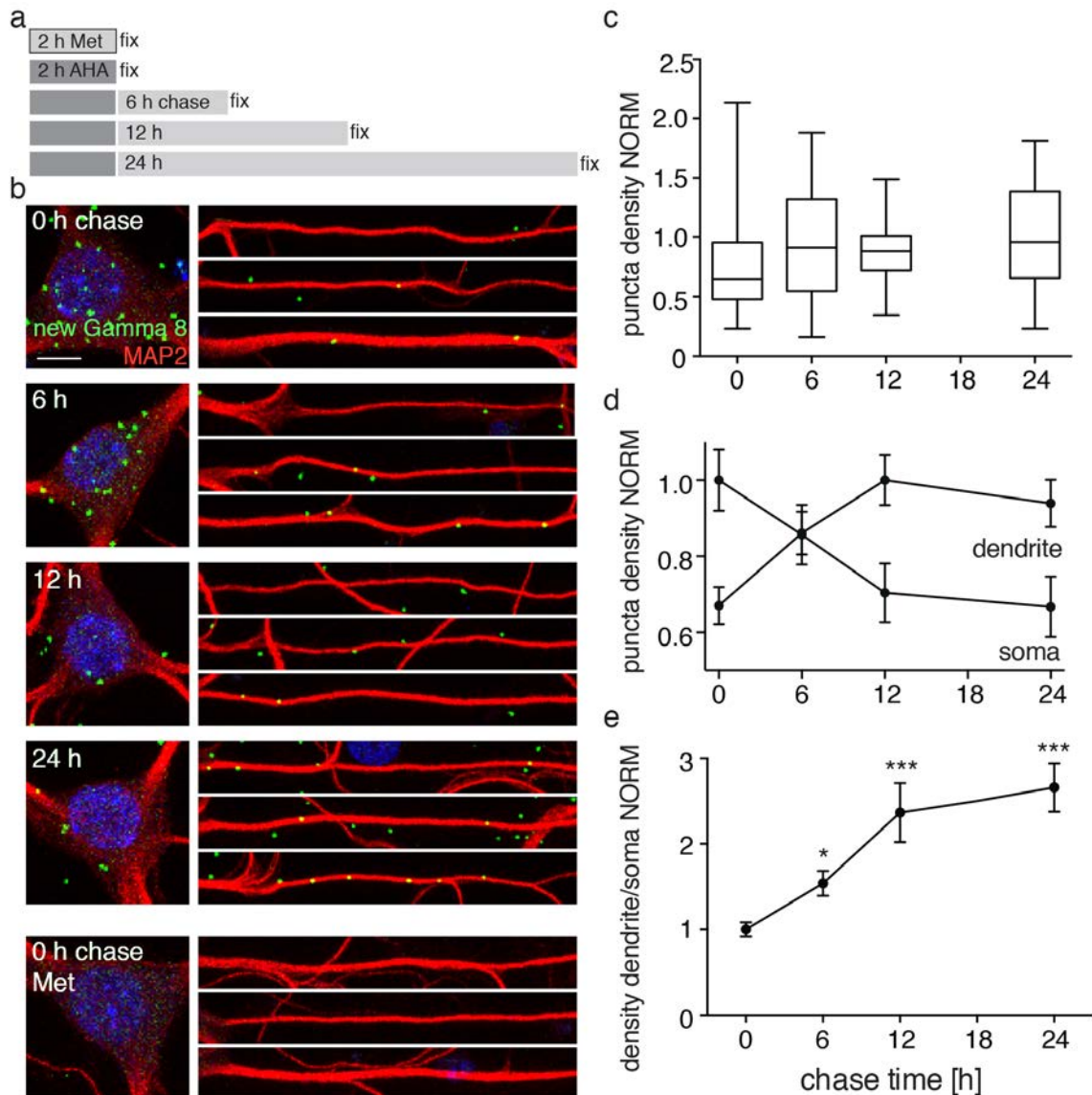


Figure 33: Pulse-chase experiments suggest a slow Gamma 8 redistribution into dendrites

a) Incubation scheme for pulse-chase experiment. b) Representative somata (left panel, DAPI blue) and straightened dendrites (right panel) of cultured hippocampal neurons (DIV 18-19) with FUNCAT-PLA signal for Gamma 8 (green) for all chase time points and methionine control (bottom). c) Box plot of total puncta density in cells (median \pm quartiles and min max values, normalized). d) Puncta density in somata and dendrites (mean \pm SEM). e) Ratio of dendritic to somatic puncta density, * $p = 0.0120$, *** $p < 0.0001$, $n = 23-43$ cells from 2 experiments.

Gamma 8 showed relatively slow redistribution kinetics. It was synthesized mainly in the soma and redistributed rather slowly over the time course of a day. The close similarities of redistribution kinetics of GluA1 and Gamma 8 will be elaborated on in the discussion.

6.5.2 FUNCAT-PLA reveals high dendritic levels of newly synthesized CNIH2

The other abundant auxiliary protein in the hippocampus is CNIH2. Its mRNA can be found in dendrites of cultured hippocampal neurons. Are these transcripts indeed used for local protein synthesis of CNIH2?

FUNCAT-PLA experiments for CNIH2 with 1 h AHA incubation were performed in cultured hippocampal neurons (Fig 34). This led to a significant labeling compared to negative controls where anisomycin was present prior and during AHA labeling or AHA was replaced by methionine (Fig 34 b).

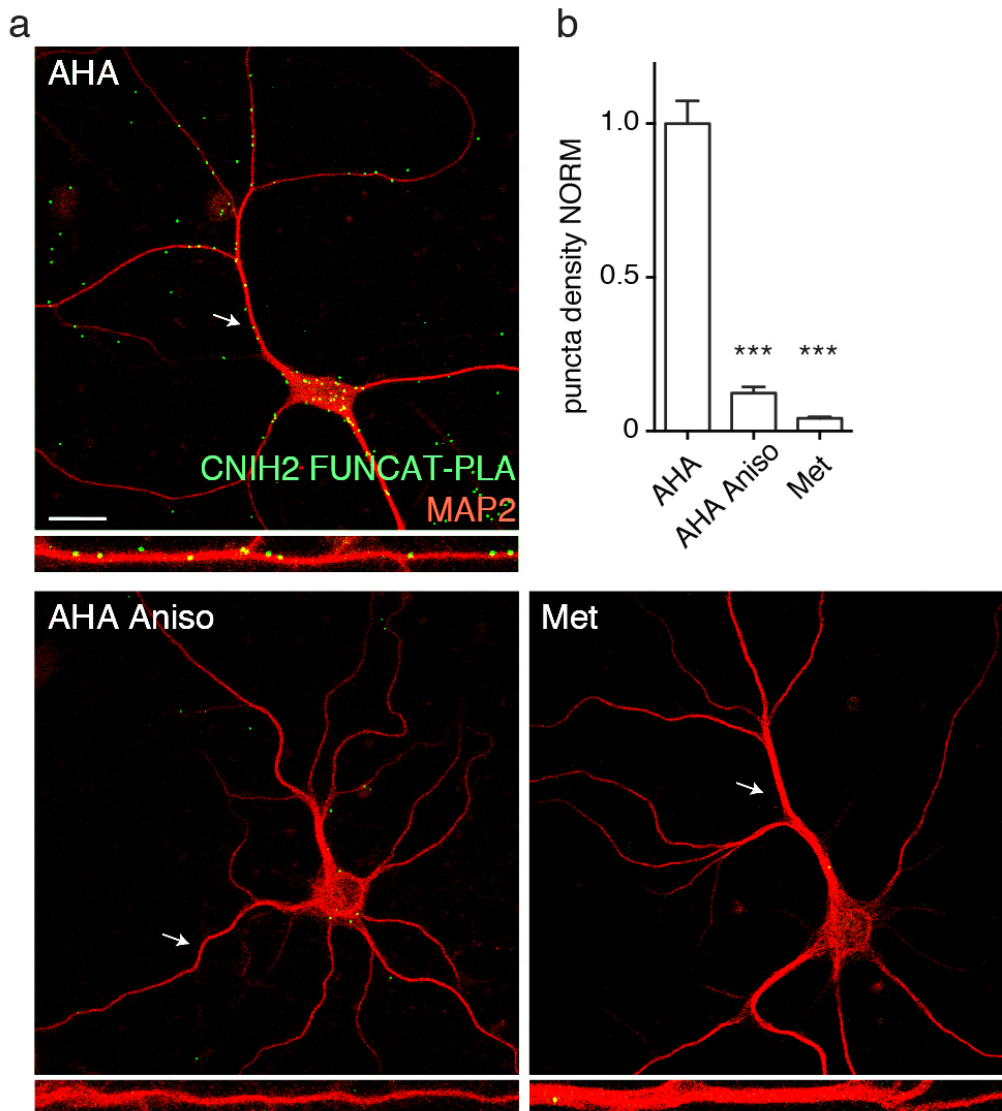


Figure 34: Newly synthesized CNIH2 can be found in neuronal somata and dendrites
a) Newly synthesized CNIH2 (green) in cultured hippocampal neurons (DIV 20, 1 h AHA). Negative controls AHA with anisomycin (Aniso) and methionine (Met). Arrows indicate straightened dendrite, scale bar = 20 μ m. b) Analysis of FUNCAT-PLA puncta density for AHA, AHA with anisomycin and methionine treated neurons, bar graph of n = 9-27 cells from 1-2 experiments, one-way ANOVA, ***p < 0.0001.

Signal to noise ratios were 8 and 24 respectively. After just 1 h of AHA labeling a lot of CNIH2 signal was observed in dendrites. On average a high fraction of the total puncta (of 80 %) were dendritic (data not shown). These data suggests the local usage of dendritic mRNA for CNIH2 for translation. Unfortunately Puro-PLA experiments for CNIH2 and Gamma 8 were not possible due to lack of available antibodies. In the future Puro-PLA experiments could confirm the local translation of CNIH2.

7. Discussion

Summary

In this study a novel technique was developed in order to, for the first time, visualize the location of specific newly synthesized proteins *in situ*. Two different labeling approaches using either AHA or puromycin were extensively tested regarding their applicability. This method was applied to answer biological questions. AMPA receptor subunits were the main focus of this study. As the main conductors of fast excitatory transmission it is crucial to understand their composition and life cycle. Investigating a subunit's site of synthesis and its redistribution after production allowed us to shed light on the eventual trajectories they might take in the secretory pathway.

Some mechanisms underlying learning and memory require the *de novo* synthesis of proteins. Neurons with their complex architecture employ localized protein synthesis in dendrites to ensure sufficient protein supply throughout the entire cell. The exact location and of protein synthesis and the identity of newly synthesized proteins is, however, not well understood in the context of synaptic plasticity. Hence, a novel method was required to investigate specific newly synthesized proteins *in situ*.

Using AHA and puromycin incorporation as a labeling strategy for nascent proteins allowed us to look at endogenous proteins and to avoid exogenous reporter systems. Combining these two metabolic labeling approaches with a co-event detection method to approach the identity of the protein we were able to probe for the first time where certain proteins are produced with subcellular resolution.

We applied this method to an open question in the synaptic plasticity field. Although incorporation of AMPA-type glutamate receptors into synapses during processes of synaptic plasticity is established, the exact regulation and localization of synthesis, trafficking and incorporation and the relative contribution of other complex constituents remain largely unresolved.

Using FUNCAT- and Puro-PLA for the main hippocampal AMPA receptor subunits GluA1, GluA2, Gamma 8 and CNIH2, we suggest a mechanism for receptor composition and synaptic receptor targeting.

7.1 Method development of FUNCAT-PLA and Puro-PLA

Combining metabolic labeling techniques for nascent proteins with a proximity ligation assay (Gustafsdottir et al. 2008) opened a new avenue to investigate specific newly synthesized proteins *in situ*. The major advantage of the method established during this thesis compared to other existing techniques is the labeling of endogenous proteins rather than using a fluorescently labeled, overexpressed protein. There are however some caveats and limitations to the technique. The co-detection is based on the relative proximity of two events. When two PLA-oligomers are brought into close proximity this leads to signal generation. Since in our technique in the current form the oligomers are coupled to secondary antibodies the

distance between the co-detected events is theoretically located anywhere in the radius of the primary antibody/secondary antibody/PLA oligomer complex. According to the manufacturers information this maximum proximity distance is 40 nm. This is relatively large compared to e.g. an AMPA receptor subunit which has a size of roughly 14 nm. Therefore a signal will be generated when the two oligos are bound via antibodies to the same protein. However, close interactions between two proteins can also give rise to close proximity (<40 nm) of the PLA oligomers – in this case if one partner is newly synthesized and the other would carry the identification epitope. The PLA technique was indeed used previously to identify interaction of proteins *in situ* (e.g. Hilbig et al. 2018; Debaize et al. 2017).

For our purpose it was hence crucial to estimate the fraction of false positive signal arising from the interaction of a pre-existing protein of interest (POI) and a different newly synthesized protein. We assessed that fraction by comparing the signals that result when an N-terminal versus C-terminal antibody against a protein of interest is used in a Puro-PLA experiment (tom Dieck et al., 2015). Our reasoning was as follows: puromycin incorporation leads to protein truncation and hence C-termini should be less abundant than N-termini in the population of puromycylated proteins. A higher Puro-PLA signal with a C-terminal antibody would argue for an intermolecular signal source. For our assay to represent intramolecular signal, the signal arising from N-terminal antibodies should hence be higher than the one from a C-terminal antibody. This was indeed the case for the protein we tested and we conclude from this finding that the majority of the signal detected represents newly synthesized protein. In principle, this control should be conducted for every POI prior to performing experiments. In reality, however, appropriate antibodies are the limiting factor and this type of investigation is not always possible.

If the majority of the signal was false positive and arose from pre-existing POI and another newly synthesized protein being close by, the PLA distribution would mirror a mix of the distribution of the total pool of the POI and the total pool of newly synthesized protein. This was, however, not the case as TARP Gamma 8 immunostaining showed labeling throughout somata and dendrites, whereas the FUNCAT-PLA signal was mainly restricted to somata (see Fig 31 and 32). In another approach we tested whether the Puro-PLA indeed depends on the *de novo* translation of the POI. We acutely knocked down CamK2 α using shRNA. Even though we were not able to identify an exact time point where mRNA levels were sufficiently reduced and at the same time pre-existing CamK2 α protein level still unchanged, Puro-PLA signal was drastically reduced in the absence of CamK2 α transcript (data not shown, revision internal figure for tom Dieck et al. 2015).

The putative contribution of signal from interactions (false positive signal) should be kept in mind while interpreting results when this point cannot be addressed experimentally. It does not prevent scientists to draw conclusions from those experiments but rather limits the type of questions which can be addressed. A disadvantageous scenario would be when an experimental manipulation results in changes in false positive or false negative detections. A complicated non-interpretable scenario would be where an experimental manipulation increases or decreases the number of level of interaction partners of the POI. More signal would be visible not because of more POI synthesized but simply because of more

interactions. Arguably this potential signal contribution is however hard to dissect out. In addition, as Puro-PLA is an antibody-based approach, the quality of the signal highly depends on antibody specificity and should be carefully evaluated prior to using it in PLA experiments (e.g. using knock out/overexpression experiments to validate the antibody).

7.1.1 Further developments of the PLA technique

How can we improve our technique?

We attempted to improve and further develop the Puro- and FUNCAT-PLA techniques. The goal of one subset of attempts was to shorten the distance for event co-detection. We tried on the one hand to directly label primary antibodies with PLA oligomers and on the other hand to click one of the oligomers directly to AHA-containing proteins. The expected advantage would be the shortening of the PLA radius and a resulting lower false positive signal.

Using a chemical reaction provided by the company (Duolink, Sigma-Aldrich), primary antibodies can be labeled directly with the PLA oligomers and as such shorten the co-detection distance. In our hands, however, this led to a very high PLA background and was not further pursued. In a second approach we clicked a PLA oligomer bearing an alkyne group directly onto AHA-labeled proteins instead of clicking biotin onto AHA and then labeling it with an anti-biotin antibody. This would reduce the co-detection radius drastically, since it removes biotin and two antibodies from the reaction. Preliminary results from this experiment did not show satisfying results as it led to a high background labeling in the absence of AHA incorporation.

A second goal for improving Puro- and FUNCAT-PLA regarded antibody choice and flexibility. In puromycin experiments antibody choice was very limited. Due to protein truncation a N-terminal antibody was needed. In addition, at the time of the work conducted in this thesis, the sole high quality anti-puromycin antibody was developed in mouse, which further limits the antibody choice against the POI since it needs to be raised in a different species. However, very recent progress in the lab includes a custom made anti-puromycin antibody in rabbit which increases the possible antibody combinations (supervised by Dr. Vidhya Rangaraju and Dr. Anne-Sophie Hafner). This new antibody showed very good results in preliminary experiments.

Even though the incorporation kinetics of metabolic labeling with AHA and puromycin were investigated in a limited time frame (5-120 min and 1-10 min for AHA and Puro, respectively, Fig 13), more experiments must be conducted to define the kinetic requirements for the two approaches over a broader time range. For AHA as well as for puromycin a saturation of labeling is expected. Long AHA labeling should eventually lead to a steady state where finally all proteins are labeled. For now, it is not clear whether or not AHA can be re-used after protein degradation. Long labeling times might also affect the cell's metabolism leading to secondary effects. A saturation curve is expected for longer puromycin labeling since truncated puromycylated proteins are degraded. Additionally puromycylated proteins are not fully functional and long puromycin labeling times might also affect cellular metabolism. The hereafter discussed unexpected signal abundance in

some pulse-chase experiments hint towards yet unknown kinetics and make further investigations of labeling kinetics crucial.

The observation of increased total FUNCAT-PLA puncta numbers in GluA1 experiments in all chase time points compared to no chase was unexpected. Since no additional labeling should be possible without AHA in the chase medium, equal or lower puncta abundances are expected in the chase conditions. One possible explanation is the close proximity of several recently synthesized GluA1 subunits which redistribute and detach from one another in chase time points. This would lead to an underestimation of newly synthesized GluA1 molecules at the earliest time point since due to steric hindrance not all newly synthesized subunits in one "cluster" can be labeled. The possibility of brighter puncta in the no chase time point due to accumulated labeling was ruled out by puncta intensity measurements (see results). Other possible explanations include the re-usage of AHA or delayed uptake of free remaining AHA within cells and delayed protein folding for proper antibody epitope recognition. If proper POI folding was not achieved within the labeling time, a higher signal in the chase conditions could arise from fully folded proteins. Additional experiments need to include a shorter chase time point (e.g. 1 h) in order to investigate if a high signal is already observed at earlier chase time points.

We decided to still use those experiments because the ratio of dendrite to soma did not vary greatly and fit into the general trend. This result suggested a similar impact of the unidentified effect on somata and dendrites.

7.1.2 Future directions of FUNCAT- or Puro-PLA experiments

The newly developed technique was already successfully used in order to address biological questions in neuroscience (Alvarez-Castelao et al., 2017; Dörrbaum, Kochen, Langer, & Schuman, 2018; Sambandan et al., 2017, tom Dieck et al., 2015 and manuscript in preparation with AMPA receptor subunit data described in the results part of this study, Hafner, Kochen et al.).

Future applications of the technique could address the following questions:

Do mRNAs have different translational efficiencies depending on their subcellular localization?

Using our technique we could investigate this on a cell-by-cell basis. High resolution FISH and Puro-PLA protocols need to be performed within the same experiment. Indeed, we started fine-tuning the two protocols in order to combine them. Together with Caspar Glock (Schuman lab) we already achieved good labeling for mRNA and newly synthesized proteins in the same sample. Due to time limitations this was not further pursued. An ideal experiment in this context would label, for example, CamK2 α mRNA and newly synthesized CamK2 α protein. Co-localization studies of the two signal species could indicate how efficient somatic and dendritic mRNA is translated.

Is the dendritic presence of an mRNA sufficient to drive translation?

It would be intriguing to know whether or not additional factors are needed for the local translation of a mRNA in dendrites. The well-known MS2/MCP system enables one to label an mRNA species of interest, artificially tagged with a stem loop sequence, with a fluorescent protein added to a coat protein tightly interacting with

that sequence (Eliscovich, Shenoy, & Singer, 2017; Park et al., 2014; Wu, Eliscovich, Yoon, & Singer, 2016). Modifications of the coat protein make it possible to target specific mRNAs to the desired subcellular location. In our lab we used e.g. a PSD95-MCP-fusion-construct to drag and target an mRNA to synapses. Experiments were started but not yet fully conclusive: we could successfully target mRNAs to dendrites. Puro-PLA experiments in order to investigate whether or not the artificial dendritic mRNA localization was sufficient to drive its translation however did not yet lead to clear results. Technical hurdles included the fine-tuning of transfection conditions, the expression period of constructs and puro labeling times.

Which cell-type specific differences are there in the production of specific proteins?

FUNCAT-PLA and Puro-PLA enable us to look at newly synthesized proteins with single cell resolution. Cell type differences in translation are often overlooked when e.g. analyzing a pool of cells using mass spectrometry. To investigate the contribution of different cell types, PLA experiments could be combined with cell-type-specific markers. Recent developments enable us to label the proteome of one specific cell type (Alvarez-Castelao et al. 2017). The expression of a mutant methionyl-tRNA-synthetase enables cells to incorporate a larger non-canonical amino acid (ANL) into newly synthesized proteins which cannot be incorporated by wild type cells carrying only the regular methionyl-tRNA-synthetase. Following ANL labeling in cells carrying the mutated version in a cell type specific manner, FUNCAT-PLA signal is only present in these cells (Alvarez-Castelao et al., 2017).

What are protein half-lives in single cells?

In order to grasp a protein's role within a cell, its full life cycle must be investigated: its synthesis and degradation rates - the protein half-life. For this purpose mRNA detection, Puro-PLA and total protein immunolabeling would ideally be performed on the same cell. This is technically challenging and not feasible at the moment. In collaboration with Yombe Fonkeu from the Tchumatchenko lab we nevertheless started looking at this question on a group data level. Distributions of CamK2 α mRNA and newly synthesized CamK2 α protein were labeled in separate dishes. Analysis on the group level could already give hints about whether or not there are differences in translation efficiency along dendrites (manuscript in preparation).

7.2 AMPA receptor complex composition and redistribution kinetics

We used the novel technique described in this thesis to intensively study the AMPA receptor complex production and redistribution kinetics. AMPA-type glutamate receptors are the main neurotransmitter of fast excitatory transmission in the CNS. Their composition of pore-forming and non-pore-forming subunits has a huge influence on their signaling properties and forward trafficking. How this composition is orchestrated is still unclear. If we knew where different subunits are made and had ideas about their redistribution kinetics we might be able to infer some general rules of how macromolecular AMPA complexes are formed and synaptically

targeted. Even though the relationship between changes in synaptic AMPA receptor abundance and synaptic plasticity is known, the role of AMPA receptor *de novo* synthesis in this context is not well understood. We used FUNCAT- and Puro-PLA to investigate site of synthesis and redistribution kinetics of the main hippocampal AMPA receptor subunits; GluA1, GluA2, TARP Gamma 8 and CNIH2. We designed the experiments to address the following core questions:

Are AMPA subunits locally synthesized in dendrites?

How fast do these newly synthesized receptors reach the plasma membrane?

Do the receptors traffic through the secretory pathway?

We first started with the pore-forming subunits GluA1 and GluA2. Are they locally synthesized and can we detect differences in their site of production? Under basal conditions local subunit production was not very high for either subunits as shown by low Puro-PLA signal of only 17 % in dendrites. We however observed stark differences in their relative dendritic abundance after a relatively short AHA labeling period. More newly synthesized GluA2 was found in dendrites.

In order to rule out that this finding is rather a detection limit problem, these experiments will be repeated in the future using different antibodies recognizing GluA1 and GluA2. Preliminary data from Dr. Anne-Sophie Hafner in the lab using an antibody pair of mouse-anti-GluA2 and rabbit-anti-puromycin confirmed our result of very low dendritic Puro-PLA labeling for GluA2 under basal activity. The higher dendritic abundance of FUNCAT-PLA for GluA2 might thus reflect faster redistribution into dendrites after synthesis compared to GluA1.

That hypothesis is strengthened by recent findings of Hanus et al. where a fraction of GluA2 subunits at the plasma membrane displays glycosylation patterns that indicate a bypass of the somatic Golgi (Hanus et al. 2016). AMPA receptor subunits as part of the membrane protein family are synthesized, post translationally modified (e.g. glycosylated) and processed along the secretory pathway, canonically including ER, ERGIC, Golgi and the trans-golgi-network. Canonical glycosylation is finalized in the Golgi apparatus, which can be found only in neuron's cell body. Most dendrites and axons are devoid of Golgi membranes. Occasionally Golgi outposts were reported in dendrites (Horton & Ehlers 2004). The low fraction of 18 % of hippocampal neurons possessing one golgi outpost in one dendrite within the first 30 microns is however barely sufficient to process all localized membrane proteins. The presence of core glycosylated proteins (bearing immature glycan trees) at the neuronal plasma membrane showed that neurons are able to bypass the Golgi apparatus and traffic membrane proteins to the surface without its function (Hanus et al. 2016). From the glycosylation pattern of a given membrane protein we can hence draw conclusions about its location within the secretory pathway and whether or not it travels through the Golgi. Surface GluA1 subunits, on the other hand show 100 % regular glycosylation patterns, indicating that they are all processed in the somatic Golgi apparatus.

Our data suggest that all newly synthesized GluA1 bearing receptors travel through the somatically localized Golgi, whereas a sub-pool of GluA2 containing receptors bypasses the somatic Golgi and gets successfully incorporated into the plasma membrane carrying immature glycan trees. In future experiments pulse-chase

FUNCAT-PLA experiments could be combined with Golgi markers (e.g. gm130 immunolabeling or VSVG transfection prior to labeling). This would enable us to investigate the route a population of newly synthesized receptors is taking, when and if it passes through the Golgi apparatus.

It would be intriguing to test whether the artificial enrichment of dendritic mRNA for a membrane protein, such as an AMPA receptor, alters its glycosylation pattern since it would be forced to bypass the somatic Golgi apparatus. These experiments are already possible using the above mentioned technique to artificially stabilize mRNAs in the vicinity of synapses.

It is important to note that from these experiments conclusions about absolute subunit production cannot be drawn. Since the PLA technique depends on antibody specificity and binding efficiency, two different proteins cannot be directly compared with respect to their total abundance. We can however assume that antibody binding is comparable in different cellular compartments and hence relative comparisons can be done (e.g. Fig 19). It remains to be elucidated in which proportion the different subunits are produced. Additional techniques (e.g. single cell/single dendrite mass spectrometry) must be applied in the future in order to address the absolute abundance of proteins.

We still cannot rule out that the low dendritic abundance of Puro-PLA signal for GluA1 and GluA2 is due to the sensitivity threshold. The presence of GluA1 and GluA2 mRNAs in dendrites (Cajigas et al. 2012) indicates at least the possibility for local subunit synthesis. All of the above mentioned experiments were conducted under basal neuronal activity. FUNCAT and Puro-PLA experiments need to be repeated in regimes of elevated or reduced neuronal activity. Under basal conditions, the somatic synthesis of AMPA receptor subunits might be prevalent whereas local changes in activity might change the rate of local synthesis. In future experiments bath applied stimulants (e.g. BDNF) to trigger synaptic potentiation could be used and site of synthesis of subunits investigated using Puro-PLA.

Even more intriguing would be experiments where local glutamate uncaging using a two-photon laser could stimulate single synapses or a stretch of dendrite. Subsequent differences in subunit production in this stimulated branch compared to un-stimulated sister dendrites could indicate the importance of local synthesis in an input-specific fashion. We already conducted pilot uncaging experiments with subsequent Puro-PLA for GluA1. The results of these initial experiments were inconclusive. This is mainly due to the complex nature of this type of experiments. Multiple parameters need to be optimized under new conditions; for example, puromycin labeling must be conducted directly under the microscope in the cell's imaging medium and with lower temperature than in the incubator. Cells must additionally be transfected with calcium indicators prior to uncaging to control for successful synaptic activation. The timing of synaptic activation, puromycin labeling and fixation must be adjusted and various stimulation protocols tested.

7.2.1 GluA1 and GluA2 surface expression

How much of a pool of newly synthesized receptors is present at the surface after a given time? How fast does a newly synthesized subunit reach its ultimate target: the synapse?

In previous experiments we observed a higher relative dendritic fraction of newly synthesized GluA2 compared to GluA1. Does that finding translate into higher surface fractions of new GluA2 or is the dendritic pool mainly intracellular?

To address this question we performed FUNCAT-PLA experiments where we in parallel labeled the total pool of newly synthesized receptor and only the fraction which was already present at the surface within the labeling period. We observed that newly synthesized GluA2 stayed mostly intracellular in the investigated time frame (68 %), whereas a large fraction (ca 75 %) of newly synthesized GluA1 was already present at the surface.

These experiments however need to be repeated side by side with a single batch of cultured hippocampal neurons. A final conclusion cannot yet be drawn since AHA labeling was done for 2 h in the GluA1 experiment whereas only 1 h in the case of GluA2. This gives GluA1 potentially a longer time to redistribute after synthesis and reach the surface. If it still holds true that there is indeed more new GluA1 at the surface it would indicate that GluA1 is more efficiently exported to the plasma membrane and dendritic GluA2 serves rather as an intracellular pool.

Future experiments should also include pulse-chase FUNCAT-PLA to investigate how fast newly synthesized subunits reach the cell's plasma membrane and whether or not there are differences in half-life for receptors at the surface and the total pool. Intriguing experiments would include neuronal stimulation and several chase time points to test whether or not changes in a cell's activity could trigger faster new GluA1 or GluA2 exocytosis from somata and dendrites.

Are exocytosis rates similar or do they vary between different compartments? We did not observe differences in plasma membrane abundance of new receptors between somata and dendrites for both subunits. In future analyses, however, it would be worth investigating this question more closely. In the current version of puncta analysis the third dimension of image stacks is not taken into account. Due to its relative roundness, the soma surface is underestimated in the current analysis and absolute density numbers for soma and dendrites cannot be compared.

Increased ER complexity was found at dendritic branch points (Cui-Wang et al., 2012). These ER complexities produced an increase in surface AMPA receptor levels. With our technique we could address whether or not newly synthesized receptors accumulate at branch points intracellularly and or at the plasma membrane by analyzing puncta accumulation around branch points for surface and total FUNCAT-PLA.

How can we label synapses in FUNCAT-PLA experiments?

One key aspect that yet remains to be elucidated is how much of the surface receptor is already located at synapses: the point of action for AMPA receptors. Surface FUNCAT-PLA experiments including synaptic markers must be conducted. Unfortunately, attempts to label synapses in this type of experiments were not successful in the past. Synaptic antibody choice is limited due to PLA (PLA antibody pair typically rabbit and mouse). Additional labeling of the cell outline (e.g. MAP2) must be always present to identify cells. Synaptic staining using phalloidin or various antibodies against synaptic markers (e.g. Vglut, bassoon) was weakened in FUNCAT-PLA experiments. Synaptic labeling using regular immunostaining showed the possibility of successfully labeling synapses in cultured hippocampal neurons of various ages (2 weeks until 2 months in culture, Fig 35).

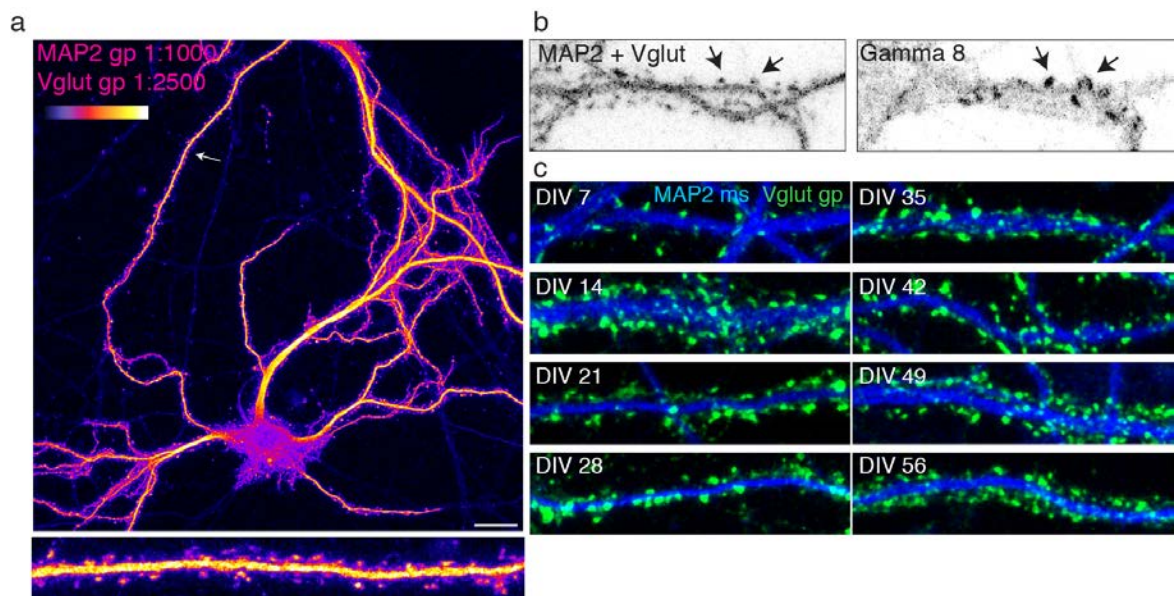


Figure 35: Synapse labeling using an anti-Vglut antibody

a) Representative image of dendrites (MAP2) and synapses (Vglut1) stained in the same color channel in cultured hippocampal neurons (DIV 49), fire look up table. Arrow indicates the dendrite straightened in the bottom panel. b) Greyscale images of stretch of dendritic arbor. Co-localization of Vglut1 and Gamma 8 staining (arrows). c) Synaptic labeling using the anti-Vglut1 antibody (green) in cultured hippocampal neurons of different ages (1-8 weeks), MAP2 in blue, scale bar = 10 μ m.

Repeated additional tests revealed that in case of phalloidin labeling the copper mediated click reaction interfered with successful staining. In case of antibody based synapse recognition the underlying reason was not yet identified.

For future experiments it is still crucial to co-label synapses. We need to know how much of the surface fraction of a newly synthesized receptor is present at synapses. Are most of the surface receptors efficiently targeted to synapses or is the bottle neck rather the process of exocytosis? This would be shown by a relatively small synaptic fraction of surface receptors. These findings would have strong implications in understanding the routes AMPA receptor subunits take. What are the points of action for modulation and regulation for synaptic AMPA receptors (local synthesis, ER export, exocytosis, synaptic targeting)? Even if more newly

synthesized GluA1 subunits make it to the neuronal surface compared to GluA2 in a given time, it might still be that most of the GluA1 subunits are extrasynaptic but the majority of new GluA2 is already synaptic.

7.2.2 Redistribution kinetics of new GluA1 and new GluA2

How fast do newly synthesized AMPA receptor subunits redistribute after synthesis? Puro-PLA experiments indicated that dendritic synthesis under basal activity conditions is rather low for both subunits. It was, however, not absent since both subunits showed 17 % of Puro-PLA signal in dendrites after a very short labeling period. Newly synthesized GluA2 however was found rapidly in dendrites whereas newly synthesized GluA1 redistributed only in the time course of a day into dendrites. This would imply that GluA2 uses more efficient means to redistribute after pronounced somatic synthesis.

Comparing pulse-chase experiments of GluA1 and GluA2 showed drastic differences, with GluA2 redistributing much faster into dendrites. A shorter AHA labeling period was needed for GluA2 to prevent pronounced dendritic signal already at the time point zero. Some dendritic labeling was already observed at a short labeling time of 20 mins, as 62 % of puncta were already found in dendrites. Intuitively one would rate this percentage as high. However, given the much higher dendritic than somatic area this is rather low. The presence of some puncta in dendrites after 20 minutes of labeling could indicate local production of GluA2 or redistributed receptors from the soma. In principle, labeling time could be decreased even more by addition of a methionine starvation step prior to AHA labeling. Methionine starvation however is a trigger for cellular stress and we hence tried to avoid it whenever possible. For GluA2 the fraction of dendritic puncta increased from 62 % to 74 % after 40 mins of chase time. In comparison, a similar increase in dendritic GluA1 fraction was observed in a much longer chase time period of 12 hours (Fig 26).

In future experiments longer chase periods must be chosen for both subunits to investigate the plateau time point at which no further shift towards dendrites can be observed. More detailed puncta analysis must be conducted to observe how puncta distances from the soma change over time. How do newly synthesized AMPA receptors populate dendrites?

GluA2 pulse-chase experiments remain to be repeated but if the results are reproduced our data would indicate that both pore-forming subunits are prevalently synthesized somatically under basal conditions. After synthesis GluA2 redistributes faster into dendrites. This result indicates a different route of secretory trafficking or at least a more efficient underlying mechanism. In this scenario GluA2 would serve as a local pool of new AMPA receptor subunits and could be used to respond fast to external stimuli. Redistribution of new GluA1 happens only in the order of a day and is hence too slow for rapid activity triggered responses. Pre-existing intracellular or surface-extrasynaptic GluA1 receptors could be however synaptically targeted in an input specific manner by auxiliary proteins. It remains to be elucidated how changes

in activity influence these mechanisms. Do certain stimuli induce local synthesis of GluA1 and GluA2 or can redistribution dynamics be altered?

7.3 Auxiliary proteins TARP Gamma 8 and CNIH2

Are non-pore-forming subunits of the hippocampus locally produced in dendrites? How do they redistribute after synthesis? At which step in the secretory pathway do they interact with pore-forming subunits?

To our surprise we found stark differences in the site of synthesis of Gamma 8 and CNIH2. Whereas FUNCAT-PLA signal for Gamma 8 was mainly found in neuronal somata, newly synthesized CNIH2 was detected in dendrites. FUNCAT-PLA distribution of both subunits matched nicely their respective mRNA localization, as only CNIH2 transcripts could be found in dendrites (high resolution FISH from Dr. Anne-Sophie Hafner and Anne Bührke). Somatic synthesized Gamma 8 redistributed into dendrites over a rather slow time course of a day. Striking similarities of redistribution kinetics between GluA1 and Gamma 8 were observed. We hypothesize that somatic GluA1 and Gamma 8 assemble and travel together to synapses. This hypothesis gets support again from their glycosylation status at the plasma membrane indicating that they both get processed in the somatic Golgi before accessing the plasma membrane (Hanus et al., 2016).

The half-life data for TARP Gamma 8 are not available probably due to its relative small size. Pulse-chase experiments for newly synthesized Gamma 8 however showed no decrease in the total abundance over the time course of 24 h. With a half-life of less than 24 h we would have observed a reduction of total puncta density in our experiments. We can hence conclude that TARP Gamma 8 is not a very short-lived protein under these conditions. Future directions could include longer chase periods to investigate its half-life as FUNCAT-PLA proved already suitable for half-life determination with single cell resolution (tom Dieck et al., 2015). In order to validate the local synthesis of CNIH2 protein, Puro-PLA experiments or FUNCAT-PLA experiments with shorter AHA labeling times must be conducted in the future. Until now Puro-PLA experiments for CNIH2 were not possible due to the lack of a suitable antibody pair. If in these experiments the local synthesis is validated, it would open a tantalizing role of CNIH2 in dendrites to mediate local AMPA receptor release into synapses after stimuli induced protein synthesis. Unpublished data from the lab (Dr. Anne-Sophie Hafner and Anne Bührke) indeed point in that direction. Knock down studies where CNIH2 protein was acutely down regulated using specific shRNAs showed a decrease in surface levels of newly synthesized GluA2. Surface new GluA1 levels however remained unchanged. This would indicate a GluA2-specific role of CNIH2. Work from the Nicoll lab (Herring et al., 2013) reports an exclusive GluA1 selectivity of CNIH2, our effect on surface GluA2 however clearly indicates otherwise.

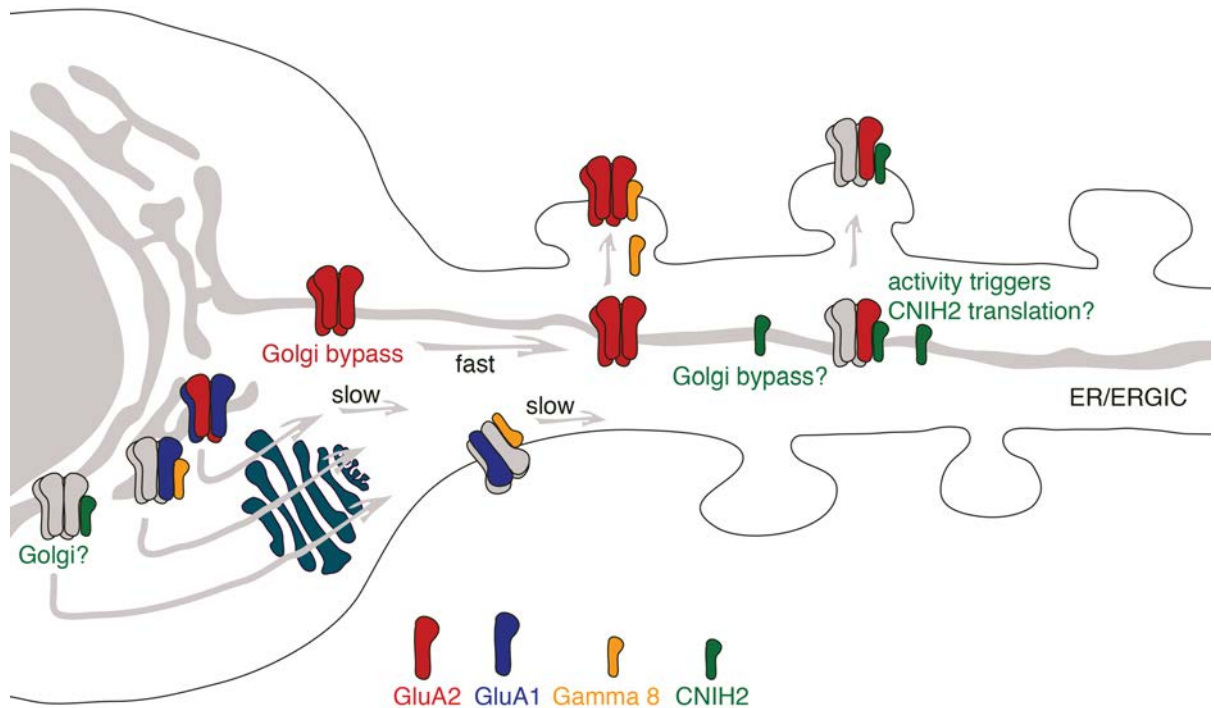


Figure 36: Proposed scenario of AMPA receptor subunit synthesis and trafficking

Summarizing a potential scenario based on the data of this study (Fig 36), Gamma 8 and GluA1 are prevalently synthesized in the soma under basal conditions and get processed through the Golgi. They co-redistribute slowly into dendrites. Along their way they might already get exocytosed given the relative high surface fraction of newly synthesized GluA1. Regulation during synaptic plasticity is possible since C-terminal phosphorylation of Gamma 8 via CamK2 α has a known role in LTP and LTD (Tomita, Stein, Stocker, Nicoll, & Brecht, 2005). CNIH2 potentially interacts in both somata and dendrites with pore-forming subunits. We hypothesize that the local translation of CNIH2 can be triggered by synaptic activity and the resulting surface targeting of AMPA receptors would be a thus far undiscovered way for activity-triggered protein synthesis-dependent AMPA receptor surface expression. GluA1/2 heteromers form in the ER and get processed through the Golgi. They are by far the most dominant combination in CA1 neurons (ca 80 %, Lu et al., 2009). Even though many X-ray crystallography studies are performed on GluA2 homomers (e.g. Rossmann et al., 2011), they are reported not to form *in vivo* (Greger & Esteban, 2007). Our data indicate however that they might form, bypass the somatic Golgi and in this way redistribute faster into dendrites. In dendrites binding to pre-existing Gamma 8 would be possible which promotes trafficking to the plasma membrane and synaptic targeting. Whether or not pre-existing tetramers can associate locally with auxiliary proteins and whether or not this could be triggered by synaptic plasticity will be a core question for future work. It remains to be elucidated whether TARP Gamma 8's main function for forward trafficking is exerted in the Golgi and CNIH2 carries a specific role in dendrites for a compartment specific regulation of AMPA surface expression. The novel technique gave us the unique opportunity to investigate protein synthesis of specific proteins of interest in single cells. We used it to answer some thrilling questions about

AMPA-type receptor life-cycles. In the future the method will enable us to answer core questions of synaptic plasticity and will certainly be of use for the scientific community beyond neuroscience.

8. References

- Aakalu, G. et al., 2001. Dynamic visualization of local protein synthesis in hippocampal neurons. *Neuron*, 30(2), pp.489–502.
- Agranoff, B.W. & Klinger, P.D., 1964. Puromycin effect on memory fixation in the goldfish. *Science*.
- Alvarez-Castelao, B. et al., 2017. Cell-type-specific metabolic labeling of nascent proteomes in vivo. *Nature biotechnology*, 35(12), pp.1196–1201.
- Alvarez-Miranda, E.A., Sinnl, M. & Farhan, H., 2015. Alteration of Golgi Structure by Stress: A Link to Neurodegeneration? . *Frontiers in Neuroscience* , 9, p.435.
- Amaral, D.G. & Witter, M.P., 1989. The three-dimensional organization of the hippocampal formation: A review of anatomical data. *Neuroscience*, 31(3), pp.571–591.
- Andersen, P., Morris, R., Amaral, D., Bliss, T., and O'Keefe, J., 2007. *The Hippocampus Book*, Oxford, Oxford University Press.
- Banker, G. & Goslin, K., 1991. *Culturing nerve cells*, Cellular and Molecular Neuroscience.
- Bedoukian, M.A. et al., 2008. The Stargazin C Terminus Encodes an Intrinsic and Transferable Membrane Sorting Signal. *Journal of Biological Chemistry* , 283(3), pp.1597–1600.
- Bedoukian, M.A., Weeks, A.M. & Partin, K.M., 2006. Different Domains of the AMPA Receptor Direct Stargazin-mediated Trafficking and Stargazin-mediated Modulation of Kinetics. *Journal of Biological Chemistry* , 281(33), pp.23908–23921.
- de Belleruche, J.S. & Bradford, H.F., 1972. Synaptosome beds: a method for the study in vitro of the metabolism and function of nerve endings. *Biochemical Journal*, 127(2), p.21P.
- Beneyto, M. & Meador-Woodruff, J.H., 2006. Lamina-specific abnormalities of AMPA receptor trafficking and signaling molecule transcripts in the prefrontal cortex in schizophrenia. *Synapse*, 60(8), pp.585–598.
- Bennett, J.A. & Dingledine, R., 1995. Topology profile for a glutamate receptor: Three transmembrane domains and a channel-lining reentrant membrane loop. *Neuron*, 14(2), pp.373–384.
- Bi, G. & Poo, M., 2001. Synaptic Modification by Correlated Activity: Hebb's Postulate Revisited. *Annual Review of Neuroscience*, 24(1), pp.139–166.
- Blaustein, M.P. & Goldring, J.M., 1975. Membrane potentials in pinched-off presynaptic nerve terminals monitored with a fluorescent probe: evidence that synaptosomes have potassium diffusion potentials. *The Journal of Physiology*, 247(3), pp.589–615.
- Bliss, T.V.P. & Collingridge, G.L., 1993. A synaptic model of memory: long-term potentiation in the hippocampus. *Nature*, 361, p.31.
- Bliss, T.V.P. & Lømo, T., 1973. Long-lasting potentiation of synaptic transmission in the dentate area of the anaesthetized rabbit following stimulation of the perforant path. *The Journal of Physiology*, 232(2), pp.331–356.
- Borgdorff, A.J. & Choquet, D., 2002. Regulation of AMPA receptor lateral movements. *Nature*, 417, p.649.
- Boudkazi, S. et al., 2014. Cornichon2 Dictates the Time Course of Excitatory Transmission at Individual Hippocampal Synapses. *Neuron*, 82(4), pp.848–858.
- Bourne, J. et al., 2006. Polyribosomes are increased in spines of CA1 dendrites 2 h after the induction of LTP in mature rat hippocampal slices. *Hippocampus*, 17(1), pp.1–4.
- Bradshaw, K., Emptage N & Bliss, T.V.P., 2003. A role for dendritic protein synthesis in

- hippocampal late LTP. *European Journal of Neuroscience*, 18(11), pp.3150–3152.
- Brink, J.J., Davis, R.E. & Agranoff, B.W., 1966. Effects of puromycin, acetoxycycloheximide and actinomycin D on protein synthesis in goldfish brain. *Journal of neurochemistry*.
- Brockie, P. & V Maricq, A., 2010. In a Pickle: Is Cornichon Just Relish or Part of the Main Dish? *Neuron*, 68, pp.1017–1019.
- Bruns, D. & Jahn, R., 1995. Real-time measurement of transmitter release from single synaptic vesicles. *Nature*, 377, pp.62–65.
- Cajigas, I.J. et al., 2012. The Local Transcriptome in the Synaptic Neuropil Revealed by Deep Sequencing and High-Resolution Imaging. *Neuron*, 74(3), pp.453–466.
- Cembrowski, M.S. et al., 2016. Hipposeq: a comprehensive RNA-seq database of gene expression in hippocampal principal neurons. *eLife*, 5, p.e14997.
- Chen, L. et al., 1999. Impaired cerebellar synapse maturation in waggler, a mutant mouse with a disrupted neuronal calcium channel γ subunit. *Proceedings of the National Academy of Sciences*, 96(21), p.12132 LP-12137.
- Chen, L. et al., 2000. Stargazin regulates synaptic targeting of AMPA receptors by two distinct mechanisms. *Nature*, 408(6815), pp.936–943.
- Cho, C.-H. et al., 2007. Two Families of TARP Isoforms that Have Distinct Effects on the Kinetic Properties of AMPA Receptors and Synaptic Currents. *Neuron*, 55(6), pp.890–904.
- Clark, B.D., Goldberg, E.M. & Rudy, B., 2009. Electrogenic Tuning of the Axon Initial Segment. *The Neuroscientist: a review journal bringing neurobiology, neurology and psychiatry*, 15(6), pp.651–668.
- Cohen, L.D. et al., 2013. Metabolic Turnover of Synaptic Proteins: Kinetics, Interdependencies and Implications for Synaptic Maintenance. *PLoS one*, 8(5), p.e63191.
- Colbert, C.M. & Johnston, D., 1996. Axonal Action-Potential Initiation and Na⁺ Channel Densities in the Soma and Axon Initial Segment of Subicular Pyramidal Neurons. *The Journal of Neuroscience*, 16(21), p.6676 LP-6686.
- Collingridge, G.L. et al., 2010. Long-term depression in the CNS. *Nature Reviews Neuroscience*, 11, p.459.
- Constals, A. et al., 2015. Glutamate-Induced AMPA Receptor Desensitization Increases Their Mobility and Modulates Short-Term Plasticity through Unbinding from Stargazin. *Neuron*, 85(4), pp.787–803.
- Cooper, L.N. & Bear, M.F., 2012. The BCM theory of synapse modification at 30: interaction of theory with experiment. *Nature Reviews Neuroscience*, 13, p.798.
- Cui-Wang, T. et al., 2012. Local Zones of Endoplasmic Reticulum Complexity Confine Cargo in Neuronal Dendrites. *Cell*, 148(1–2), pp.309–321.
- Cylwik, B. et al., 2013. Congenital disorders of glycosylation. Part I. Defects of protein N-glycosylation. *Acta biochimica Polonica*, 60(2), pp.151–161.
- Debaize, L. et al., 2017. Optimization of proximity ligation assay (PLA) for detection of protein interactions and fusion proteins in non-adherent cells: application to pre-B lymphocytes. *Molecular Cytogenetics*, 10, p.27.
- Dikic, I., 2017. Proteasomal and Autophagic Degradation Systems. *Annual Review of Biochemistry*, 86(1), pp.193–224.
- Dörrbaum, A.R. et al., 2018. Local and global influences on protein turnover in neurons and glia M. V Chao, ed. *eLife*, 7, p.e34202.
- Doyle, J.P. et al., 2008. Application of a Translational Profiling Approach for the Comparative Analysis of CNS Cell Types. *Cell*, 135(4), pp.749–762.
- Edward, K., 1967. Synthetic mechanisms in the axon - in vitro incorporation of [3H] precursors into axonal protein and RNA. *Journal of Neurochemistry*, 14(4), pp.437–446.

- Ehlers, M.D. et al., 2007. Diffusional Trapping of GluR1 AMPA Receptors by Input-Specific Synaptic Activity. *Neuron*, 54(3), pp.447–460.
- Flexner, J.B. & Flexner, L.B., 1969. Studies on memory: evidence for a widespread memory trace in the neocortex after the suppression of recent memory of puromycin. *Proceedings of the National Academy of Sciences of the United States of America*, 62(3), pp.729–732.
- Fukaya, M. et al., 2005. Spatial diversity in gene expression for VDCC γ subunit family in developing and adult mouse brains. *Neuroscience Research*, 53(4), pp.376–383.
- Govindarajan, A. et al., 2011. The dendritic branch is the preferred integrative unit for protein synthesis-dependent LTP. *Neuron*, 69(1), pp.132–146.
- Graber, T.E. et al., 2013. Reactivation of stalled polyribosomes in synaptic plasticity. *Proceedings of the National Academy of Sciences of the United States of America*, 110(40), pp.16205–16210.
- Granger, A.J. et al., 2013. LTP requires a reserve pool of glutamate receptors independent of subunit type. *Nature*, 493(7433), pp.495–500.
- Greger, I. & Esteban, J., 2007. AMPA receptor biogenesis and trafficking. *Current opinion in neurobiology*, 17, pp.289–297.
- Greger, I.H. et al., 2003. AMPA Receptor Tetramerization Is Mediated by Q/R Editing. *Neuron*, 40(4), pp.763–774.
- Guillaud, L., Wong, R. & Hirokawa, N., 2008. Disruption of KIF17-Mint1 interaction by CaMKII-dependent phosphorylation: a molecular model of kinesin-cargo release. *Nature Cell Biology*, 10(1), pp.19–29.
- Gustafsdottir, S.M. et al., 2008. Use of Proximity Ligation to Screen for Inhibitors of Interactions between Vascular Endothelial Growth Factor A and Its Receptors. *Clinical chemistry*, 54(7), pp.1218–1225.
- Hafner, A.-S. et al., 2015. Lengthening of the Stargazin Cytoplasmic Tail Increases Synaptic Transmission by Promoting Interaction to Deeper Domains of PSD-95. *Neuron*, 86(2), pp.475–489.
- Hanus, C. et al., 2014. Synaptic Control of Secretory Trafficking in Dendrites. *Cell Reports*, 7, pp.1771–1778.
- Hanus, C. et al., 2016. Unconventional secretory processing diversifies neuronal ion channel properties. *eLife*.
- Harmel, N. et al., 2012. AMPA Receptors Commandeer an Ancient Cargo Exporter for Use as an Auxiliary Subunit for Signaling. *PLoS ONE*, 7(1), p.e30681.
- Hashimoto, K. et al., 1999. Impairment of AMPA Receptor Function in Cerebellar Granule Cells of Ataxic Mutant Mouse Stargazer. *The Journal of Neuroscience*, 19(14), p.6027 LP-6036.
- Heiman, M. et al., 2008. A Translational Profiling Approach for the Molecular Characterization of CNS Cell Types. *Cell*, 135(4), pp.738–748.
- Heine, M. et al., 2008. Surface mobility of postsynaptic AMPARs tunes synaptic transmission. *Science*, 320(5873), pp.201–205.
- Henley, J.M. & Wilkinson, K.A., 2016. Synaptic AMPA receptor composition in development, plasticity and disease. *Nature Reviews Neuroscience*, 17, p.337.
- Herring, B.E. et al., 2013. Cornichon Proteins Determine the Subunit Composition of Synaptic AMPA Receptors. *Neuron*, 77(6), pp.1083–1096.
- Hilbig, D. et al., 2018. The Interaction of CD97/ADGRE5 With β -Catenin in Adherens Junctions Is Lost During Colorectal Carcinogenesis. *Frontiers in Oncology*, 8, p.182.
- Hirokawa, N., Niwa, S. & Tanaka, Y., 2010. Molecular motors in neurons: transport mechanisms and roles in brain function, development, and disease. *Neuron*, 68(4), pp.610–638.
- Hollmann, M. & Heinemann, S., 1994. Cloned glutamate receptors. *Annual Review of Neuroscience*, 17, pp.31–108.

- Horton, A.C. & Ehlers, M.D., 2004. Secretory trafficking in neuronal dendrites. *Nature Cell Biology*, 6(7), pp.585–591.
- Huber, K.M., Kayser, M.S. & Bear, M.F., 2000. Role for Rapid Dendritic Protein Synthesis in Hippocampal mGluR-Dependent Long-Term Depression. *Science*, 288(5469), p.1254 LP-1256.
- Hughes, J.R., 1958. Post-Tetanic Potentiation. *Physiological Reviews*, 38(1), pp.91–113.
- Ingolia, N.T. et al., 2009. Genome-Wide Analysis in Vivo of Translation with Nucleotide Resolution Using Ribosome Profiling. *Science (New York, N.Y.)*, 324(5924), pp.218–223.
- Ingolia, N.T., Lareau, L.F. & Weissman, J.S., 2011. Ribosome Profiling of Mouse Embryonic Stem Cells Reveals the Complexity and Dynamics of Mammalian Proteomes. *Cell*, 147(4), pp.789–802.
- Iwasaki, S. & Ingolia, N.T., 2016. Seeing translation. *Science*, 352(6292), p.1391 LP-1392.
- Jackson, A.C. & Nicoll, R.A., 2009. AMPA receptors get ‘pickled.’ *Nature*, 458(7238), pp.585–586.
- Jackson, A.C. & Nicoll, R.A., 2011a. Stargazin (TARP γ -2) Is Required for Compartment-Specific AMPA Receptor Trafficking and Synaptic Plasticity in Cerebellar Stellate Cells. *The Journal of neuroscience*, 31(11), pp.3939–3952.
- Jackson, A.C. & Nicoll, R.A., 2011b. The Expanding Social Network of Ionotropic Glutamate Receptors: TARPs and Other Transmembrane Auxiliary Subunits. *Neuron*, 70(2), pp.178–199.
- Kang, H. & Schuman, E.M., 1996. A Requirement for Local Protein Synthesis in Neurotrophin-Induced Hippocampal Synaptic Plasticity. *Science*, 273(5280), p.1402 LP-1406.
- Kato, A.S. et al., 2010. Hippocampal AMPA receptor gating controlled by both TARP and cornichon proteins. *Neuron*, 68(6), pp.1082–1096.
- Kennedy, M.J. & Ehlers, M.D., 2011. Mechanisms and function of dendritic exocytosis. *Neuron*, 69(5), pp.856–875.
- Kott, S. et al., 2009. Comparative analysis of the pharmacology of GluR1 in complex with transmembrane AMPA receptor regulatory proteins γ 2, γ 3, γ 4, and γ 8. *Neuroscience*, 158(1), pp.78–88.
- Kott, S. et al., 2007. Electrophysiological Properties of AMPA Receptors Are Differentially Modulated Depending on the Associated Member of the TARP Family. *The Journal of Neuroscience*, 27(14), p.3780 LP-3789.
- Lein, E.S. et al., 2006. Genome-wide atlas of gene expression in the adult mouse brain. *Nature*, 445, p.168.
- Li, Z. et al., 2004. The Importance of Dendritic Mitochondria in the Morphogenesis and Plasticity of Spines and Synapses. *Cell*, 119(6), pp.873–887.
- Link, J., Vink, M. & Tirrell, D., 2007. Preparation of the functionalizable methionine surrogate azidohomoalanine via copper-catalyzed diazo transfer. *Nature Protocols*, 2, p.1879.
- Lu, W. et al., 2009. Subunit Composition of Synaptic AMPA Receptors Revealed by a Single-Cell Genetic Approach. *Neuron*, 62(2), pp.254–268.
- Mazor, K.M. et al., 2018. Effects of single amino acid deficiency on mRNA translation are markedly different for methionine versus leucine. *Scientific Reports*, 8, p.8076.
- Menuz, K. et al., 2007. TARP Auxiliary Subunits Switch AMPA Receptor Antagonists into Partial Agonists. *Science*, 318(5851), p.815 LP-817.
- Milstein, A.D. et al., 2007. TARP Subtypes Differentially and Dose-Dependently Control Synaptic AMPA Receptor Gating. *Neuron*, 55(6), pp.905–918.
- Moremen, K.W., Tiemeyer, M. & Nairn, A. V., 2012. Vertebrate protein glycosylation: diversity, synthesis and function. *Nature Reviews Molecular Cell*

- Biology*, 13(7), pp.448–462.
- Nakagawa, T. et al., 2005. Structure and different conformational states of native AMPA receptor complexes. *Nature*, 433, p.545.
- Neff, R.A. et al., 2009. Postsynaptic scaffolds for nicotinic receptors on neurons. *Acta Pharmacologica Sinica*, 30(6), pp.694–701.
- Neves, G., Cooke, S.F. & Bliss, T.V.P., 2008. Synaptic plasticity, memory and the hippocampus: a neural network approach to causality. *Nature Reviews Neuroscience*, 9, p.65.
- Nguyen, P. V, Abel, T. & Kandel, E.R., 1994. Requirement of a critical period of transcription for induction of a late phase of LTP. *Science*, 265(5175), p.1104 LP-1107.
- Nowak, L. et al., 1984. Magnesium gates glutamate-activated channels in mouse central neurones. *Nature*, 307, p.462.
- Opazo, P. et al., 2010. CaMKII Triggers the Diffusional Trapping of Surface AMPARs through Phosphorylation of Stargazin. *Neuron*, 67(2), pp.239–252.
- Opazo, P. & Choquet, D., 2011. A three-step model for the synaptic recruitment of AMPA receptors. *Molecular and Cellular Neuroscience*, 46(1), pp.1–8.
- Ostroff, L.E. et al., 2002. Polyribosomes Redistribute from Dendritic Shafts into Spines with Enlarged Synapses during LTP in Developing Rat Hippocampal Slices. *Neuron*, 35(3), pp.535–545.
- Pestka, S., 1971. Inhibitors of Ribosome Functions. *Annual Review of Microbiology*, 25(1), pp.487–562.
- Popov, V. et al., 2005. Mitochondria form a filamentous reticular network in hippocampal dendrites but are present as discrete bodies in axons: A three-dimensional ultrastructural study. *The Journal of comparative neurology*, 492(1), pp.50–65.
- Ramón y Cajal, S., 1909. *Histologie du système nerveux de l'homme & des vertébrés*. Ed. française rev. & mise à jour par l'auteur, de l'espagnol par L. Azoulay., Paris : Maloine,.
- Rao, A. & Steward, O., 1991. Evidence that protein constituents of postsynaptic membrane specializations are locally synthesized: analysis of proteins synthesized within synaptosomes. *The Journal of Neuroscience*, 11(9), p.2881 LP-2895.
- Remondes, M. & M. Schuman, E., 2004. Role for a cortical input to hippocampal area CA1 in the consolidation of a long-term memory. *Nature*, 431.
- Rouach, N. et al., 2005. TARP γ -8 controls hippocampal AMPA receptor number, distribution and synaptic plasticity. *Nature neuroscience*, 8(11), pp.1525–1533.
- Salin, P.A. et al., 1996. Distinct short-term plasticity at two excitatory synapses in the hippocampus. *Proceedings of the National Academy of Sciences of the United States of America*, 93(23), pp.13304–13309.
- Scheiffele, P., 2003. Cell-cell signaling during synapse formation in the CNS. *Annual Review of Neuroscience*, 26(1), pp.485–508.
- Schmidt, E.K. et al., 2009. SUnSET, a nonradioactive method to monitor protein synthesis. *Nature Methods*, 6(4), pp.275–277.
- Schwenk, J. et al., 2009. Functional Proteomics Identify Cornichon Proteins as Auxiliary Subunits of AMPA Receptors. *Science*, 323(5919), p.1313 LP-1319.
- Schwenk, J. et al., 2012. High-Resolution Proteomics Unravel Architecture and Molecular Diversity of Native AMPA Receptor Complexes. *Neuron*, 74(4), pp.621–633.
- Schwenk, J. et al., 2014. Regional Diversity and Developmental Dynamics of the AMPA-Receptor Proteome in the Mammalian Brain. *Neuron*, 84(1), pp.41–54.
- Scott, H. & Panin, V.M., 2014. The role of protein N-glycosylation in neural transmission. *Glycobiology*, 24(5), pp.407–417.
- Scoville, W.B. & Milner, B., 1957. Loss of recent memory after bilateral hippocampal

- lesions. *Journal of Neurology, Neurosurgery, and Psychiatry*, 20(1), pp.11–21.
- Setou, M. et al., 2000. Kinesin superfamily motor protein KIF17 and mLin-10 in NMDA receptor-containing vesicle transport. *Science*, 288(5472), pp.1796–1802.
- Sheng, M. & Hoogenraad, C.C., 2007. The Postsynaptic Architecture of Excitatory Synapses: A More Quantitative View. *Annual Review of Biochemistry*, 76(1), pp.823–847.
- Shi, Y. et al., 2010. Functional comparison of the effects of TARPs and cornichons on AMPA receptor trafficking and gating. *Proc Natl Acad Sci USA*, 107(37), pp.16315–16319.
- Shi, Y. et al., 2009. The stoichiometry of AMPA receptors and TARPs varies by neuronal cell type. *Neuron*, 62(5), pp.633–640.
- Silberberg, G. et al., 2008. Stargazin involvement with bipolar disorder and response to lithium treatment. *Pharmacogenetics and genomics*, 18, pp.403–412.
- Sjöström, P.J. et al., 2008. Dendritic Excitability and Synaptic Plasticity. *Physiological Reviews*, 88(2), pp.769–840.
- Sommer, B. et al., 1991. RNA editing in brain controls a determinant of ion flow in glutamate-gated channels. *Cell*, 67(1), pp.11–19.
- Sonenberg, N. & Hinnebusch, A.G., 2009. Regulation of Translation Initiation in Eukaryotes: Mechanisms and Biological Targets. *Cell*, 136(4), pp.731–745.
- Soto, D. et al., 2009. Selective regulation of calcium-permeable AMPA receptors by a novel TARP. *Nature neuroscience*, 12(3), pp.277–285.
- Squire, L.R. et al., 1992. Activation of the hippocampus in normal humans: a functional anatomical study of memory. *Proceedings of the National Academy of Sciences of the United States of America*, 89(5), pp.1837–41.
- Stuart, G. et al., 1997. Action potential initiation and backpropagation in neurons of the mammalian CNS. *Trends in Neurosciences*, 20(3), pp.125–131.
- Südhof, T.C. & Rothman, J.E., 2009. Membrane Fusion: Grappling with SNARE and SM Proteins. *Science*, 323(5913), pp.474–477.
- Sumioka, A. et al., 2011. PDZ binding of TARP γ -8 controls synaptic transmission but not synaptic plasticity. *Nature neuroscience*, 14(11), pp.1410–1412.
- Sutton, M. & Schuman, E., 2005. Local translational control in dendrites and its role in long-term synaptic plasticity. *Journal of Neurobiology*, 64(1), pp.116–131.
- Sutton, M.A. et al., 2006. Miniature neurotransmission stabilizes synaptic function via tonic suppression of local dendritic protein synthesis. *Cell*, 125(4), pp.785–799.
- Sutton, M.A. et al., 2007. Postsynaptic Decoding of Neural Activity: eEF2 as a Biochemical Sensor Coupling Miniature Synaptic Transmission to Local Protein Synthesis. *Neuron*, 55(4), pp.648–661.
- Sutton, M.A. et al., 2004. Regulation of dendritic protein synthesis by miniature synaptic events. *Science*, 304(5679), pp.1979–1983.
- Sutton, M.A. & Schuman, E.M., 2006. Dendritic Protein Synthesis, Synaptic Plasticity, and Memory. *Cell*, 127(1), pp.49–58.
- Suzuki, E., Kessler, M. & Arai, A.C., 2008. The fast kinetics of AMPA GluR3 receptors is selectively modulated by the TARPs γ 4 and γ 8. *Molecular and Cellular Neuroscience*, 38(1), pp.117–123.
- Tao, X. et al., 1998. Ca²⁺ Influx Regulates BDNF Transcription by a CREB Family Transcription Factor-Dependent Mechanism. *Neuron*, 20(4), pp.709–726.
- Tardin, C. et al., 2003. Direct imaging of lateral movements of AMPA receptors inside synapses. *The EMBO Journal*, 22(18), pp.4656–4665.
- Tichelaar, W. et al., 2004. The Three-dimensional Structure of an Ionotropic Glutamate Receptor Reveals a Dimer-of-dimers Assembly. *Journal of Molecular Biology*, 344(2), pp.435–442.
- Tigaret, C. & Choquet, D., 2009. More AMPAR Garnish. *Science*, 323, pp.1295–1296.

- tom Dieck, S. et al., 2015. Direct visualization of newly synthesized target proteins in situ. *Nature Methods*.
- tom Dieck, S. et al., 2012. Metabolic labeling with noncanonical amino acids and visualization by chemoselective fluorescent tagging. *Current protocols in cell biology*.
- Tomita, S. et al., 2003. Functional studies and distribution define a family of transmembrane AMPA receptor regulatory proteins. *The Journal of Cell Biology*, 161(4), pp.805–816.
- Tomita, S. et al., 2005. Stargazin modulates AMPA receptor gating and trafficking by distinct domains. *Nature*, 435, p.1052.
- Torre, E.R. & Steward, O., 1992. Demonstration of local protein synthesis within dendrites using a new cell culture system that permits the isolation of living axons and dendrites from their cell bodies. *The Journal of Neuroscience*, 12(3), p.762 LP-772.
- Tsien, J.Z. et al., 1996. Subregion- and cell type-restricted gene knockout in mouse brain. *Cell*, 87(7), pp.1317–1326.
- Tsui, J. & Malenka, R.C., 2006. Substrate Localization Creates Specificity in Calcium/Calmodulin-dependent Protein Kinase II Signaling at Synapses. *Journal of Biological Chemistry*, 281(19), pp.13794–13804.
- Turetsky, D., Garringer, E. & Patneau, D.K., 2005. Stargazin Modulates Native AMPA Receptor Functional Properties by Two Distinct Mechanisms. *The Journal of Neuroscience*, 25(32), p.7438 LP-7448.
- Vickers, C.A. & Wyllie, D.J.A., 2007. Late-phase, protein synthesis-dependent long-term potentiation in hippocampal CA1 pyramidal neurones with destabilized microtubule networks. *British Journal of Pharmacology*, 151(7), pp.1071–1077.
- Vitureira, N. & Goda, Y., 2013. The interplay between Hebbian and homeostatic synaptic plasticity. *The Journal of Cell Biology*, 203(2), p.175 LP-186.
- Wang, Z. & Ehlers, M.D., 2008. Myosin Vb Mobilizes Recycling Endosomes and AMPA Receptors for Postsynaptic Plasticity. *Cell*, 135(3), pp.535–548.
- Weiler, I.J. & Greenough, W.T., 1991. Potassium ion stimulation triggers protein translation in synaptoneurosomal polyribosomes. *Molecular and Cellular Neuroscience*, 2(4), pp.305–314.
- Yamasaki, M. et al., 2016. TARPs 2 and 8 Differentially Control AMPAR Density Across Schaffer Collateral/Commissural Synapses in the Hippocampal CA1 Area. *Journal of Neuroscience*, 36(15), pp.4296–4312.
- Zalutsky, R. & Nicoll, R.A., 1992. Mossy fiber long-term potentiation shows specificity but no apparent cooperativity. *Neuroscience letters*, 138, pp.193–197.

9. Appendix

9.1 List of Abbreviations

AHA	Azidohomoalanine
AMPA	α -amino-3-hydroxy-5-methyl-4-isoxazolepropionic acid
Aniso	Anisomycin
BB	Blocking buffer
BO	Branch order
BONCAT	Bio-orthogonal non-canonical amino acid tagging
CA	<i>Cornu ammonis</i>
CaCl ₂	Calcium chloride
CCT	Cacahouete
CDS	Coding sequence
CTD	C terminal domain
CNIH	Cornichon homolog
CNS	Central nervous system
CuAAC	Copper-catalyzed [3+2] azide-alkyne cycloaddition
DAPI	4',6-diamidino-2-phenylindole
DMSO	Dimethylsulfoxid
DIV	Days <i>in vitro</i>
DNA	Desoxyribonucleic acid
EPSC	Excitatory postsynaptic current
EPSP	Excitatory postsynaptic potential
ER	Endoplasmic Reticulum
ERGIC	ER to Golgi intermediate compartment
FLIM	Fluorescence lifetime imaging microscopy
FRAP	Fluorescent recovery after photobleaching
FRET	Fluorescence resonance energy transfer
FUNCAT	Fluorescent non-canonical amino acid tagging
GA	Golgi apparatus
GFAP	Glial fibrillary acidic protein
GM130	Golgi Matrix Protein of 130 kDa
LSM	Laser scanning microscope
LTD	Long term depression
LTP	Long term potentiation
MAP2	Microtubule - associated protein 2
Met	Methionine
MgCl ₂	Magnesium chloride
MIP	Maximum intensity projection
mRNA	Messenger RNA
NMDA	N-methyl-D-aspartate
NGM	Neuronal growth medium
Oligo	Oligonucleotide
PBS	Phosphate-buffered saline
PFA	Paraformaldehyde
PLA	Proximity ligation assay
POI	Protein of interest
PSD	Post synaptic density
Puro	Puromycin
ROI	Region of interest
RT	Room temperature
SILAC	Stable isotope labeling by/with amino acids in cell culture

TARP	Transmembrane AMPA receptor regulatory protein
TGN	Trans Golgi network
Tris	Tris hydroxy methyl aminomethan

9.2 List of Figures

<i>Figure 1: The hippocampal formation</i>	15
<i>Figure 2: Model of a glutamatergic synapse</i>	16
<i>Figure 3: Pre and postsynaptic changes during synaptic potentiation</i>	18
<i>Figure 4: All components of the translational machinery are present in dendrites</i>	21
<i>Figure 5: Impact of TARPs on channel properties</i>	29
<i>Figure 6: Secretory pathway</i>	32
<i>Figure 7: AHA labeling of newly synthesized proteins in cultured hippocampal neurons</i>	41
<i>Figure 8: Puromycylation in COS7 cells</i>	42
<i>Figure 9: Puromycin labeling in cultured hippocampal neurons</i>	43
<i>Figure 10: Working principle of FUNCAT- and Puro-PLA</i>	44
<i>Figure 11: FUNCAT-PLA for newly synthesized CamK2α and negative controls</i>	45
<i>Figure 12: Puro-PLA for newly synthesized CamK2α and negative control</i>	46
<i>Figure 13: Linear relationship between labeling time and signal density</i>	46
<i>Figure 14: No obvious influence of methionine starvation on global protein synthesis</i>	47
<i>Figure 15: Workflow of puncta analysis with the custom written ImageJ script</i>	50
<i>Figure 16: Workflow of puncta analysis in neurons with Neurobits (MATLAB)</i>	51
<i>Figure 17: High reproducibility of neuron tracing with different script users</i>	53
<i>Figure 18: FUNCAT-PLA for AMPA receptor subunits GluA1 and GluA2</i>	56
<i>Figure 19: Newly synthesized GluA2 is relatively more abundant in dendrites than GluA1</i>	57
<i>Figure 20: Surface labeling of GluA1 using an N-terminal antibody</i>	58
<i>Figure 21: Surface labeling of GluA2 using an N-terminal antibody</i>	59
<i>Figure 22: High fraction of newly synthesized GluA1 at the cell surface</i>	60
<i>Figure 23: Low fraction of newly synthesized GluA2 at the surface</i>	61
<i>Figure 24: Comparison of surface to total fraction of newly synthesized AMPA receptor subunits</i>	62
<i>Figure 25: Puro-PLA for GluA1 and GluA2 shows very low dendritic signal</i>	63
<i>Figure 26: Pulse-chase experiment for GluA1 suggests a slow redistribution into dendrites</i>	64
<i>Figure 27: No puncta intensity differences between different chase times for GluA1 FUNCAT-PLA</i>	65
<i>Figure 28: Define AHA labeling conditions for GluA2 pulse-chase experiments</i>	66
<i>Figure 29: Newly synthesized GluA2 redistributes rapidly into dendrites</i>	67
<i>Figure 30: Specific labeling using custom-produced Gamma 8 antibody</i>	69
<i>Figure 31: Custom-produced anti-Gamma 8 antibody shows staining enriched at synapses</i>	70
<i>Figure 32: Low Gamma 8 FUNCAT-PLA signal in dendrites</i>	71
<i>Figure 33: Pulse-chase experiments suggest a slow Gamma 8 redistribution into dendrites</i>	72
<i>Figure 34: Newly synthesized CNIH2 can be found in neuronal somata and dendrites</i>	74
<i>Figure 35: Synapse labeling using an anti-Vglut antibody</i>	84
<i>Figure 36: Proposed scenario of AMPA receptor subunit synthesis and trafficking</i>	87

9.3 List of Info-Boxes

<i>Infobox 1: FUNCAT and BONCAT - chemistry and principle</i>	25
<i>Infobox 2: Topology of AMPA GluA subunits</i>	27
<i>Infobox 3: TARPs</i>	29
<i>Infobox 4: CNIH2 and 3</i>	31

9.4 List of Tables

<i>Table 1: Properties and range of applications for Puro-PLA and FUNCAT-PLA</i>	48
<i>Table 2: Output parameters for Neurobits (MATLAB)</i>	53

Lisa Verena Kochen

Hügelstraße 179, 60431 Frankfurt am Main
+491577/1916687, lisa.kochen@googlemail.com
Date of birth: 16/06/1987

Research Experience

- 2013 – 2018 **PhD student** at Max Planck Institute for Brain Research (MPI-BR), Frankfurt/Main, Supervisor Prof. Dr. Erin Schuman, Topic: Synaptic plasticity, technique development to visualize endogenous newly synthesised target proteins *in situ*. **PhD fellowship** International Max Planck Research School (IMPRS) for Neural Circuits.
- 2012 – 2013 **Research assistant** at Max Planck Institute for Brain Research.
- 2011 – 2012 **Diploma thesis** (Master equivalent) at the MPI-BR, Title: Secretory pathway dynamics in synaptic plasticity, grade: very good.
- 2008 – 2010 Internships with Prof. Dr. H. Osiewacz (Ageing in the model organism *Podospora anserina*), Prof. Dr. H. Zimmermann (Adult neurogenesis), Prof. Dr. M. Kössl (Psychophysics and electrophysiology in young bats and humans) at the Goethe University, Frankfurt/Main and Prof. Dr. E. Schuman (GRASP55, a ribbon formation protein in the Golgi apparatus) at the MPI-BR.

Education

- Autumn 2018 Expected PhD reception (Dr. rer. nat.)
- 2006 – 2012 Diplom in Biology (Master equivalent) Goethe University, Frankfurt/Main
Grade: very good, Majors: Neurobiology, Genetics, Cell biology

Languages

German	native
English	bilingual
French	fluent

Science Communication

Scientific Writing: Prepared research proposals in English and German, manuscripts (text and figures) for publication in English, edited grant applications in English and French, animal protocols, bachelor and master theses in English and German.

Presentations and posters: Prepared and presented monthly progress report in group meetings (English, up to 1 hour), yearly presentation at the Institute's seminar (audience of up to 100 researchers), gave talk at the young investigator colloquium (YIC) at the Interdisciplinary Center for Neuroscience in Frankfurt, presented poster at international conferences (EMBO, Wellcome Trust) and for the scientific advisory board at the MPI-BR.

Teamwork and Organisation

Organisation of the MPI-BR Institute's Seminar (2014 – 2017, monthly talks): As head of the organisation committee, defined seminar format with the MPI-BR directors, organised speaker schedule, created communication media (posters, website, mailing lists), set up discussion platform with catering for scientists from diverse backgrounds.

Coordination of Collaborations with internal and external research groups (2013 – present):

Developed software for analysis of neuronal morphology and molecular tools to assess RNA and protein dynamics *in situ* for joint research projects (see publications no. 2 and 4) with bioinformaticians (Dr. G. Tushev, head of the scientific computing facility), mathematicians (S. Suchan, S. Lang), physicists (Dr. T. Tchumatchenko) and chemists (Prof. A. Heckel), adapted those tools to other researcher's needs, taught them to use these tools.

Teaching Lab at the MPI-BR (2013 – 2017): Defined format and content of experiments and presentations, trained scientists, prepared, organised and executed teaching activities for school classes and students.

Event Organisation for academic and lay audiences (2011 – 2017): For the Night of Science (www.nightofscience.de) gave lab tours and summarised the institute's research topics to lay audience, institute summer and Christmas parties, family events, up to 200 people.

Institute's Choir (2013 – present): Founder and leader of the MPI-BR and Frankfurt Institute for Advanced Studies (FIAS) choir with 25 members.

Mentoring (2011 – 2017): Defined and supervised short and mid term research programs and experiments for 11 students between 2011 and 2017. This included one PhD rotation student, two master students, four bachelor students with diverse backgrounds (Mathematics, Physics, Medicine and Biomedicine) and four high school internship students.

Proficiency in Productivity and Scientific Software

Productivity and Graphics Software: MS Office (Word, Excel, PowerPoint, Outlook), Adobe Creative Suite (Photoshop, Illustrator, InDesign), TheBrain.

Computing and Data Analysis: Excel, ImageJ, Prism, Matlab, Metamorph, Zen, Amira, Pubmed, GeneProt.

Publications

Dörrbaum A, **Kochen L**, Langer J, Schuman EM. Local and global influences on protein turnover in neurons and glia. In press at **eLife 2018**

Sambandan S, Akbalik G*, **Kochen L***, Rinne J, Kahlstatt J, Glock C, Tushev G, Alvarez-Castelao B, Heckel A, Schuman EM. Activity-dependent spatially localized miRNA maturation in neuronal dendrites. **Science 2017** * Equal contribution

Hanus C, Geptin H, Tushev G, Garg S, Alvarez-Castelao B, Sambandan S, **Kochen L**, Hafner AS, Langer J, Schuman EM. Unconventional secretory processing diversifies the properties of neuronal membrane proteins. **eLife 2016**

TomDieck S*, **Kochen L***, Hanus C, Heumüller M, Bartnik I, Nassim-Assir B, Merk K, Mosler T, Garg S, Bunse S, Tirrell DA, Schuman EM. Direct visualization of newly synthesized target proteins *in situ*. **Nature Methods 2015** * Equal contribution

Hanus C, **Kochen L**, Sibarita JB, Racine V, Schuman EM, Ehlers MD. Synaptic control of early secretory trafficking in dendrites. **Cell Reports 2014**

Will TJ, Tushev G, **Kochen L**, Nassim-Assir B, Cajigas IJ, TomDieck S, Schuman EM. Deep sequencing and high-resolution imaging reveal compartment-specific localization of BDNF mRNA in hippocampal neurons. **Science Signaling 2013**

THE END